VIETNAM JOURNAL OF

ISSN 2815 - 6110

AGRICULTURE & RURAL DEVELOPMENT

Volume 2. No 2 (2022)

MINISTRY OF AGRICULTURE AND RURAL DEVELOPMENT

EDITORIAL COMMITTEE

VIETNAM JOURNAL OF AGRICULTURE AND RURAL DEVELOPMENT
ISSN 2815 - 6110

THE TWENTY SECOND YEAR

VOL 2. No. 2 (2022)

Head-office
No 10 Nguyenconghoan
Badinh - Hanoi - Vietnam
Tel: 024.37711072
Fax: 024.37711073
Email: tapchinongnghiep@mard.gov.vn
Website:www.tapchikhoahocnongnghiep.vn

Representative Office
135 Pasteur
Dist 3 - Hochiminh City
Tel/Fax: 028.38274089

Printing in Hoang Quoc Viet
technology and science
joint stock company

CONTENTS

DESIGN OF CRISPR/CAS9 SYSTEM FOR EDITING *OsNRAMP7* INVOLVED IN METAL TRANSPORT IN TBR225 RICE VARIETY

Phung Thi Thu Huong[1], Cao Le Quyen[1], Ngo Thi Van Anh[1], Pham Phuong Ngoc[1], Pham Thi Van[1], Le Quynh Mai[2], Pham Xuan Hoi[1], Nguyen Duy Phuong[1,*]

ABSTRACT

Rice (*Oryza sativa* L.) is one of the major food crops but is deficient in minerals such as Zn. In rice, there were eight genes belonging to *the Natural resistance-associated macrophage protein* (*NRAMP*) family, of which *OsNRAMP1*, *OsNRAMP4, OsNRAMP5, OsNRAMP6*, and *OsNRAMP8* were reported to transport metals such as iron (Fe), zinc, mangan (Mn). Recently, *AtNRAMP5*, closely related to *OsNRAMP7*, has been identified as a function in Zn uptake in *Arabidopsis.* To identify the function of *OsNRAMP7* in a local rice variety -TBR225, the expression of the interested gene was evaluated and a Clustered regular interspaced short palindromic repeats/CRISPR-associated Cas9 (CRISPR/Cas9) system for editing TBR225 *OsNRAMP7* was constructed. The accumulation of *OsNRAMP7* mRNA was increased in Zn-treated TBR225 rice plants. Two single guide RNAs for the *OsNRAMP7*-editing using CRISPR/Cas9 system was designed based on 0.52 kb DNA fragment containing the ExonII region of *OsNRAMP7* isolated from the genomic DNA of TBR225. The CRISPR/Cas9 system for directed editing TBR225 *OsNRAMP7* containing two CRISPR RNA (crRNA) sequences recognizing two different sites on the ExonII of *OsNRAMP57* was developed. The recombinant vector was validated by PCR and sequencing analysis. The results will be used for studying possible function of OsNRAMP7 via knocking out of the gene.

Keywords: *CRISPR/Cas9, OsNRAMP7, TBR225, Zinc.*

Received: 4 August 2022; revised: 1 September 2022; accepted: 30 November 2022.

1. INTRODUCTIONS

Rice (*Oryza sativa* L.) is one of the major food crops of the world in general and Vietnam in particular. Rice is a rich energy source, gluten-free, easy to digest, and low in fat. However, the most emerging issue is that rice is deficient in minerals, including zinc (Zn), which significantly affects the human immune system. This disadvantage results in micronutrient deficiencies in the diet, especially in countries where rice is the staple food [1]. One of the practical solutions to this problem is generating new rice varieties with high zinc content in the grain. TBR225 is one of the mega rice varieties for some northern provinces of our country with a significant proportion of rice production. Production of rice variety TBR225 with high Zn content will improve the value of this rice variety and bring many benefits to consumers.

The NRAMP (natural resistance-associated macrophage protein) transporter protein family has eight members in rice,

[1] Insitute of Agricultural Genetics
[2] VNU-University of Science
*Email: phuongnd.bio@gmail.com

including *OsNRAMP1*, *OsNRAMP2*, *OsNRAMP3*, *OsNRAMP4*, *OsNRAMP5*, *OsNRAMP6*, *OsNRAMP7* and *OsNRAMP8* [2]. NRAMPs transport metal ions such as Zn2+, Mn2+, Fe2+, Cd2+, and others in plants. *OsNRAMP1*, *OsNRAMP2* and *OsNRAMP3* express primarily in roots, leaves and both tissues, respectively [3]. Furthermore, *OsNRAMP5* and *OsNRAMP2* are the major transporters responsible for Fe, Mn, and Cd, whereas *OsNRAMP4* functions as a transporter for Al [2, 4, 5]. However, relatively little information about these transporters is available, especially information regarding *OsNRAMP7*. The close genetic relationship between *OsNRAMP7* and the identified Zn transporter AtNRAMP4 in *Arabidopsis* [2] suggested the role of *OsNRAMP7* in Zn accumulation in rice.

CRISPR/Cas9 (Clustered Regular Interspaced Short Palindromic Repeats/ CRISPR-Associated Cas9) is a commonly used technique in reverse-genetics research to knock out a gene of interest [4]. Because of its simplicity, efficiency, and versatility, the CRISPR/Cas9 system has revolutionized gene editing and is widely used. The generation of target gene-inactivating mutants based on the specific double-stranded DNA cleavage of the sgRNA-Cas9 complex and the strand break repair machinery is one of the most widely used applications of the CRISPR/Cas9 system. The cell's non-homologous end joining (NHEJ) mechanism causes a double-strand break (DSB) [6]. Many valuable agro-biological traits of plants, such as tolerance to abiotic and biotic stresses, yield, and quality, have been improved by this method [7].

In order to understand the possible involvement of *OsNRAMP7* as Zn transporter in rice plants, the expression of *OsNRAMP7* under Zn treatment was investigated and a CRISPR/Cas9 system-mediated *OsNRAMP7* editing was developed for lightening up *OsNRAMP7* function in TBR225 rice in coming studies

2. MATERIALS AND METHODS

2.1. Materials

The rice variety TBR225 was provided by Thaibinh Seed Corporation. The *Escherichia coli* strains DH5α and DB3.1 were purchased from Thermo Scientifics (USA).

Vectors pENTR4-V1 and pCas9 were provided by the research team of Dr. Sebastien Cunnac (Research Center for Development, Montpellier, France).

The primer pairs used in the study were designed based on the reference sequences (Os12g0581600 and Os03t0718100-01) and ordered from PHUSA Biochem Cor. (Vietnam).

2.2. Methods

2.2.1. Expression analysis

Zn treatment experiments and gene expression analysis were carried out according to the description of Sasaki *et al.* (2012) [8]. Four-week-old rice plants were grown in a nutrient solution containing 10 µM $ZnSO_4$ for 0.5 h, 1 h, 3 h, and 6 h. Total RNA was extracted from the treated plant and used for first-strand cDNA with primers oligo dT. Expression of *OsNRAMP7* was evaluated by amplifying 177 bp of the gene using primers NRAMP7-RT-F: 5'-TTGAAAACTACGGGGTG AGG-3' and NRAMP7-RT-R: 5'- AACAACCCCA ACTGCTTGTC-3'. PCR mixture contains 0.5 µL of cDNA template (100 ng), 0.3 µL of each 10 pmol/ml primer (1.5 µL of 2 mM dNTP and 1.5 µL of 10 X *Taq* DNA polymerase buffer, 0.5 µL of 5 U/µL *Taq* DNA polymerase, 10.3 µL of deionized sterilized water. Meanwhile, *OsActin* was used as a internal control using *Actin1* specific primers (Actin-F: 5'-

TGATGGTGTCAGCCACACT-3', and Actin-R: 5'-TGGTCTTGGCAGTCTCCATT-3'; 221 bp). The RT-PCR was performed in 3 independent experiments.

2.2.2. OsNRAMP5 isolation

Total DNA was extracted from TBR225 plants as described by Doyle and Doyle (1990) [9] using a 2% CTAB solution. The rice leaf sample (100 mg) was ground in liquid nitrogen to a fine powder, then 500 µL of 2% CTAB solution (containing 40 mg/mL RNase) was added and centrifuged at 13,000 rpm to collect the solution. Five hundred µL of a mixture of phenol:chloroform:isoamyl (25: 24: 1) was added to the solution to precipitate the protein. The mixture was then centrifuged at 13,000 rpm to remove the protein. DNA was precipitated by adding 500 µL of isopropanol to the solution and finally redissolved in TE buffer.

A part of *OsNRAMP7* (referred to as *OsNRAMP7-TBR*) was isolated from TBR225 genomic DNA using specific primers (NRAMP7-F: TCTCAACGCTTCACGGACTT-3' and NRAMP7-R: 5'-TGAGGATTTCT GCCTTGTGCT-3'; Os12g0581600; 517 bp). The PCR conditions were as follows: denaturation at 95˚C for 30 s and 35 cycles of 95˚C for 30 s, 55˚C for 30 s, and 72˚C for 60 s. The PCR products were directly sequenced by Marorgen Cor. (Korea). Sequencing results were analyzed using BioEdit 4.0 software; a homology search was performed using the NCBI BLAST program on GenBank.

2.2.3. Design of sgRNA

The *OsNRAMP7-TBR* editing sgRNA was determined using CRISPR-P v2.0 software (http://crispr. hzau. edu. cn/ CRISPR2). The secondary structure of sgRNA was predicted by Mfold 2.3 software (http://unafold.rna. albany.edu/). The DNA sequences homologous to the crRNA region of designed sgRNA in the rice genome were identified using CCTop software (http://crispr.cos.uni-heidelberg.de). The crRNA sequences were then synthesized by PHUSA Biochem Cor. (Vietnam).

2.2.4. Construction of T-DNA vector

Two oligonucleotide pairs BtgZI-crRNA1-F/BtgZI-crRNA1-R (5'-tgttGTATGGCTGTCT CCTTTGCA-3'/5'-aaacTGCAAAGGAGACAG CCATAC-3') and BsaI-crRNA2-F/BsaI-crRNA 2-R (5'-gtgtGTGTCTCTTGAAAA CTACG-3'/5'-aaa cCGTAGTTTTCAAGAGAC AC-3') were annealed to each other by heat treatment at 95°C for 10 min to form two double-stranded crRNAs (called as *crRNA1-OsNRAMP7* and *crRNA2-OsNRAMP7*). These DNA fragments were then inserted at the *Btg*ZI and *Bsa*I sites on the pENTR4-V2/sgRNA vector, respectively (Figure 1). After PCR validation of recombinant vector with BsaI-crRNA2-F/pENTR4-R (5'- ATGGC TCATAACACCCC TTG-3') (443 bp in length) and pENTR4-F (5'- CTACAAACTC TTCCTGTTAGTTAG-3')/BtgZI -crRNA1-R (527 bp in length), the DNA region containing two sgRNA expression constructs driven by *U6* promoter (0.45 kb) was ligated into the pCas9 binary vector using the Gateway kit (Invitrogen). The pCas9/sgRNA-OsNRAMP7 recombinant vector was tested by PCR with primer pairs BtgZI-crRNA1-F/BsaI-crRNA2-R (0.45 kb in length), Ubi-F (5'-CCCTGC CTTCATAC GCTATT-3')/Cas9-t-R (5'-GCCTCGGCTGTC TCGCCA-3') (0.35 kb in length) and Hpt -F (5'-AAGGAGGTGATC CAGCC-3')/Hpt-R (5'-GAGTTTGATCCTGGCT CAG-3') (0.8 kb in length) and DNA sequencing.

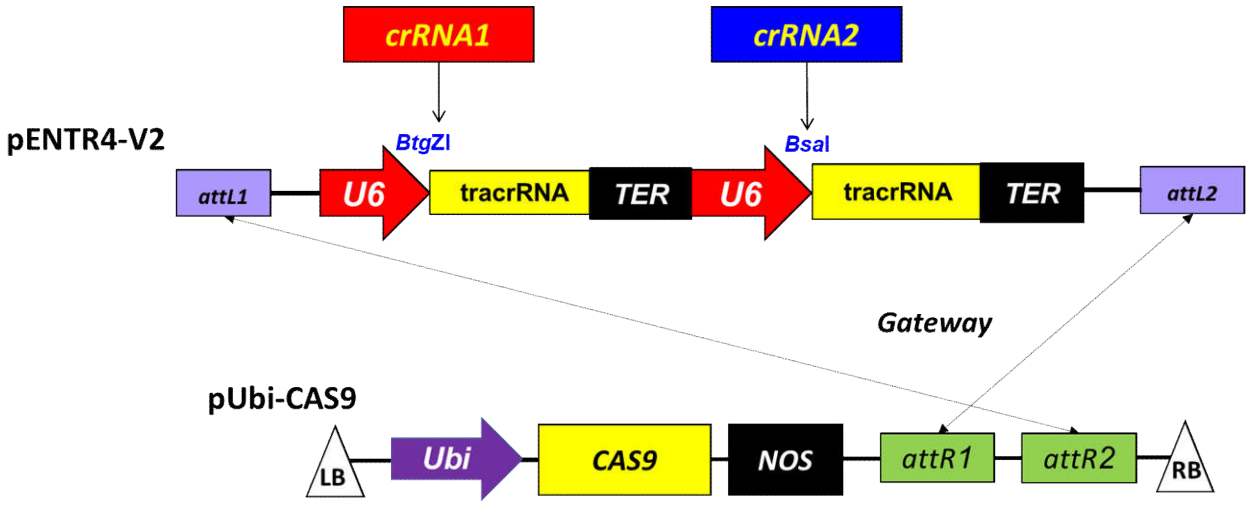

Figure 1. Schematic illustration of pCas9/sgRNA-*OsNRAMP7* vector construction

Note: (U6) OsU6 promoter; (TER) Terminator; (Ubi) ZmUbiquitin promoter; (NOS) nopaline synthase terminator; (LB) Left border; (RB) right border; (attL1/attL2; attR1/attR2) recognition sites of Gateway LR clonase

3. RESULTS AND DISCUSSION

3.1. Analysis of *OsNRAMP7* expression

Many members of the *NRAMP* gene family have been shown to increase their expression under metal ions treatment [8, 00]. In this study, the responses of *OsNRAMP7* expression in the plants exposed to the addition of micronutrient Zn in the hydroponic solution were investigated. The RT-PCR results revealed the accumulation of *OsNRAMP7* transcripts in the different Zn treatment time points (0.5 h, 1 h, 3 h, and 6 h) (Figure 2). The *OsNRAMP7* expression increased immediately in response to the addition of Zn and peaked at 3 h after treatment. Despite the slight decrease, the high expression level of *OsNRAMP7* still remained at 6 h point. These observations initially suggested that *OsNRAMP7* involves in Zn transportation in rice variety TBR225.

Among the *OsNRAMPs* involved in metal transportation in rice, some are strongly expressed under normal conditions, such as *OsNRAMP4* and *OsNRAMP6*, while others are weakly expressed (*OsNRAMP1*, *OsNRAMP2*, and *OsNRAMP5*) or no expression (*OsNRAMP6* and *OsNRAMP7*) [11]. In the current study, *OsNRAMP7* expression was only observed under the Zn treatment condition but not the normal growth condition. The expression of *OsNRAMPs* in response to different metal treatments also varies widely. *OsNRAMP1* strongly expressed in addition of Fe [3]; in contrast, *OsNRAMP2* and *OsNRAMP5* were induced in deficiency of Fe, Cu, Mn, and Zn [4]. Here, the accumulation of *OsNRAMP7* mRNA increased significantly by Zn addition treatment, suggesting that *OsNRAMP7* may have a certain role in the Zn transportation of TBR225 rice.

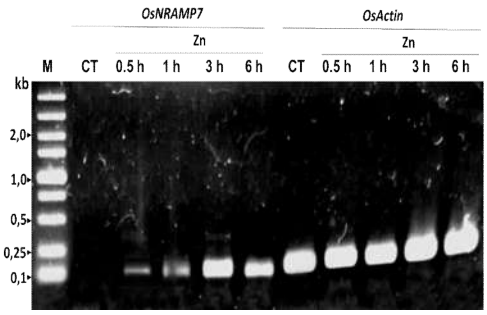

Figure 2. Expression of *OsNRAMP7* in Zn-treated TBR225 rice plants

Note: RT-PCR analysis of OsNRAMP7 and OsActin (internal control) expression in Zn-treated TBR225 rice plants at 0.5 h, 1 h, 3 h, and 6 h post-treatment. (Zn) Zn treated rice samples; (CT): rice samples without Zn treatment; (M) 1.0 kb DNA ladder (Cleaver Scientific).

3.2. Isolation of TBR225 *OsNRAMP7*

To design an *OsNRAMP7*-editing CRISPR/Cas9 system for functional identification of TBR225 *OsNRAMP7* through gene knocking-out, the ExonII-containing region of *OsNRAMP7* was isolated from the total DNA of TBR225. The PCR amplification produced a single DNA band corresponding to approximately 0.52 kb (Figure 3) as the theoretically calculated size of the expected *OsNRAMP7* fragment.

The sequencing analysis showed that the isolated DNA fragment was 99% homology to both Indica rice variety Shuhui498 (CP018168.1) and Japonica rice variety Nipponbare (AP014968.1) published on GenBank (Figure 4). These indicated that *OsNRAMP7* was successfully isolated from TBR225. The complete ExonII region of *OsNRAMP7* with the size of 137 bp was selected from the amplified *OsNRAMP7-TBR* fragment for designing *OsNRAMP7*-edited sgRNA.

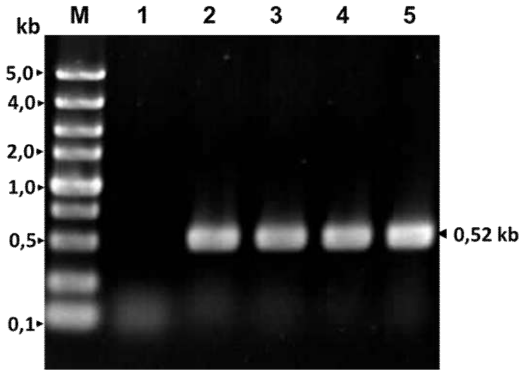

Figure 3. Isolation of *OsNRAMP7-TBR* by PCR

Note: PCR products were electrophoresed on 1% agarose gel. Lane M: 1.0 kb DNA ladder (Cleaver Scientific); lane 1: blank control (no DNA template); lane 2-5: templates were TBR225 genomic DNAs with dilutions of 1: 1, 1: 5, 1: 20 and 1: 50.

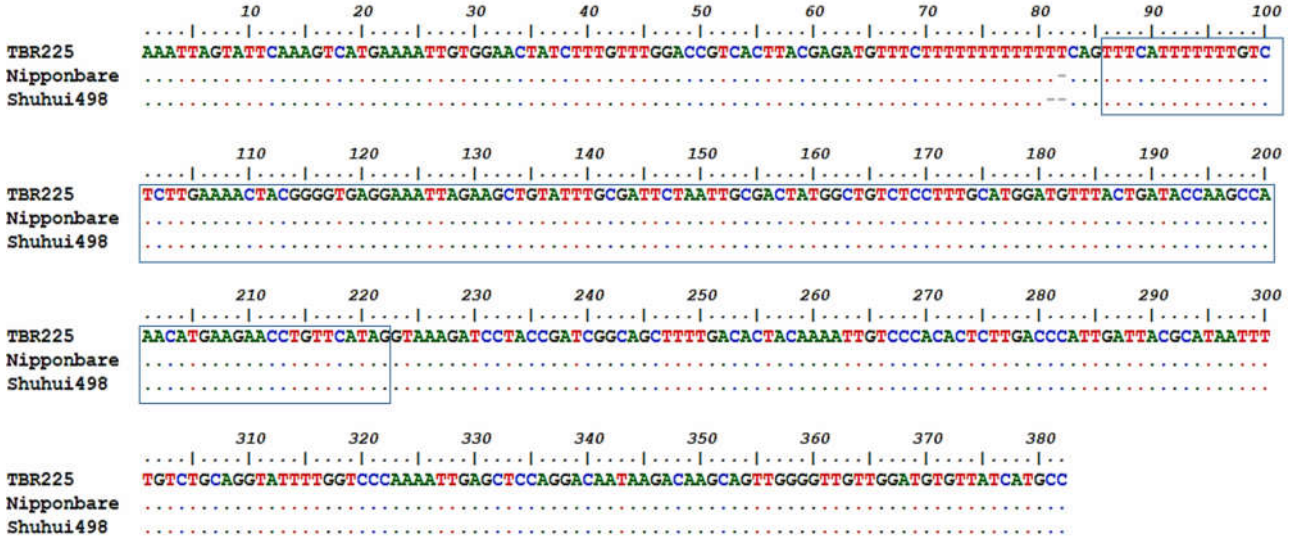

Figure 4. Alignment of *OsNRAMP7* fragments

Note: Dots indicate the similar nucleotides. ExonII regions are showed in the box. (TBR225, Nipponbare, Shuhui498) OsNRAMP7 sequences of TBR225, Nipponbare (AP014968.1) Shuhui498 (CP018168.1) rice varieties.

3.3. Design of *OsNRAMP7*-editing sgRNA sequences

The gene editing CRISPR/Cas9 system works on its ability to precisely cut double-stranded DNA at the desired location of the RNA-protein complex. This complex consists of two main components: (i) the Cas9 protein with endonuclease activity and (ii) the single guide RNA (sgRNA) that guides the complex to the targeted DNA site. The specificity of the CRISPR/Cas9 complex depends on the 17 - 22 nucleotide CRISPR RNA (crRNA) sequence on the sgRNA molecule [12].

In order to ensure the best performance of the sgRNA expression construct and the DNA cutting ability of the CRISPR/Cas9 system, the crRNA sequences must comply with the following conditions: (i) target DNA sequence complementary to crRNA located upstream the protospacer adjacent motif (PAM) sequence (NGG), (ii) 19-22 Nu length, (iii) the DNA cut site is on the target sequence (ExonII of *OsNRAMP7*) [12]. Using CRISPR-P v2.0 software, 11 sgRNAs satisfying the above requirements were determined (Table 1). Furthermore, to maintain the activity and specificity of the Cas9-sgRNA complex in the cell nucleus, in the secondary structure of the sgRNA molecule, three structural loops, RAR, SL2, and SL3, must be remained [13]. The total base pairs (TBP - total base pairs), the number of consecutive base pairs (CBP - consecutive base pairs) and the number of base pairs inside the crRNA structure (IBP - internal base pairs) should be less than 13, 8 and 7, respectively [14]. The content of GC in crRNA sequences ranges from 30-80% [12]. Two sgRNAs (sgRNA-1 and sgRNA-6) (Table 2) satisfying all these requirements and having the highest on-score were selected for the design of a T-DNA vector expressing the TBR *OsNRAMP7*-editing CRISPR/Cas9 system.

Table 1. Characteristics of TBR *OsNRAMP7*-editing sgRNAs

Name	Sequences of crRNA (5'-3')	Size	TSL	GSL	CBP	TBP	IBP	% GC	On-score
sgRNA-1	CTATGGCTGTCTCCTTTGCA	20	3	0	7	11	0	50	0.5766
sgRNA-2	ATGAACAGGTTCTTCATGTT	20	3	0	3	9	0	35	0.1029
sgRNA-3	ATCAGTAAACATCCATGCAA	20	3	0	3	5	0	35	0.0736
sgRNA-4	TGCGATTCTAATTGCGACTA	20	4	1	5	10	5	40	0.0305
sgRNA-5	CTCTTGAAAACTACGGGGTG	20	3	0	5	10	0	50	0.0266
sgRNA-6	TTGTCTCTTGAAAACTACG	19	3	0	3	9	0	40	0.6158
sgRNA-7	GCGATTCTAATTGCGACTA	19	4	1	6	11	5	40	0.3845
sgRNA-8	TCTTGAAAACTACGGGGTG	19	3	0	5	10	0	45	0.1228
sgRNA-9	ACATGAAGAACCTGTTCAT	19	3	0	5	7	0	35	0.1065

sgRNA-10	TGAACAGGTTCTTCATGTT	19	3	0	3	10	0	35	0.1029
sgRNA-11	TCAGTAAACATCCATGCAA	19	3	0	3	5	0	35	0.0736

(TBP) total number of base pairs, (CBP) number of continuous base pairs, (IBP) number of base pairs of the crRNA sequence in the secondary structure of sgRNA, (TSL) total number of loops, (GSL) number of loops containing crRNA; (% GC) content of GC in the crRNA sequence; (On-score): the score predicts the ability to correctly recognize the target location.

The specificity of CRISPR/Cas9 is dependent on the crRNA sequence (~20 Nu); however, Cas9 can still function even if there are a few mismatches between the target DNA sequence and crRNA [7, 12, 15]. Therefore, the specificity of the two engineered sgRNAs was further analyzed using CCTop software. The analysis showed that one and six sequences in the rice genome were homologous to the crRNA sequence of sgRNA-1 and sgRNA-6, respectively. All these homologs locate in the non-coding region of different gene (Table 2); therefore, they will be less likely to affect the biochemical and physiological processes if CRISPR/Cas9-induced off-target mutations occur. Nevertheless, these potential off-target sites still need to be validated (by sequencing analysis) at a later step in screening the gene-edited rice plants to ensure that there will be no unexpected mutations in the genome [6, 12, 13, 14].

Table 2. DNA sequences homologous to *OsNRAMP7*-TBR-editing crRNAs

Name	crRNA homologous sequences	Coordinates	Distance (bp)*	Gene ID
sgRNA-1	C**C**AT**CT**CT[GTCTCCTT**G**GCA]	-	1868	Os04g0207501
sgRNA-6	TT**TCA**TC[TTGAAAA**T**TACG]	-	31040	Os09g0311600
	T**CC**TCTT[TTGAAAAA**T**ACG]	-	232	Os03g0111200
	TTA**T**TAC[TTGAAAA**T**TACG]	-	1022	Os09g0516300
	T**GT**TCC**C**[TTGAAAAC**A**ACG]	I	261	Os04g0495400
	TTGT**G**T**T**[TTGAAAACTA**T**G]	-	645	Os04g0565200
	TTGT**G**T**T**[TTGAAAACTA**T**G]	-	6624	Os11g0472500

The letters in brackets [] represent sequences homologous to the core region (12 nu) of crRNA; bold letters represent positions that are different from the corresponding nucleotide sites on crRNA; (I) intron; (-): neither exon nor intron.

**Distance to nearest Exon in rice genome.*

Additionally, in this study, the *U6* promoter was used in the sgRNA expression construct (Figure 1), from which transcription necessarily starts from the +1 (G) position

[12]. Thus, two pairs of oligonucleotide were synthesized with a 4-nu sequence complementary to the end of the *U6* promoter and tracrRNA sequences, followed by a G nucleotide at the 5' end and designed crRNA sequence for the next vector construction experiment.

3.4. Design of T-DNA construct and CRISPR-mediated TBR *OsNRAMP7* editing

To design an *OsNRAMP7-TBR*-recognized sgRNA expression construct, the *crRNA1-OsNRAMP7* (containing crRNA of sgRNA-1) and *crRNA2-OsNRAMP7* (containing crRNA of sgRNA-6) DNA fragments were inserted into the pENTR4-V2 vector (Figure 1), which was previously cut by *Btg*ZI and *Bsa*I, respectively (Figure 5 A&B, lane 2). The recombinant plasmid was tested by PCR with primer pairs BsaI-crRNA2-F/pENTR4-R, pENTR4-F/BtgZI-crRNA1-R, respectively; the obtained PCR products were approximately 0.44 kb (Figure 5 C, lane 3) and 0.53 kb (Figure 5 C, lane 6) in sizes, consistent the theoretical calculation of the DNA fragments. This result proves that the recombinant vector (pEN/sgRNA-OsNRAMP7) contains two sequences, *crRNA1-OsNRAMP7* and *crRNA2-OsNRAMP7*, at the desired position.

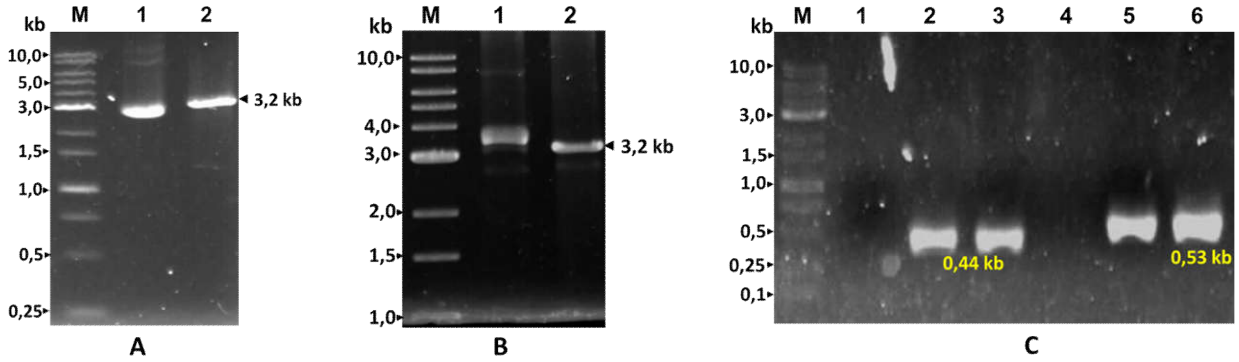

Figure 5. Insertion of *crRNA1-OsNRAMP7* and *crRNA2-OsNRAMP7* into pENTR4-V2

Notes: (A) Digestion of pENTR4-V2 with BtgZI; lane 1: original vector, lane 2: digested vector. (B) Digestion of pENTR4-V2/crRNA1 with BsaI; lane 1: original vector, lane 2: digested vector. (C) Validation of pEN/sgRNA-OsNRAMP7 by PCR; lanes 1-3: primers were BsaI-crRNA2-F/pENTR4-R; lanes 4-6: primers were pENTR4-F/BtgZI-crRNA1-R; lanes 1 & 4: negative control (template was pENTR4-V2); lanes 2 & 5: template was cells transformed ligation products; lanes 3 & 6: template was pEN/sgRNA-OsNRAMP7. Lane M: 1.0 kb DNA ladder (Cleaver Scientific and Thermo Scientific).

Next, to design the plant transformation vector containing the sgRNA expression cassette and the Cas9 gene, sgRNA-OsNRAMP7 from donor vector pEN/sgRNA-OsNRAMP7 was ligated to the destination pCas9 vector using Gateway LR reaction. The recombinant transformation vector was validated by PCR for the presence of sgRNA and *Cas9* expression cassettes with the specific primer pairs (BtgZI-crRNA1-F/BsaI-crRNA2-R, Ubi-F/Cas9-t-R, respectively). The PCR product analysis in Figure 6 (lane 4) shows bands with approximately 0.45 kb (Figure 6, lane 4) and 0.36 kb (Figure 6, lane 8) in size, corresponding with the theoretical size of the amplicons for sgRNA and Cas9. These results revealed that the final vector pCas9/sgRNA-OsNRAMP7 was constructed habouring the complete Cas9 gene (driven by *Ubiquitin* promoter) and TBR *OsNRAMP7*-editing sgRNA expression construct.

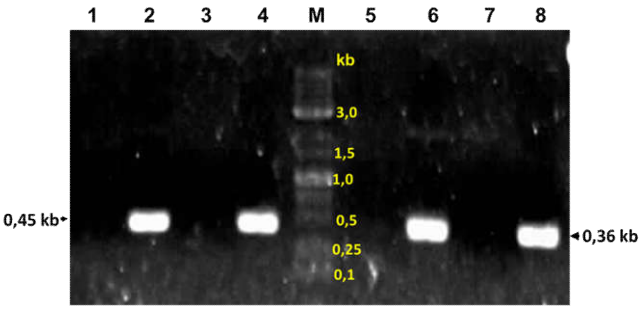

Figure 6. Validation of recombinant vector pCas9/sgRNA-OsNRAMP7

Note: PCR products were electrophoresed on 1% agarose gel. Lanes 1-4: primers was BtgZI-crRNA1-F/BsaI-crRNA2-R; lanes 5-8: primers was Ubi-F/Cas9-t-R; lanes 1 & 5: blank control (no template DNA); lanes 2 & 7: template was pEN/sgRNA-OsNRAMP7; lanes 3 & 6: template was pCas9; lanes 4 and 8: template was pCas9/sgRNA-OsNRAMP7. Lane M: 1.0 kb DNA ladder (Clever Scientifics).

To confirm the expected DNA fragments were correctly inserted into the targeted vector without changes, the recombinant pCas9/sgRNA-OsNRAMP7 vector was sequenced and analyzed using BioEdit 2.0 software (Figure 7). The sequencing analysis showed that two sequences crRNA1-OsNRAMP7 and crRNA2-OsNRAMP7 were accurately inserted between the promoter (*U6.1* and *U6.2*) and the tracrRNA encoding sequence in the sgRNA expressing structure and the complete OsNRAMP7-TBR-editing sgRNA expression construct were ligated into the pCas9 vector.

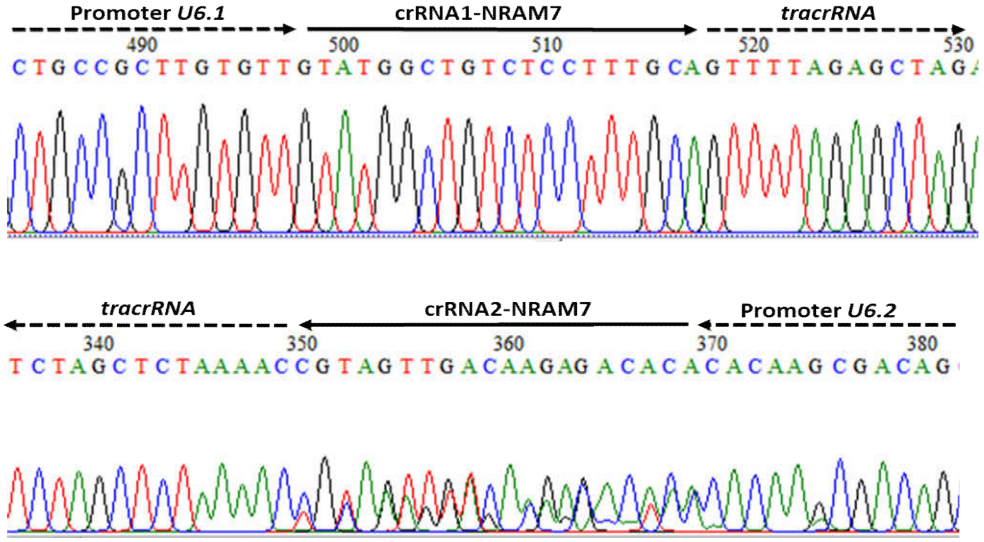

Figure 7. Sequencing pCas9/sgRNA-OsNRAMP7

Note: Part of pCas9/sgRNA-OsNRAMP7 sequencing results. The crRNA sequences are shown by arrows (→), the sequences of promoter U6 and tracrRNA are shown by the broken arrows (⇢).

4. CONCLUSIONS

In this study, the expression of *OsNRAMP7* of rice TBR225 was found to be increased under Zn treatment. Two single guide RNA (sgRNAs) was selected from potential target sites based on exon II sequence of *OsNRAMP7*isolated from rice TBR225 using the bioinformatics tool. The plant transformation vector expressing the OsNRAMP7-TBR editing CRISPR/Cas9 complex was developed for further evaluating *OsNRAMP7* function as Zn or other metal transporters in TBR225 rice variety.

ACKNOWLEDGEMENTS

This study was funded by the Ministry of Science and Technology under the project

"Application of biotechnology to improve micronutrient content of rice varieties" (NĐT/CN/21/24).

REFERENCES

1. Junaid-ur-Rahman S., Chughtai M.F.J., Khaliq A. (2022). Rice: a potential vehicle for micronutrient fortification. *Clin. Phytosci.*, 8: 14.

2. Peris-Peris C., Serra-Cardona A., Sánchez-Sanuy F., Campo S., Ariño J., San Segundo B. (2017). Two NRAMP6 isoforms function as iron and manganese transporters and contribute to disease resistance in rice. *Mol. Plant Microbe. Interact.*, 30(5): 385-398.

3. Xiangjun Z. & Yang Y. (2004). Differential expression of rice Nramp genes in response to pathogen infection, defense signal molecules and metal ions. *Physiol. Mol. Plant Pathol.*, 65: 235–243.

4. Tang L., Mao B., Li Y., Lv Q., Zhang L., Chen C., He H., Wang W., Zeng X., Shao Y., Pan Y., Hu Y., Peng Y., Fu X., Li H., Xia S. & Zhao B. (2017). Knockout of *OsNRAMP5* using the CRISPR/Cas9 system produces low Cd-accumulating indica rice without compromising yield. *Scientific reports*, 7(1): 14438.

5. Chang J., Xie Y., Zhang H., Zhang S. & Zhao F. (2022). The vacuolar transporter OsNRAMP2 mediates Fe remobilization during germination and affects Cd distribution to rice grain. *Research Square*,

6. Li J.F., Norville J.E., Aach J., McCormack M., Zhang D., Bush J., Church G.M. & Sheen J. (2013). Multiplex and homologous recombination-mediated genome editing in *Arabidopsis* and *Nicotiana benthamiana* using guide RNA and Cas9. *Nature biotechnology*, 31(8): 688–691.

7. Bortesi L. & Fischer R. (2015). The CRISPR/Cas9 system for plant genome editing and beyond. *Biotechnology advances*, 33(1): 41-52.

8. Sasaki A., Yamaji N., Yokosho K. & Ma J.F. (2012). NRAMP5 is a major transporter responsible for manganese and cadmium uptake in rice. *The Plant Cell*, 24(5): 2155–2167.

9. Doyle J.J. & Doyle J.L. (1990). Isolation of plant DNA from fresh tissue. *Focus*, 1: 13-15.

10. Zhou X. & Yang Y. (2011). Differential expression of rice *NRAMP* genes in response to pathogen infection, defense signal molecules and metal ions. Physiological and Molecular *Plant Pathology,* 65(5): 235-243.

11. Mani A. & Sankaranarayanan K. (2018). In silico analysis of natural resistance-associated macrophage protein (NRAMP) family of transporters in rice. *The Protein journal*, 37(3): 237–247.

12. Liang G., Zhang H., Lou D. & Yu D. (2016). Selection of highly efficient sgRNAs for CRISPR/Cas9-based plant genome editing. *Scientific reports*, 6: 21451.

13. Doench J.G., Fusi N., Sullender M., Hegde M., Vaimberg E.W., Donovan K.F., Smith I., Tothova Z., Wilen C., Orchard R., Virgin H.W., Listgarten J. & Root D.E. (2016). Optimized sgRNA design to maximize activity and minimize off-target effects of CRISPR-Cas9. *Nature biotechnology*, 34(2): 184–191.

14. Fu Y., Sander J.D., Reyon D., Cascio V.M. & Joung J.K. (2014). Improving CRISPR-Cas nuclease specificity using truncated guide RNAs. *Nature biotechnology*, 32(3): 279–284.

15. Bae S., Park J. & Kim J.S. (2014). Cas-OFFinder: a fast and versatile algorithm that searches for potential off-target sites of Cas9 RNA-guided endonucleases. *Bioinformatics*, 30(10): 1473-1475.

BREEDING THIRTEEN MUTANT LINES FROM DX208 MUNGBEAN (*Vigna radiata*) WITH SYNCHRONY IN POD MATURITY BY DNA MARKER

Truong Trong Ngon[1,*], Tran Thi Thanh Thuy[2]

ABSTRACT

Mungbean yield is affected by many biological and abiotic factors, in which the blooming flowers and asynchronous in pods are the main causes. The fastest way to improve mungbean yield is to use genotypes available through Ethyl Methane Sulphonate (EMS) mutations and in combination with molecular markers (SSRs and SNPs). The project was implemented in the spring-winter crop of 2019-2020, at the Experimental Farm of Can Tho University and Phu Sa Biochemistry Company to select 1 to 2 mutant lines in M_6 with short days, high yield and synchronous maturity. Thirteen lines of mutant mungbeans in M_6 and DX208 varieties (control varieties) were tested for yield. Set up a randomized block, 1 factor, 3 replicates, spacing of 45x20 cm, the density of 22 plants/m^2, 9 m^2 per plot, applying 60N-60P_2O_5-40K_2O fertilizer. At the same time, the purity of genotypes of 1,000 seedlings and flowering dates of these 13 mutant mungbean lines and parent varieties (DX208) were determined by SSR and the sequences of the three lines of DX6-5-1- 10, DX6-6-28-14, DX8-1-28-8B in M_6 and DX208 with SNPs. The results showed that 4 lines of DX8-1-28-8B, DX6-5-1-10, DX4A-3-3-1, DX2-1-26-5 have yield of 2.99 to 3.29 tons/ha, which is higher than that of the control variety (DX208) (2.60 tons/ha) ($p<0.01$). All 13 mutant lines had short maturity (61-64 days), and synchrony in pod maturity; 13 DX208 mutant lines in the M_6 population were homozygous genotypes in 1.000 seed weight as well as flowering day, the genotype between these mutant lines compared to the DX208 variety (origin variety) and the genotype between the mutant lines have changed; Genetic sequences related to genes of 1,000 seed weight between the three lines of DX6-5-1-10, DX6-6-28-14, DX8-1-28-8B and the original variety are different, line DX6-6-28-14 was identified as the most genetic difference compared to the DX208 variety.

Keywords: *Ethyl Methane Sulphonate (EMS), mungbean, mutation, polymorphism, synchronous maturity.*

Received: 6 June 2022; revised: 11 July 2022; accepted: 22 November 2022.

1. INTRODUCTION

Mungbean (*Vigna radiata* (L.) Wilczek) is one crop with high nutritional value. Mungbean seed contains 60.4% carbohydrate, 24.2% protein, 1.3% lipid, 118 mg canxi (Ca) and 340 mg phosphorus (P) per 100 g of seed [1]. Mungbean plants have the ability to fix nitrogen in the air. Roots can improve soil fertility and limit erosion. It plays an important role in models of crop rotation. With the advantages of a short life cycle, low water demand, good drought tolerance and wide adaptability, the mungbean is considered as a

[1] Biotechnology Research & Development Institute - Can Tho

[2] College of Agriculture - Can Tho University

* Corresponding author: ttngon@ctu.edu.vn

potential crop and well adapted to severe global climate change. Despite efforts to improve mungbean varieties, the mungbean yield is still low in the Mekong delta, averaging about 1.1 tons/ha. Except for soil factors, climate and cultural practices of growers, local varieties are used to grow everywhere, and flower bloom sporadically leading to inconsistent development pods and not synchronized maturity is the main reason for low yield [2], [3]. According to the orientation of the Ministry of Agriculture and Rural Development, by 2020 [4], our country strives to achieve an area of one million hectares of legume group and breed mungbean variety with 1.5-2.5 tons/ha, short maturity, synchronized maturity and less infected pests and diseases meeting rotation, increasing crops. Therefore, in order to make a new mungbean variety with these characteristics in a short time, the fastest way to carry out breeding is with the combination of the induced mutation method and the molecular marker method (SSR and SNP marker). Currently, mutagenesis is considered as a way of providing genetic resources in plant breeding. Of which, using mutant agent like Ethyl Methane Sulphonate (EMS) is high effective in new plant breeding with high yield, good quality, resistance to pests and diseases, and tolerance to adverse environmental conditions [5], [6], [7]. When a mutation occurs, some mutants can be observed by phenotype. However, some mutants do not express themselves due to degenerate codons. To detect these mutants, a gene is sequenced also known as the Single Nucleotide Polymorphism (SNP) marker. In addition, to quickly direct the desired genotype as well as check whether the genotype under study is pure or not; even though certain mutants in M_2 or M_3 generation, Single Sequence Repeat (SSR) marker can be used. As the property of this marker is codominant, it can detect homozygous or heterozygous loci quickly and exactly [8]. From the above points, this experiment was carried out to select from 2 to 4 mungbean mutant lines with stable and high yield, synchronized pod maturity. New mutants can be used to enlarge the cultivated areas for mungbean in the Mekong delta.

2. MATERIALS AND METHODS

2.1. Materials

DX208 variety and 13 mutant lines in M_6 generation were grown at an experimental farm, Can Tho University from April 2020 to December 2021. The list of these varieties/lines is presented in table 1.

Table 1. Fourteen mungbean lines/varieties were used in the experiment

No.	Line/variety name	Source	No.	Line/variety name	Source
1	DX208 (Control)	AVRDC	8	DX4A-3-5-6	AVRDC
2	DX2-1-26-5	Can Tho University	9	DX6-5-1-10	Can Tho University
3	DX2-1-26-6	Can Tho University	10	DX6-6-28-14	Can Tho University
4	DX2A-6-3-1	Can Tho University	11	DX8-1-28-8A	Can Tho University
5	DX4-6-1-1	Can Tho University	12	DX8-1-28-8B	Can Tho University

6	DX4A-3-3-1	Can Tho University	13	DX8-5-1-3	Can Tho University
7	DX4A-3-32-1	Can Tho University	14	DX8A-5-18-2	Can Tho University

The chemical agents in this experiment were purchased from Sigma-Aldrich, Merck, NEXpro, Korea. Seventeen SSR primers were bought from Phu Sa Biochemistry company table 2.

Table 2. Seventeen SSR primers, PCR product size and Linkage groups

No.	Primer name	Sequences 5' - 3'		Size	Linkage groups
1	CEDAAG002	F: GCAGCAACGCACAGTTTCATGG	R: GCAAAACTTTTCACCGGTACGACC	140-170	2
2	CEDG014	F: GCTTGCATCACCCATGATTC	R: AAGTGATACGGTCTGGTTCC	152-158	5
3	CEDG026	F: TCAGCAATCACTCATGTGGG	R: TGGGACAAACCTCATGGTTG	142	2
4	CEDG030	F: TGAGGGAATGGGAGAGAGGC	R: TCCGCAGATAGAGGCTCACG	105	8
5	CEDG037	F: GAAGAAGAACCCTACCACAG	R: CACCAAAAACGTTCCCTCAG	160-170	6
6	CEDG088	F: TCTTGTCATTTAGCACTTAGCACG	R: TTGTTGTTTACTAAGAGCCCGTGT	119	4
7	CEDG198	F: CAAGGAAGATGGAGAGAATC	R: CCTTCTAAGAACAGTGACATG	227	10
8	CEDG232	F: GATGACCAAGGTAACGTG	R: GGACAGATCCAAAACGTG	200	4
9	DMBSSR160	F: GGTGGATCAAATCCATTTTAGG	R: ACAGATCACATAGCAACCAAACA	-	2A
10	DMBSSR167	F: TGGGACTCAAACCACACTTTC	R: GAACTATGAAGGTTTCACAGAAATCA	-	4
11	MBSSR039	F: GAAAAATTACCCTTTCAAGCAG	R: TTGGTTGTTACTGAGGGAAG	197	5
12	MBSSR087	F: TCCCTTGTGGGAGATCCT	R: CTTTGCCACACTCCTTGC	-	2A
13	VM37	F: TGTCCGCGTTCTATAAATCAGC	R: CGAGGATGAAGTAACAGATGATC	270	8
14	VR095	F: GAAATGGGAGTTCAAAGAGGAA	R: TGGAGAAGTCTGGAAGAGAACC	115-121	6
15	VR293	F: GTGGCTCACAAGGTAGTGCTAA	R: GAGAGAAACAACCAACCAAAGG	222-225	10
16	VR304	F: GAAGCGAAGAAGCCATAGAAAA	R: CCTCACACACAACACAACAGAA	170-188	11
17	VRSSR035	F: CCAATGAAACCAAAGGTCCA	R: GGGGAGAGGGGTAAGTGTGT	-	4

2.2. Methods

13 lines of mungbean mutants at M_6 generation were selected from induced mutant populations at four levels of 0.2; 0.4, 0.6, and 0.8% of EMS on the DX208 variety. After treating EMS, single seed descent (SSD) was carried out in the M_1 and M_2 generations. In M_3 generation, the desired phenotype was selected for mutant lines. Selected mutants were multiplied in the M_4 generation. The mutant lines were compared with the origin cultivar in agronomical traits, and desired lines were selected. Pod maturity and yield of promising mutant lines were tested as compared to DX208 (commonly cultivated cultivar) until M_6, generation.

2.3. Yield test for 13 mungbean mutant lines

This experiment was carried out at Campus 2 experimental farm, Can Tho University in Winter-Spring crop 2019-2020. The experimental design was a Randomized Complete Block Design (RCBD) with three replications and one factor including fourteen treatments. In which DX208 was chosen as the control variety and thirteen mungbean mutant lines in M_6 generation. The area of one plot was 14.4 m^2 (3.2 x 4.5 m); the sowing distance was 45 x 20 cm, with 2 plants/hole, and a density of 22 plants/m^2. Fertilizer was applied by the following formula 60N-60P_2O_5-40K_2O. Traits involve flowering time (days), maturity (day), plant height at R1 and R8 stages (cm), number of branches, number of pods/plant, pod length (cm), number of seeds/pod, 1.000 seed weight (g) and seed yield (tons/ha) were recorded. The evaluation of traits was observed and measured based on the descriptions of IBPGR, (1980) [9] and the Vietnamese standard of QCVN 01-62: 2011/BNNPTNN (2011) [10]. The classification of pod maturity type was evaluated based on the method of Mondal *et al.* (2011) [11]. SPSS 21.0 software was used for the Analysis of Variation (ANOVA) and the Duncan test for treatment means.

2.4. Molecular marker method

DNA extraction and purification: young leaves of mungbean plants in the M_6 population were collected to extract and purify DNA based on CTAB [12].

DNA test by gel agarose electrophoresis: DNA was extracted and then tested by electrophoresis on gel agarose 0.8% (w/v). Samples with DNA high quality were used for PCR.

Pure line test and evaluation of genetic difference by SSR marker

There are seventeen primers of SSR were used for amplifying DNA. The sequence of 17 primers was presented in table 2. PCR for SSR marker was carried out on GenAmp PCR system 2700 with steps such as following: 5 minutes at 95°C, then 35 cycles involving 30 seconds at 95°C, 30 seconds next depending on the annealing temperature of each primer so that it was adjusted accordingly on the machine, 72°C in 30 seconds, 72°C in 5 minutes. PCR products were stored at 10°C for 20 min. PCR products were carried out on polyacrylamide 12% gel, in TBE 0.5X solution by electrophoresis machine with 24 V in 60 minutes. Gel was dyed with ethidium bromide (10 mg/l) for 15 to 20 minutes. The gel was washed with distilled water for 5 minutes, then the gel was taken by the photo machine under UV. The presence of loci was amplified on the gel will be shown polymorphism or monomorphism of mungbean cultivars/lines used in this experiment. GenAlEx 6.5 software was used to analyze the database of SSR markers, and the UPGMA method was applied

to estimate genetic distance among mungbean mutant lines.

PCR and determination of gene sequences

Design primer of "VrSrThr" for discovering Single Nucleotide Polymorphisms

Two sequences of gene "*Ca_04364*" and "*Ca_04607*" encoding for 1000 seed weight of chickpea [13] were used and then blast based on the database of mungbean genome (https://legumeinfo.org/blast/nucleotide/nucleotide) for finding out similarity sequence. The results found a similar sequence on the 8th chromosome in VC1973A variety *(Vigna radiata)* NC_028358.1. Then, Primer3 software was used to design primers of *VrSrThr*. The forward primer sequence is 5'-TGGGC TTCATAAGGGCAAGG-3', and the Reverse primer sequence is 5'-AAGGAGGGAGATCC CCGAAA-3'. PCR was conducted with a total volume of 50 µl. Forward and reverse primers were used to amplify the region of 1,000 seed weights in 4 mungbean varieties/lines. PCR products were carried out on gel electrophoresis, then purified by Wizard SV kit and PCR Clean-up System (Promega). *VrSrThr* gene of mungbean varieties/lines was sequenced by ABI 3130 machine, USA. Gene sequence encoding 1,000 seed weight was analyzed by BioEdit 7.2 software.

3. RESULTS

3.1. Flowering time and maturity

Figure 1. Synchronized pod maturity of DX4A-3-3-1 line (A) and partial-synchronized pod maturity of DX208 (B)

The time from sowing to the flowering of mungbean varieties/lines was short, about 35-37 days (** $p<0.01$) presented in table 3. The flowering time of those varieties is relatively concentrated. Most varieties/lines bloomed from the 6th day to the 10th day and finished from the 11th day to the 15th day from the first flowering. Maturity of fourteen mungbean varieties/lines varied from 60 to 64 days (** $p<0.01$). Mungbean varieties are short maturity, so they are always favoured, because they are suitable for many models of intensive farming in the Mekong delta. This is also the first objective of our crop improvement program. All mungbean mutant lines are in M_6 generation, sown in the Winter-Spring crop 2015-2016 and had synchronized pod maturity. The percentage of pod maturity in the first harvest of thirteen mutant lines ranged from 94.7 to 100.0% (>90% pod maturity: synchronize; from 80-90% pod maturity: partial-synchronize; <80% pod maturity: unsynchronized). DX208 has partially synchronized pod maturity (Table 3). Synchronized pod maturity variety is always paid attention, due to shortening harvest time, decreased yield loss and cultivation cost. In addition, synchronized pod maturity is the

first condition for breeding new mungbean varieties adapted to machine-based harvest. With the aim of breeding for synchronized pod maturity mungbean variety, so 13 mutant lines had few branches, ranging from 0.3-1 branch, this is similar to previous studies of Mondal *et al.* (2011) [11] the genotype of mungbean synchronized pod maturity has only the main stem or few branches.

Table 3. Growth and agronomic traits, ration of pod maturity of 14 varieties/line in Winter-Spring Crop in 2019-2020 (MeansOSD)

No	Varieties/ lines	Flowering time (day)	Maturity (day)	Ratio of Pod maturity (%)	Classification	Number of branches	Plant height (cm)
1	DX208 (ĐC)	36.0±0.00^{bc}	62.3±1.15^{abc}	88.2	Partial synchronise	0.6±0.08^{bcd}	69.9±0.52^{c-f}
2	DX2-1-26-5	35.3±0.58^{cd}	61.0±0.00^{bcd}	95.4	synchronize	0.6±0.06^{a-d}	69.6±3.97^{def}
3	DX2-1-26-6	35.3±0.58^{cd}	62.3±1.15^{abc}	98.3	synchronize	0.8±0.12^{abc}	73.8±3.07^{abc}
4	DX2A-6-3-1	36.3±1.15^{ab}	63.7±0.58^{a}	95.1	synchronize	1.1±0.15^{a}	72.4±1.96^{a-e}
5	DX4-6-1-1	35.0±0.00^{d}	62.7±1.53^{ab}	99.1	synchronize	0.5±0.11^{cd}	65.9±2.00^{f}
6	DX4A-3-3-1	37.0±0.00^{a}	60.7±1.15^{cd}	95.1	synchronize	0.7±0.02^{a-d}	73.4±2.82^{a-d}
7	DX4A-3-32-1	37.2±0.29^{a}	60.0±0.00^{d}	100.0	synchronize	0.7±0.08^{a-d}	68.8±1.29^{ef}
8	DX4A-3-5-6	37.0±0.00^{a}	62.0±0.00^{bc}	95.2	synchronize	0.3±0.14^{d}	75.2±1.02^{a}
9	DX6-5-1-10	35.0±0.00^{d}	61.7±1.15^{bc}	99.5	synchronize	0.9±0.06^{abc}	74.2±0.35^{ab}
10	DX6-6-28-14	35.3±0.58^{cd}	61.0±0.00^{bcd}	98.8	synchronize	0.8±0.03^{abc}	67.2±1.06^{f}
11	DX8-1-28-8A	37.0±0.00^{a}	62.0±0.00^{bc}	97.4	synchronize	0.8±0.08^{abc}	72.1±3.33^{a-e}
12	DX8-1-28-8B	37.0±0.00^{a}	62.0±0.00^{bc}	100.0	synchronize	1.0±0.11^{ab}	69.4±3.96^{def}
13	DX8-5-1-3	35.7±0.58^{bcd}	62.7±0.58^{ab}	94.7	synchronize	0.6±0.05^{a-d}	67.3±1.89^{f}
14	DX8A-5-18-2	37.0±0.00^{a}	61.3±1.15^{bcd}	98.9	synchronize	0.9±0.06^{abc}	70.1±0.09^{b-f}
F test		**	**			*	**
CV (%)		1.25	1.38			6.53	3.10

Remarks: In the same column, any treatment means having the same letter are not significantly different at 5% by Duncan test; (**): significance at 1% level; (*): significance at 5% level; ns: no significance; SD: standard deviation

3.2. Yield components and yield

Table 4 showed that 4 mungbean mutant lines such as DX8-1-28-8B, DX6-5-1-10, DX4A-3-3-1, DX2-1-26-5 with yield from 2.99 to 3.29 tons/ha) higher than the yield of DX208 (control variety) (2.6 tons/ha). The yield of 4 lines is high, due to many pods/plant and heavy sustained 1000 seed weight. In addition, four of these lines had main characteristics such as higher maturity height of the main stem (69.4-74.2 cm), flowering time about 35-37 days after sowing, maturity varied from 61 to 63 days, and uniform population.

Table 4. Yield components & yield of 14 varieties/lines in M_6, Winter-Spring crop 2019-2020 (Means ± SD)

No.	Cultivar/lines	Number of pods/plant	Pod length (cm)	Number of seeds/pod (seed)	1,000 seed weight (g)	Yield (tons/ha)
1	DX208 (ĐC)	19.6±1.29^{ef}	10.5±0.26^{b}	11.0±0.69	77.7±3.12^{abc}	2.60±0.09^{fgh}
2	DX2-1-26-5	21.9±0.78^{bc}	10.6±0.43^{b}	11.7±0.22	74.8±1.70^{bcd}	2.99±0.28^{bcd}
3	DX2-1-26-6	22.3±0.81^{bc}	10.7±0.25^{b}	11.4±0.35	76.6±0.72^{a-d}	2.59±0.11^{fgh}
4	DX2A-6-3-1	22.9±0.82^{ab}	10.9±0.12^{b}	11.4±0.34	77.0±0.69^{a-d}	2.40±0.14^{h}
5	DX4-6-1-1	20.9±0.92^{cde}	10.5±0.28^{b}	11.1±0.09	81.2±6.02^{a}	2.84±0.13^{c-f}
6	DX4A-3-3-1	21.1±0.70^{cde}	10.7±0.43^{b}	12.3±2.52	76.1±4.41^{a-d}	3.08±0.01^{abc}
7	DX4A-3-32-1	20.4±0.40^{def}	10.5±0.37^{b}	11.6±0.21	71.56±1.69^{d}	2.68±0.11^{e-h}
8	DX4A-3-5-6	19.3±1.01^{f}	9.5±0.21^{c}	11.7±0.35	59.90±3.36^{e}	2.44±0.27^{gh}
9	DX6-5-1-10	23.8±0.70^{a}	11.9±1.67^{a}	11.3±0.16	75.6±3.17^{a-d}	3.16±0.13^{ab}
10	DX6-6-28-14	24.0±0.90^{a}	10.8±0.22^{b}	11.4±0.39	79.1±1.16^{abc}	2.82±0.21^{c-f}
11	DX8-1-28-8A	19.3±0.35^{f}	10.8±0.18^{b}	11.0±0.92	78.4±0.42^{abc}	2.71±0.10^{d-g}
12	DX8-1-28-8B	22.9±0.55^{cde}	10.5±0.41^{b}	11.5±0.13	75.5±2.35^{a-d}	3.29±0.06^{a}
13	DX8-5-1-3	21.4±0.21^{bcd}	10.7±0.14^{b}	11.3±0.07	79.5±5.23^{ab}	2.71±0.15^{d-g}
14	DX8A-5-18-2	20.8±0.89^{cde}	10.4±0.38^{bc}	11.0±0.46	73.2±2.63^{cd}	2.94±0.16^{b-e}

F test	**	*	ns	**	**
CV (%)	3.75	4.77	6.79	4.04	5.73

Remarks: In the same column, any treatment means having the same letter are not significantly different at 5% level by Duncan test, (**): significant at 1% level; (*): significant at 5% level; (ns): no significance; SD: Standard deviation

Homozygous test for thirteen mungbean mutant lines in M_6 generation and DX208

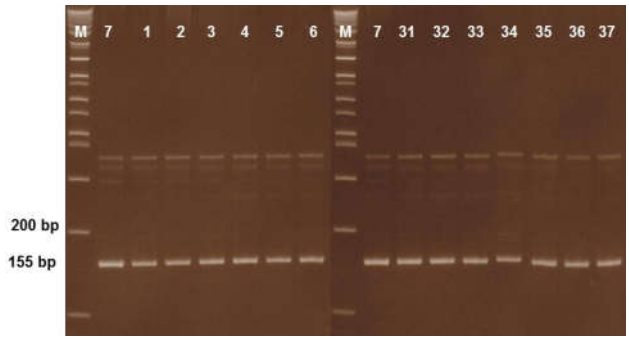

Figure 2. PCR product electrophoresis of 13 mungbean mutant lines and DX208 with VRSSR035 primer

Remarks: M: 1 kb plus ladder; 7: DX208 (Control); 1: DX4A-3-3-1; 2: DX4-6-1-1; 3: DX6-5-1-10; 4: DX6-6-28-14; 5: DX8A-5-18-2; 6: DX8-1-28-8B; 31: DX2A-6-3-1; 32: DX2-1-26-5; 33: DX2-1-26-6; 34: DX4A-3-32-1; 35: DX4A-3-5-6; 36: DX8-1-28-8; 37: DX8-5-1-3

17 primers of SSR related to 1,000 seed weight and flowering date were used to test homozygosity as well as polymorphism of 13 mungbean mutant lines and DX208 (origin variety). The result of gel electrophoresis showed that all varieties/lines are homozygous (Figure 2), due to one amplified band. That means all mutant lines are pure lines in the M_6 generation.

Genetic difference evaluation of 12 mungbean mutant lines

After PCR product electrophoresis, SSR database of 17 primers was analyzed by GenAlEx 6.5 software with UPGMA method, and estimated Nei distance.

Table 5. Nei distance among mungbean mutant lines in M6 generation and DX208 variety

7	1	2	3	4	5	6	31	32	33	34	35	37	
0													**7**
32	0												1
48	28	0											2
36	28	28	0										3
44	40	56	40	0									4
52	48	56	40	24	0								5
64	56	40	48	48	40	0							6
36	36	48	40	40	44	64	0						31

36	36	36	40	52	60	56	28	0					32
48	52	52	52	52	56	56	36	32	0				33
48	60	64	56	56	60	64	40	40	20	0			34
36	44	48	52	52	56	64	40	52	52	48	0		35
36	44	52	48	48	52	64	36	44	36	32	36	0	37

Remarks: 1: DX4A-3-3-1; 2: DX4-6-1-1; 3: DX6-5-1-10; 4: DX6-6-28-14; 5: DX8A-5-18-2; 6: DX8-1-28-8B; 7: DX208; 31: DX2A-6-3-1; 32: DX2-1-26-5; 33: DX2-1-26-6; 34: DX4A-3-32-1; 35: DX4A-3-5-6; 37: DX8-5-1-3

Analysis of genetic distance among mungbean mutant lines, the result showed that these lines are far distance from DX208 (origin variety) at 17 loci. There is a genetic difference as well as genetic distance among mutant lines. The genetic difference is so large ranging from 20 to 64, which the DX8-1-28-8B line has the furthest genetic distance from DX208. This result demonstrates that there is success in making good variation material sources to meet the needs for breeding and variety improvement in the future.

Gene sequences

To identify genetic variation with the difference of nucleotides among mutant lines with DX208 (origin variety), 3 lines of DX6-5-1-10, DX6-6-28-14, DX8-1-28-8B in M_6 generation and DX208 variety were selected to determine nucleotide sequence related to 1,000 seed weight. The result showed that the gene length of 4 mungbean varieties/lines is 1.299 nucleotides. However, the variation level of nucleotide performed clearly in gene fragments of 900 nucleotides. Table 6 showed that among 3 mungbean mutant lines having nucleotide variation and different from DX208 (origin variety), the DX6-6-28-14 line has a value of 3,415 most difference compared with DX208. Besides, there is also showing a difference of nucleotide among the 3 mutant lines in this gene fragment (Table 6).

Table 6. Nucleotide difference of 3 promising mungbean mutant lines as compared with DX208

	DX6-5-1-10	DX6-6-28-14	DX8-1-28-8B	DX208 (Control)
DX6-5-1-10	0			
DX6-6-28-14	3.145	0		
DX8-1-28-8B	3.023	0.113	0	
DX208 (Control)	2.882	3.415	3.124	0

The nucleotide difference of 1,000 seed weight gene has Pi = 0.618 and The value at one site is 0.708 ± 0.269, the nucleotide variation occurs clearly from 400th to 750th position and non-crossing-over.

There are 7 substitution positions on the fragment of a gene from 420 to 440 nucleotide of 3 mungbean mutant lines and DX208 variety (origin variety). 2 mutants had the same substitution group from A → G at the nucleotide of 420 of DX6-5-1-10 and DX6-6-28-14 as compared with DX208. There are 2 mutant lines with substitution different group from G -→ T at the 425th nucleotide position, these lines are DX6-5-1-10 and DX8-1-28-8B lines, from G→C of DX6-5-1-10 and DX8-1-28-8B lines at nucleotide position of 428, from C→A of DX6-5-1-10 and DX8-1-28-8B lines at 430th nucleotide position, besides, DX6-6-28-14 and DX8-1-28-8B lines at the 431th nucleotide position, from G→T of DX6-5-1-10 and DX6-6-28-14 lines at 435th nucleotide position and from T→G of DX6-6-28-14 and DX8-1-28-8B lines (Figure 3).

	420					425					430					435					440
ĐX6-5-1-10	G	T	G	A	A	T	C	C	C	C	A	C	C	C	C	T	C	C	C	T	T
ĐX6-6-28-14	G	A	T	G	G	G	T	G	G	C	C	A	A	G	G	T	G	G	T	T	G
ĐX8-1-28-8B	A	T	G	G	G	T	G	G	C	C	A	A	G	G	T	G	G	T	T	G	G
ĐX208 (ĐC)	A	G	A	T	G	G	G	T	G	G	C	C	A	A	G	G	T	G	G	T	T

Figure 3. Gene sequences from 420 to 440 nucleotide positions of three mutant lines and DX208

4. CONCLUSIONS

The 4 mungbean lines DX8-1-28-8B, DX6-5-1-10, DX4A-3-3-1 and DX2-1-26-5 had good yield components and higher yield than DX208 (control variety). 13 mungbean mutant lines in the M_6 generation are homozygous genotypes of 1000 seed weight, and all are quite different as compared with DX208 (origin variety). The DX8-1-28-8B line has the furthest genetic distance from the DX208 variety. The sequences for the 1000 seed weight gene of three mungbean mutant lines as DX6-5-1-10, DX6-6-28-14, DX8-1-28-8B in M_6 generation were quite different and also different from the gene sequence of the DX208 variety (origin control). The DX6-6-28-14 line has the furthest genetic difference as compared to DX208 (origin variety). These promising lines have been released to growers so that they can cultivate new lines contributing to increasing their income.

REFERENCES

1. Imran, H. I., Khattak I., Ahamd, A.U., Zada, F.H. and Naveed, S. (2015). Roots nodulation, yield and yield contributing parameters of mungbean cultivars as influenced by different Phosphorous level in Swat-Pakistan. *Pure & Applied Biology* 4: 557–567.

2. Bushby, H. and Lawn R. (1992). Accumulation and partitioning of nitrogen and dry matter by contrasting genotypes of mungbean *Vigna radiata* (L.) Wilczek. *Australian Journal of Agricultural Research* 43: 1609-1628.

3. Egli, D. and Bruening, W. (2006). Fruit development and reproductive survival in soybean: Position and age effects. *Field Crops Research* 98: 195-202.

4. Ministry of Agriculture and Rural Development. (2020). *Result of mid term rural and agricultural survey*. Statistical Publishing House

5. Kozgar, M.I., Goyal, S. and Khan, S. (2011). EMS induced mutational variability in *Vigna radiata* and *V. mungo*. *Research Journal Botany* 6: 31-37.

6. Wattoo, J. I., Aslam, K., Shah, S. M., Shabir, G., Sabar, M. and Naveed, S. A. (2012). Ethyl methanesulphonate (EMS) induced mutagenic attempts to create genetic variability in Basmati rice. *Journal of Plant Breeding and Crop Science* 4, 101-105.

7. Bhosale, U.P., Hallale, B.V. and Dubhashi, S.V. (2013). M_1 generation studies in urdbean *Vigna mungo* (L.) Hepper Advances. *Applied Science Research* 4: 95-97.

8. Shehata, A.I., Al-Ghethar, H. A. and Al-Homaidan, A. A. (2009). Application of simple sequence repeat (SSR) markers for molecular diversity and heterozygosity analysis in maize inbred lines. *Saudi Journal of Biological Sciences* (16): 57-62.

9. IBPGR Executive Secretariat (1980). Descriptors for mungbean.

10. QCVN 01-62: 2011/BNNPTNT (2011), National technical standard regulation on testing for cultivation and use of mungbean varieties.

11. Mondal, M.M.A., Solaiman, M.D., Fakir, F., Abdul, S.J., Hakim, M.A., Islam, M. M. and Shamsuddoha, A. T. M. (2011). Effects of flowering behavior and pod maturity synchrony on yield of mungbean (*Vigna radiata* (L.) Wilczek). *Australian Journal of Crop Science* 5 (8): 945-953.

12. Doyle, J.J. and Doyle, J.L. (1990). Isolation of plant DNA from fresh tissue. *Focus* 12: 13-15.

13. Singh, V. K., Khan, A W., Jaganathan, D., Thudi, M., Roorkiwal, M., Takagi, H., Garg, V., Kumar, V., Chitikineni, A., Gaur, P. M., Sutton, T., Terauchi, R. and Varshney, R. K. (2016). QTL-seq for rapid identification of candidate genes for 100-seed weight and root/total plant dry weight ratio under rainfed conditions in chickpea. *Plant Biotechnol Journal* 14: 2110–2119.

PHENOTYPIC VARIATION AND CORRELATION OF FRUIT TRAITS IN DIVERSE MUSKMELON MATERIALS

Nguyen Trung Duc [1,*], Pham Quang Tuan[1], Nguyen Thi Nguyet Anh[1], Vu Van Liet[1]

ABSTRACT

Understanding the phenotypic variation, correlation, and identification of important agronomic traits will speed up the selection efficiency of elite melon materials for nutritious hybrid melon breeding in Vietnam. This study utilized three approaches *viz.*, correlation analysis, principal component analysis, and cluster analysis methods to investigate the primary and secondary relationships of the main agronomic traits affecting the yield and quality of 20 muskmelon materials originated from Taiwan-China, India, Thailand, and Japan in the Spring and Autumn season 2021 in Gia Lam, Ha Noi. The results showed that the highest significant positive correlation at $p < 0.001$ was observed between fruit weight (FW) and fruit length (FL) (0.744***), fruit diameter (FD) (0.716***) and fruit thickness (FT) (0.527***). A total of ten quantitative traits could be reduced to just four components, which could explain more than 90% of the total variation. The first four traits *viz.*, FW, FL, FD, and FT contributed more than 90% of their cumulative contribution, these principal component values representing genetic characteristics of eight agronomic traits. Hierarchical clustering based on principal component analysis showed that 20 muskmelon materials were divided into three distinct groups in the Spring season and four distinct groups in the Autumn season. To the best of our knowledge, this is the first report on applying dimension reduction methods to investigate phenotypic variability in muskmelon materials in Vietnam.

Keywords: *Muskmelon, variability, correlation, principal component analysis, cluster analysis.*

Received: 18 August 2022; revised: 12 September 2022; accepted: 21 November 2022.

1. INTRODUCTION

With sweetness, delicious, and nutritious, muskmelon (*Cucumis melo* L.) is widely grown around the world [1]. In Vietnam, with great economic potential, muskmelon has been cultivated in high-tech greenhouses and polyhouses with an area constantly increasing throughout the country. However, apart from some muskmelon varieties such as TL3, King KN, Queen KN, most of the high-quality cantaloupe varieties are imported from Thailand, Taiwan, and Japan. This poses a challenge to the selection and breeding of domestic melon varieties, it is necessary to develop domestic melon varieties soon to help agricultural production have more choices and actively produce seeds. As a result of high growth vigor, uniform fruit size and shape, and high yield with suitable quality, all muskmelon growth in Vietnam were hybrid varieties. The fundamentals in hybrid muskmelon breeding were the collection, screening, classification, development, and selection of muskmelon inbred lines. Melons have been bred and grown in nearly all of the warmer regions of the world, leading to the wide diversity of phenotypic traits, especially

[1] Vietnam National University of Agriculture, Ha Noi, Vietnam
* Corresponding author: ntduc@vnua.edu.vn

in terms of fruit traits such as size, shape, rink thickness, flesh thickness, sugar content, acidity, texture and aroma [2, 3, 4]. This wide variety is a source for ongoing breeding and genetic research aimed at mapping QTLs and identifying genes that influence key horticultural traits and consumer needs [5, 6, 7]. Many genetic studies using diverse collections or isolated populations have focused on fruit quality traits in melons, including fruit size and shape [8].

Phenotypic evaluation is an important method for selecting pure melon lines. Keeping observed of all phenotypic traits across a large breeding population is a challenge for breeders. The principal component analysis is an effective analytical method to extract important information from highly correlated phenotypic complex traits while retaining the original information [9, 10]. Principal component analysis and cluster analysis are believed to be effective in multidimensional data processing, helping to get the best approximation of the dataset from which to draw important results in agricultural research [10]. Understanding the correlation and identification of important agronomic traits improves selection efficiency and more accurately identifies promising melon lines for target breeding programs.

This study applied principal component analysis and cluster analysis to investigate the primary and secondary relationships of the main agronomic traits affecting yield and quality and phenotypic diversity of 20 muskmelon materials in the Spring and Autumn season 2021 in Gia Lam, Ha Noi. The result of this study provided valuable information for muskmelon pre-breeding in Vietnam.

2. MATERIALS AND METHODS

2.1. Plant materials

Plant materials included 19 muskmelon materials *viz.*, ML01, ML02, ML03, ML04, ML05, ML06 originated from Taiwan, China; ML07, ML08, ML09, ML10, ML11 originated from India; ML12, ML13, ML14, ML15 originated from Thailand; and ML16, ML17, ML18, ML19 originated from Japan, with check variety TL3 (Chanh Phong Agriculture Co., Ltd distributed).

2.2. Experimental design

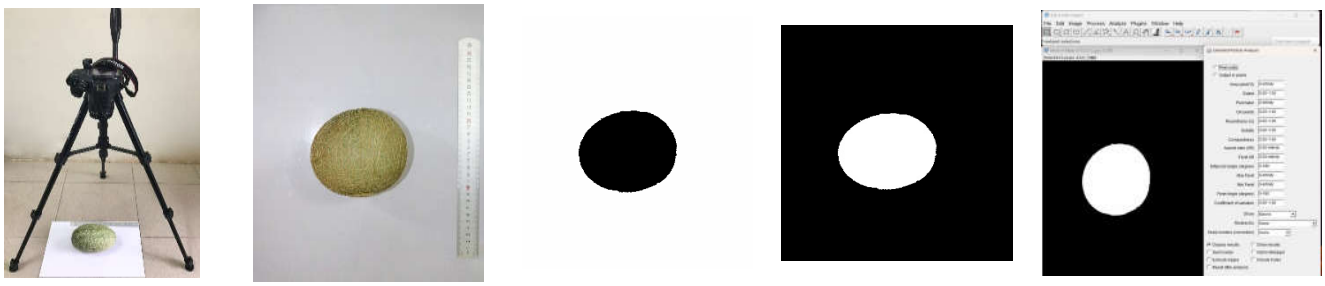

(A) Capture image | (B) Raw image | (C) Thresholding | (D) Segmentation | (E) Data extraction

Figure 1. Image-based phenotyping on muskmelon fruits

The experiment was arranged in a randomized complete block design (RCBD), with 3 replications in a polyhouse at Vietnam National University of Agriculture, Ha Noi, Vietnam in Spring and Autumn seasons of 2021. Experimental plot area was 12 m^2 (1.2 m x 10 m), each seed sample was planted in 2 rows of 10 m long. Planting spacing was 60 cm between rows, 55 cm between plants (24,000 plants/ha). Fertilizer application per ha *viz*,

1,400 kg of manure + 600-800 kg of superphosphate + 1,000 kg of NPK (15-5-20) + 50 kg of urea + 50 kg of potassium chloride. Each plant kept only one fruit for about 7-10 days after hand pollination. Ten important agronomic traits were monitored namely: harvest time (HT, day), fruit weight (FW, kg), fruit length (FL, cm), fruit diameter (FD, cm), fruit flesh thickness (FT, cm), rind thickness (RT, cm), total soluble solids (TSS, °Brix), seed number (SN, number of seeds/fruit), seeds weight/fruit (SW, g), and thousand seed weight (TSW, g).

Fruit length and fruit diameter were extracted from the image taken by Canon EOS 1500D, by BioVoxxel Toolbox on ImageJ software. The main steps were described in Figure 1.

2.3. Data analysis

Data were handled by Microsoft Excel, and analyzed by the one-way ANOVA method in Statistix 10. Descriptive statistics using "*rstatix*" package, correlation analyzed by "*GGally*" package in R 4.1.1. Principal component analysis and hierarchical clustering based on principal component analysis were performed by "*factoextra*" and "*FactoMineR*" packages in the R 4.1.1 [11].

3. RESULTS AND DISCUSSION

3.1. Descriptive statistics and correlation analysis between investigated traits

Descriptive parameter results included mean, minimum, maximum, standard deviation, and coefficient of variation, and statistically significant of 10 traits over two seasons (Table 1). ANOVA showed that there were statistical significant at $p \leq 0.01$ for all investigated traits. Overall, these yield traits showed high variability, and muskmelon materials have a longer duration in Autumn season compared with Spring season. HT of muskmelon materials ranged from 73.0 days to 79.0 days in the Spring season and ranged from 78.0 days to 87.0 days in the Autumn season. Fruit-related traits namely FW, FL, FD, FT are important economical parameters in melon breeding program, affected both demand and supply [12, 7]. FW of muskmelon materials ranged from 1.4 kg to 2.9 kg in Spring season and ranged 1.3 kg to 3.2 kg in the Autumn season. FL fluctuated from 13.5 cm to 19.0 cm in Spring season and ranged between 12.6 cm and 20.4 cm in the Autumn season. FD of muskmelon materials ranged from 9.2 cm to 14.5 cm in the Spring season and ranged from 8.0 cm to 16.7 cm in the Autumn season. FT ranged between 2.7 cm and 4.2 cm in Spring season and ranged between 2.5 cm and 3.9 cm in the Autumn season. RT is affected by both genetic [13] and cultivation methods [14]. RT ranged from 0.4 to 0.7 cm in Spring season and ranged 0.4 to 0.8 cm in the Autumn season. TSS is a vital quality trait, governed by additive effects, can be improvement through recurrent selection [15, 4]. TSS ranged between 11.1 and 15.0 cm in Spring season and ranged 12.1 to 16.0 in Autumn season. SN, SW and TSW are valuable traits of the fruit in terms of taxonomy and evolution, also had a significant effect the commercial product for melon seed companies [16]. SN trait of muskmelon materials ranged between 158.0 and 258.0 seeds/fruit in Spring season and ranged from 130.0 to 270.0 seeds/fruit in the Autumn season. SW variated from 5.0 to 7.7 g in Spring season and 5.8 to 8.3 g in the Autumn season. TSW ranged from 20.9 to 45.9 g in Spring season and ranged from 22.1 to 46.9 g in Autumn season. Three traits *viz*, FW, SN, and TSW showed highest variability with coefficient of variation of FW reached 20.2 in Spring season and 27.3 in the Autumn season, SN had a coefficient of variation reached 22.0

in Spring season and 19.5 in the Autumn season, TSW had efficient variation and reached 21.7 in Spring season and 21.1 in Autumn season. Thus, selection on those traits can be applied to select more suitable genotypes have more phenotypic variation.

Table 1. Descriptive statistics of eight agronomic traits over two seasons

Trait	Season	Min	Max	Mean	Range	Standard deviation	Coefficient of variation	Statistical significance
HT	Spring 21	73.0	79.0	75.5	6.0	1.8	2.3	**
	Autumn 21	78.0	87.0	82.4	9.0	2.7	3.3	**
FW	Spring 21	1.4	2.9	1.8	1.5	0.4	20.2	**
	Autumn 21	1.3	3.2	1.6	1.9	0.4	27.3	**
FL	Spring 21	13.5	19.0	16.2	5.5	1.6	9.8	**
	Autumn 21	12.6	20.4	15.4	7.8	2.2	14.5	**
FD	Spring 21	9.2	14.5	11.1	5.3	1.7	15.2	**
	Autumn 21	8.0	16.7	10.4	8.7	1.9	18.4	**
FT	Spring 21	2.7	4.2	3.4	1.5	0.4	12.9	**
	Autumn 21	2.5	3.9	3.2	1.4	0.4	13.3	**
RT	Spring 21	0.4	0.7	0.5	0.3	0.1	11.2	**
	Autumn 21	0.4	0.8	0.5	0.4	0.1	17.4	**
TSS	Spring 21	11.1	15.0	13.1	3.9	1.2	9.2	**
	Autumn 21	12.1	16.0	13.7	3.9	1.3	9.7	**
SN	Spring 21	108.0	258.0	216.4	150.0	47.5	22.0	**
	Autumn 21	130.0	270.0	226.2	140.0	44.2	19.5	**
SW	Spring 21	5.0	7.7	6.4	2.7	0.9	13.8	**
	Autumn 21	5.8	8.3	6.9	2.6	0.8	11.8	**
TSW	Spring 21	20.9	45.9	30.6	25.0	6.7	21.7	**
	Autumn 21	22.1	46.9	31.6	24.8	6.7	21.1	**

*Note: ** mean statistically significant at $p \leq 0.01$.*

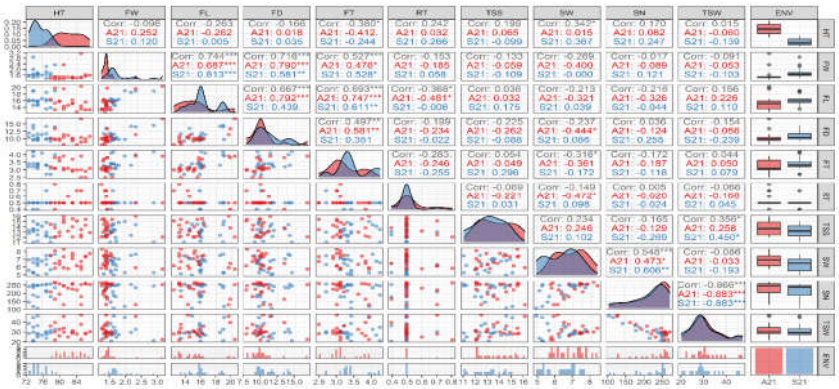

Figure 2. Correlogram chart for ten agronomic traits over two seasons

*Note: ** mean statistically significant at $p \leq 0.01$; A21: Autumn season 2021; S21: Spring season 2021.*

Correlogram chart for ten agronomic traits over two seasons was presented in Figure 2. The density distribution of each trait is shown diagonally with blue color indicating

Spring season 2021 and pink color indicating Autumn season 2021. At the top-right of Figure 2, a two-variable scatter plot is shown while at the top, with the symbols *, **, *** indicating statistical significance at P ≤ 0.05, P ≤ 0.01 and P ≤0.001, respectively. The boxplot on the right illustrates the difference between two seasons. Knowledge of the correlation between yield and its components can help breeders to decide the selection pressures on the traits involved in order to simultaneously improve the yield traits [17]. FW is a polygenic inherited trait and governed by many genes, located on different chromosomes [4]. Overall, in this study, the highest significant positive correlation at p < 0.001 was observed between FW and FL (0.744***), FD (0.716***), and FT (0.527***) suggesting that simultaneous selection of these characters would lead to yield improvement of muskmelon (Figure 2). Significant positive correlations at p <0.001 were also found between FL and FD (0.667***), FT (0.693***). This information can be useful for future melon breeding programs to obtain high yield muskmelon varieties. For example, crosses can be made between cultivars with large fruit. The above results have served as a basis for the selection of elite muskmelon materials by multivariate method. Despite of HT of those muskmelon materials in Autumn season were longer than Spring season, the variation and FW and it related traits were higher than Spring season. The quality traits *viz.*, TSS were also higher in Autumn season compared with Spring season. These results might due to the difference in temperature between day time and night time in the Autumn season in the North of Vietnam.

3.2. Principal component analysis

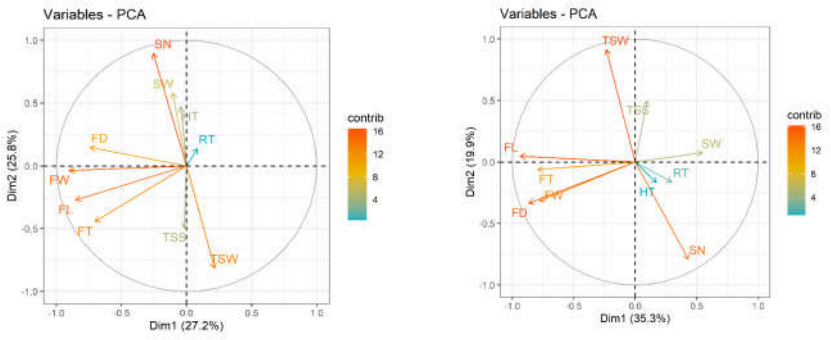

(A) Spring season 2021 (B) Autumn season 2021

Figure 3. Contribution of traits on the first two major components

By applying principal component analysis (PCA), the most important characteristics in the data set were revealed. PCA is a technique that falls within the data framework of multivariate statistical analysis. To determine genetic variation and relationships between muskmelon materials, PCA was used. Total of 8 quantitative traits could be reduced to just four components, which could explain more than 90% of the total variation. A PCA diagram is presented based on the first two components (Figure 3). The arrangement of traits on PC1 and PC2 demonstrates that some traits are highly correlated with each other as seen in the overlap pattern of traits. Variables on the same PC and next to each other indicate a positive correlation between them, and an increase in one will lead to an increase

in the other. However, the traits at the opposing ends are not correlated and an increase in one point will decrease the other traits and vice versa. In both seasons, based on the first component, accessions exhibit high positive component values representing relatively high fruit weight (FW), fruit length (FL), fruit diameter (FD), and fruit thickness (FT).

The market value of melons is influenced by fruit quality in terms of fruit size, and fruit shape [18, 1]. In both seasons, FW, FL, FD, and FT which were fruit-related traits strongly contributed to the total variation of 20 muskmelon materials. However, in the Autumn season, the total of the two first components achieved 55.2%, which was slightly higher than the Spring season (54.0%) (Figure 3). The first component, accounting for 27.2% of the total variation in the Spring season and 35.3% in the Autumn season, was closely related to fruit weight and fruit shape, including fruit length, fruit diameter, and fruit thickness (Figure 4). The first two components accounted for 54% of the morphological variation, and fruit length, being the most important variable constituting PC1. Kaur *et al.* (2022) [12] highlighted the importance of fruit traits in muskmelon breeding for yield improvement. The second component, which accounted for 25.8% of the total variation in the Spring season and 19.9% in the Autumn season, was mainly correlated with the characteristics of seed number (SN), one-thousand seed weight (TSW), and seed weight/fruit (SW) (Figure 5).

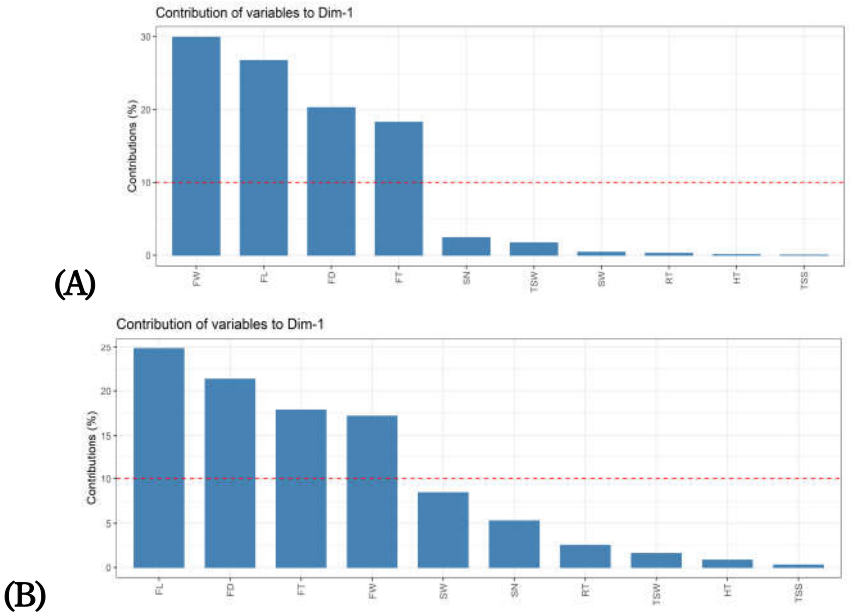

Figure 4. Contribution of agronomic traits to PC1 in (A) Spring season, (B) Autumn season

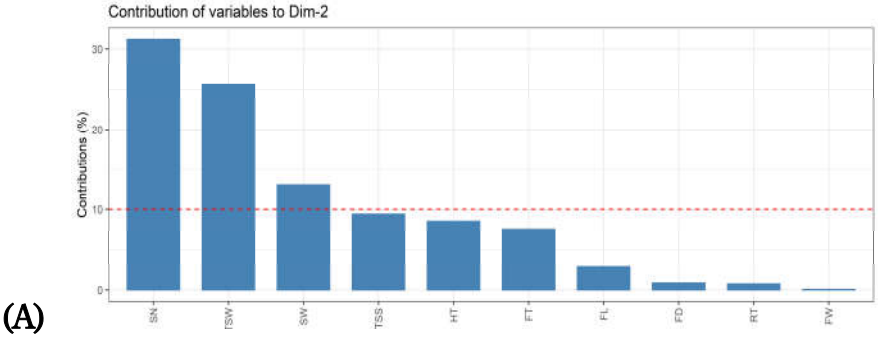

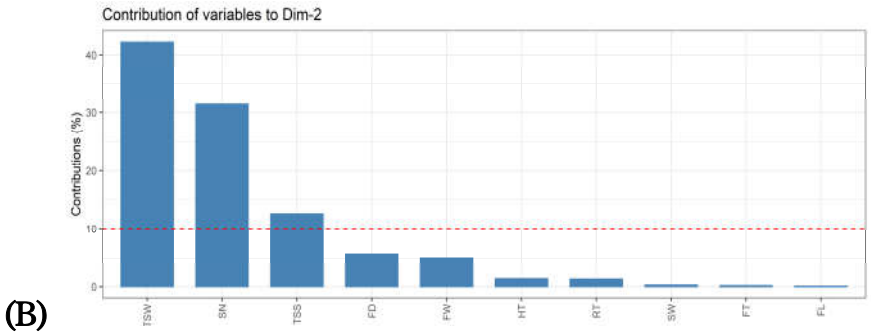

(B)

Figure 5. Contribution of agronomic traits to PC2 in (A) Spring season, (B) Autumn season

3.3. Cluster analysis

Diversity and the relationship between traits are essential information in crop improvement programs, and the success of plant breeding programs relies heavily on the existence of phenotypic variation and inheritance for specific traits. In this study, hierarchical clustering based on principal component analysis was used to investigate genetic similarity. The euclidean distance was used as a measure to measure this phenotypic similarity among 20 muskmelon materials based on 8 investigated traits. The dendrogram showed 20 muskmelon materials were divided into three distinct groups in the Spring season and four distinct groups in the Autumn season (Figure 6).

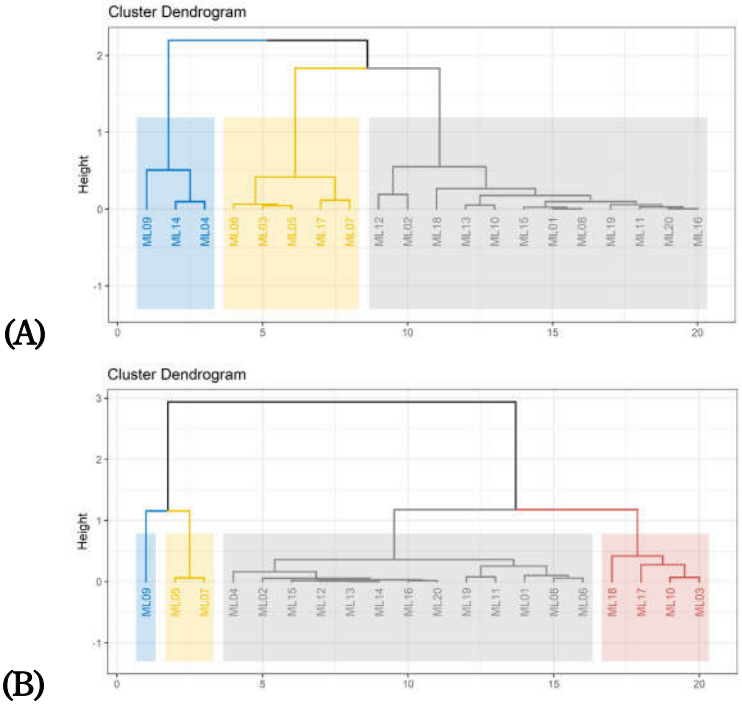

(A)

(B)

Figure 6. Cluster dendrogram of 20 muskmelon materials in (A) Spring season, and (B) Autumn season

Based on the phenotypic traits in the Spring season, hierarchical clustering based on principal component analysis showed three major groups *viz.*, the first group included 3 muskmelon materials (ML09, ML14, and ML04), the second group included 5 muskmelon materials (ML06, ML03, ML05, ML07, and ML17) and the largest third group included 12 muskmelon materials along with the check variety TL3. On the other hand, based on phenotypic traits in the Autumn season, hierarchical clustering based on

principal component analysis showed four major groups *viz.*, the first group included only one material ML09 which showed the highest fruits weight, the second group included 2 muskmelon materials (ML05, and ML07), the third group included 4 muskmelon materials (ML18, ML17, ML10, and ML03) and the largest fourth group included 13 muskmelon materials along with check variety TL3 (Figure 5). Those muskmelon lines responded dynamically under two seasons, responsiveness to the weather conditions, and presented useful information for breeding high adaptation muskmelon varieties in Vietnam. Recently, hierarchical clustering based on principal component analysis has been used by Gong *et al.* (2014) [19] to study diversity in apples. Iqbal *et al.* (2014) [20] studied genetic diversity in tomato. To the best of our knowledge, this is the first study applied hierarchical clustering based on principal component analysis to investigate phenotypic diversity on the agronomic traits in muskmelon in Vietnam.

4. CONCLUSION

This study investigated the phenotypic diversity of 20 muskmelon materials in the Spring and Autumn seasons based on ten agronomical traits in Hanoi, Vietnam. Three quantitative traits *viz.*, fruit weight, seed number, and one-thousand seed weight showed the highest variability. Fruit weight, fruit length, fruit diameter, and fruit thickness contributed more than 90% of their cumulative contribution suggesting that those traits can be used to classify muskmelon materials. The result of this study is highly useful for effective utilization of muskmelon germplasm, provided a foundation breeding population for the hybrid muskmelon breeding program in Vietnam.

ACKNOWLEDGEMENTS

This study is part of a Key Science and Technology project at the Vietnam National University of Agriculture: "A pilot study on image-based phenotyping, building big data and application in plant breeding" - code "T2021-41-15TĐ". The authors acknowledge financial support from Vietnam National University of Agriculture.

REFERENCES

1. Wang X., Ando K., Wu S., Reddy U. K., Tamang P., Bao K., Hammar S. A., Grumet R., McCreight J. D. & Fei Z. (2021). Genetic characterization of melon accessions in the U.S. National Plant Germplasm System and construction of a melon core collection. *Molecular Horticulture,* 1(1): 11.

2. Burger Y., Sa'ar U., Paris H. S., Lewinsohn E., Katzir N., Tadmor Y. & Schaffer A. A. (2006). Genetic variability for valuable fruit quality traits in *Cucumis melo*. *Israel Journal of Plant Sciences,* 54(3): 233-242.

3. Pereira L., Santo Domingo M., Ruggieri V., Argyris J., Phillips M. A., Zhao G., Lian Q., Xu Y., He Y., Huang S., Pujol M. & Garcia-Mas J. (2020). Genetic dissection of climacteric fruit ripening in a melon population segregating for ripening behavior. *Horticulture Research,* 7(1): 187.

4. Kesh H. & Kaushik P. (2021). Advances in melon (*Cucumis melo* L.) breeding: An update. *Scientia Horticulturae,* 282: 110045.

5. Lian Q., Fu Q., Xu Y., Hu Z., Zheng J., Zhang A., He Y., Wang C., Xu C., Chen B., Garcia-Mas J., Zhao G. & Wang H. (2021). QTLs and candidate genes analyses for fruit size under domestication and differentiation in melon (*Cucumis melo* L.) based on high resolution maps. *BMC Plant Biology,* 21(1): 126.

6. Du X., Liu H., Zhu Z., Liu S., Song Z., Xia L., Zhao J., Luan F. & Liu S. (2022).

Identification of Candidate Chromosome Region Related to Melon (*Cucumis melo* L.) Fruit Surface Groove Trait Through Biparental Genetic Mapping and Genome-Wide Association Study. *Frontiers in Plant Science,* 13.

7. Oren E., Tzuri G., Dafna A., Rees E. R., Song B., Freilich S., Elkind Y., Isaacson T., Schaffer A. A., Tadmor Y., Burger J., Buckler E. S. & Gur A. (2022). QTL mapping and genomic analyses of earliness and fruit ripening traits in a melon Recombinant Inbred Lines population supported by de novo assembly of their parental genomes. *Horticulture Research,* 9, uhab081.

8. Pouyesh A., Lotfi M., Ramshini H., Karami E., Shamsitabar A. & Armiyoun E. (2017). Genetic analysis of yield and fruit traits in cantaloupe cultivars. *Plant Breeding,* 136(4): 569-577.

9. Ringnér M. (2008). What is principal component analysis? *Nature Biotechnology,* 26(3): 303-304.

10. Lever J., Krzywinski M. & Altman N. (2017). Principal component analysis. *Nature methods,* 14(7): 641-642.

11. R Development Core Team (2022). R: A language and environment for statistical computing. R Foundation for Statistical Computing, Vienna, Austria. Retrieved from https://cran.r-project.org/bin/windows/base on March 10, 2022.

12. Kaur S., Sharma S. P., Sarao N. K., Deol J. K., Gill R., Abd-Elsalam K. A., Alghuthaymi M. A., Hassan M. M. & Chawla N. (2022). Heterosis and combining ability for fruit yield, sweetness, beta-carotene, ascorbic acid, firmness and fusarium wilt resistance in muskmelon (*Cucumis melo* L.) involving genetic male sterile lines. *Horticulturae,* 8(1).

13. Lázaro A., Fernández I. C., Borrero M. J., Cabello F., López-Sesé A. I., Gómez-Guillamón M. L. & Picó B. (2017). Agromorphological genetic diversity of Spanish traditional melons. *Genetic Resources and Crop Evolution,* 64(7): 1687-1706.

14. Cosme C. R., da Silva Dias N., Silva K. M. P., Silva C. V. T., de Queiroz Í. S. R., Rebougas T. C. & dos Santos Fernandes C. (2017). Yield and quality of gália melon grown in coconut fiber under different concentrations of macronutrients in the nutrient solution. *Idesia,* 35(4): 119-128.

15. Akrami M. & Arzani A. (2019). Inheritance of fruit yield and quality in melon (*Cucumis melo* L.) grown under field salinity stress. *Scientific Reports,* 9(1): 7249.

16. Zhang H., Zhang X., Li M., Yang Y., Li Z., Xu Y., Wang H., Wang D., Zhang Y., Wang H., Fu Q., Zheng J. & Yi H. (2022). Molecular mapping for fruit-related traits, and joint identification of candidate genes and selective sweeps for seed size in melon. *Genomics,* 114(2): 110306.

18. Shajari M., Soltani F., Reza Bihamta M. & Alabboud M. (2021). Genetic analysis and inheritance of floral and fruit traits in melon (Cucumis melo) in the full diallel cross. *Plant Breeding,* 140(3): 486-496.

17. Thakur H., Sharma S. & Thakur M. (2019). Recent trends in muskmelon (*Cucumis melo* L.) research: an overview. *The Journal of Horticultural Science and Biotechnology,* 94(4): 533-547.

19. Gong L., Meng X., Liu N. & Bi J. (2014). Evaluation of apple quality based on principal component and hierarchical cluster analysis. *Transactions of the Chinese Society of Agricultural Engineering,* 30(13): 276-285.

20. Iqbal Q., Saleem M. Y., Hameed A. & Asghar M. (2014). Assessment of genetic divergence in tomato through agglomerative hierarchical clustering and principal component analysis. *Pakistan Journal of Botany,* 46(5): 1865-1870.

RESEARCH ON *IN VITRO* SHOOT PROLIFERATION OF *Stemnona tuberosa* L.

Vu Hoai Sam [1,*], Nguyen Thi Xuyen [1], Hoang Thi Nhu Nu [1],
Le Thi Quynh Nga[1], Dinh Thanh Giang [1], Nguyen Thi Huong [1]

ABSTRACT

Stemona tuberosa Lour. (Stemonaceae) is known as an antitussive medicinal plant in traditional medicine. Recently, its tuberous roots have been seriously exploited for medicinal materials in Vietnam. Therefore, it is necessary to conduct research on the propagation of *S. tuberosa* by tissue culture for its conservation and rapid production. In this study, the strong positive influence of coconut water (CW) on *in vitro* shoot proliferation and the effective shoot formation in *S. tuberosa* was recorded. MS medium supplemented with 1.5 mg/L BAP, 30 g/L sucrose, and 10% CW was determined as the optimal medium for the shoot multiplication of *S. tuberosa* shoots from the nodal explants. On that medium, 8.87 effective shoots per explant were obtained.

Keywords: *Stemona tuberosa, proliferation, BAP, explant, coconut water.*

Received: 12 August 2022; revised: 14 September 2022; accepted: 21 November 2022.

1. INTRODUCTION

"Bach bo" is a crucial medicinal plant with the scientific name *Stemona tuberosa* Lour., which belongs to the family Stemonaceae. Its tuberous roots are rich in alkaloids such as stemoninine, tuberostemonine and neotuberostemonine [1] and therefore has been recorded as an antitussive medicinal plant in Vietnamese pharmacopeia [2]. Currently, there are many herbal products containing ingredients from the tuberous roots of *S. tuberosa*. The natural material source of *S. tuberosa*, therefore, has been significantly declining, not only in Vietnam but also in its distribution places around the world. Demand recently for high-quality seedlings of medicinal plants in general, and of *S. tuberosa*, in particular, ensure the standards and traceability which are required by the Ministry of Health in the making process of herbal products is on the rise in Vietnam. Research on micropropagation of *S. tuberosa* - a valuable medicinal plant is essential for conservation and cultivation.

Protocols for *in vitro* culture of *S. tuberosa* have been established in Bangladesh and India, in which the MS medium was used as the basic medium for the culture. In those protocols, plant growth regulators used for multiplication purposes were high in concentration and it is noticed that there were no correlations or agreements between the publications [3, 4, 5]. Although the type of explants of *S. tuberosa* were the same, the differences in age and characteristics of donor plants, as well as different collection seasons could be the causes of these differences [3, 4, 5]. To produce large-scale plantlets with all the inherited traits of the donor plant, we carried out *in vitro* regeneration of *S. tuberosa* from nodes of the selected domestic 4-year-old

[1] National Institute of Medicinal Materials
* Corresponding author: samthavn@yahoo.com

mother plant. In this paper, we present the results on the investigation of plant growth regulators, coconut water, and sugar content on *in vitro* shoot proliferation to establish an efficient micropropagation protocol for *S. tuberosa*. The results can be applied for a large-scale production of *S. tuberosa* plantlets for cultivation in Vietnam.

2. MATERIALS AND METHODS

2.1. Materials

The juvenile nodes (1,0 -1,5 cm) of the 4-year-old *S.temona tuberosa* were collected during Spring season in Thanh Hoa province were used as the explants.

2.2. Methods

Explants were cleaned under a running water tap for 20 min to remove dust, and then they were shaken gently in 1% detergent powder for 10 min and washed for 4-5 times with distilled water. In a laminar, explants were treated with 70% ethanol in a sterile flask for 30 sec, following 8 – 10 min surface sterilized with 0.1% $HgCl_2$ to determine the appropriate period for sterilization of *S. tuberosa* nodal explants. After sterilization, the two ends of the explants were dissected and discarded (the wounded tissue which directly contacted with $HgCl_2$ solution) and explants were inoculated on MS medium supplemented with 0.5 mg/L BAP and 30 g/L in test-tubes (22 x 200 mm).

The nodal segments of the regenerated shoots were fortified with MS medium supplemented with BAP (0 - 2.0 mg/L), NAA (0 - 0.3 mg/L), IBA (0 - 0.3 mg/L) and sucrose (0 - 60 g/L), coconut water (0 - 20%) at different concentrations and combinations to explore the optimal medium for proliferation.

pH of the medium was adjusted to 5.7 - 5.8 before dispensing in a flask and autoclaving at 121^0C and 1.1 kg/cm^2 for 20 min. Inoculation room was maintained at 25 ± 2°C, < 70% in humidity, illuminance level of 2,000 - 3,000 lux, 16 hours of light a day. The experiments were completely randomized design. Each experiment was repeated thrice using 15 replicates. The data were subjected to Analysis of Variance (ANOVA) for one factor at $P \leq 0.05$ per experiment. The significant difference between the means was compared with Duncan's Multiple Range Test by the program SPSS 20.

3. RESULTS AND DISSCUSSION

3.1. Effect of duration treatment of 0.1% $HgCl_2$ on surface sterilization of *S. tuberosa* explants

Table 1. Effect of duration treatment of 0.1% $HgCl_2$ on *S. tuberosa* explants

Duration* (min)	Survival percentage** (%)	Contaminated percentage** (%)	Death percentage** (%)
8	46.67	46.67	6.67
10	83.33	10.00	6.67
12	53.33	6.67	40.00

**Culture medium: MS + 30 g/L sucrose + 0.5 mg/L BAP*

*** Data indicate the mean of three replicates of the experiment with ten explants used per replication.*

Figure 1. Surface sterilization of *S. tuberosa* explants. A: the juvenile nodal segments of *S. tuberosa* explants; B: The explants of *S. tuberosa* 4 weeks after sterilization with 0.1% $HgCl_2$ for 10 min.

Surface sterilization is the main aspect of tissue culture to prevent it from contamination, to obtain sterile plant material is difficult because during sterilization the microorganism should be eliminated, while the living materials should be survived. In this experiment, we investigated the effect of the duration of $HgCl_2$ 0.1% treatment on *S. tuberosa* explants. After 4 weeks of culture, the percentage of explant survival and microbial contamination was observed.

The results in table 1 showed that, the longer the exposure time of the explants to $HgCl_2$ solution, the lower the rate of bacterial contamination (6.67%, 12 min). However, when explants exposed longer time to $HgCl_2$, the explants turned brown and eventually died. The percentage of browning and dying explants was quite high (up to 40%) as the exposure time of 0.1% $HgCl_2$ was 12 min.

In this experiment, we have succeeded in controlling the contamination, determining that 10 min is the optimal exposure time of 0.1% $HgCl_2$ to the juvenile nodal segments of *S. tuberosa.*

3.2. Effect of BAP on *in vitro* shoot proliferation of *S. tuberosa*

In previous studies on *in vitro* shoot multiplication in *S. tuberosa* indicated that BAP, Kin, and TDZ were suitable for proliferation. However, those results also showed that the different combinations and concentrations of these substrates brought the various number of regenerated shoots [3, 4, 5]. BAP is considered to be one of the effective cytokinins for induction of organogenesis and thereby it enhanced the ability of micropropagation in many plant species. In the present study, we investigated the effect of BAP concentration (0-2 mg/L) on the number of shoots and on the growth of shoots of *S. tuberosa* explants. The given results showed that the percentage of multiple shoot formation reached 73.33% in treatment 0.5 mg/L BAP, and the maximum of this rate (100%) was obtained from the third treatment (1.0 mg/L BAP) onwards (Table 2). It is clearly indicated that the increase of BAP concentration has increased the percentage of multiple shoot formation, as well as the number of new shoots per the nodal explant. The average number of new shoots was significantly influenced by different concentration of BAP. It increased from 2.43 to 4.63 shoots/explant according to the increase of BAP concentration (0.5 mg/L - 2.0 mg/L) in the culture medium. The maximum number of shoots obtained at the highest concentration of BAP in the experiment. Their regenerated shoots, however, were less vigorous than the others (Table 2, Figure 2).

Table 2. Effects of various concentrations of BAP on *in vitro* shoot proliferation in *S. tuberosa*

BAP* (mg/L)	Percentage of multiple shoot formation	No. of shoots**	Length of the shoots** (cm)	Vigor of shoots
0,0	-	-	-	
0.5	73.33	$2.43^{c} \pm 1.09$	$2.39^{c} \pm 0.92$	++
1.0	100	$2.82^{b} \pm 0.81$	$3.06^{bc} \pm 0.69$	++
1.5	100	$4.57^{a} \pm 0.56$	$3.82^{a} \pm 0.43$	++
2.0	100	$4.63^{a} \pm 1.16$	$3.28^{b} \pm 1.02$	+
		$P < 0.05$	$P < 0.05$	

** Supplemented to MS + 30 g/L sucrose (Control medium)*

*** Data indicate mean±SD; mean followed by the same letter was not significantly different by Duncan's test at 0.05% probability.*

Fifteen replicates were used per treatment and the experiment was repeated thrice.

+++: green leaves, short internodes; ++: pale green leaves, long internodes; +: small leaves, long internodes;

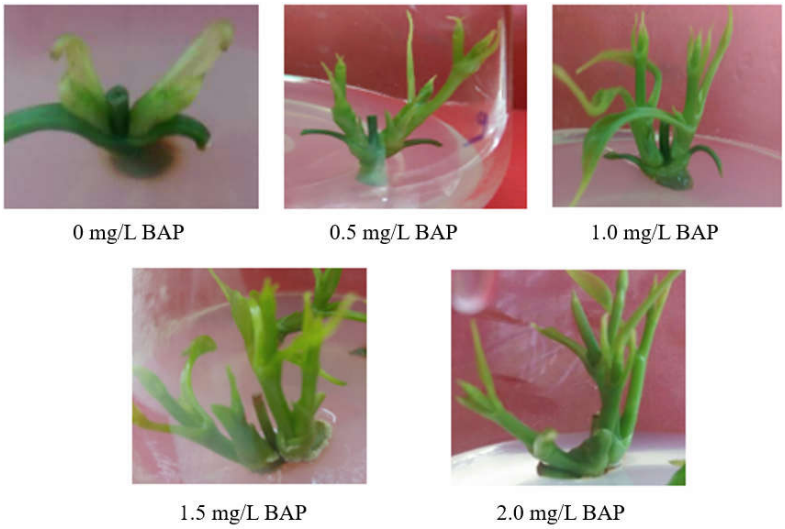

Figure 2. Effect of BAP concentration on *in vitro* shoot proliferation in *S. tuberosa*

In terms of the analysis results, the number of shoots in 1.5 mg/L and 2.0 mg/L BAP treatments were the same rank according to Duncan's test (Table 2). The length and vigour of shoots in 1.5 mg/L BAP treatment, however, were better than another one. Besides, the change of their shoot length was a significant difference. In previous studies of *in vitro* propagation in *S. tuberosa*, the percentage of shoot multiple responses was quite low. At the same concentration range of BAP, the number of shoots per explant was also lower than this result, only got under 50% in percentage response with 1.00 shoot/explant. This might be due to the differences of genetic resources or the origin of the used chemicals. No multiple shoot formation occurred in plant growth regulators free medium after 6 weeks of culture.

Therefore, we concluded that 1.5 mg/L of BAP was the most suitable concentration for the following experiments of *in vitro* shoot proliferation.

3.3. Effect of BAP in combination with auxin (IBA, NAA) on *in vitro* shoot proliferation

Normally cytokinin inhibits the root induction and enhances the shoot proliferation and elongation during *in vitro* propagation of plants. However, many studies have demonstrated that lower concentrations of auxins in combination with higher concentrations of cytokinin enhance the rate of shoot proliferation in micropropagation of plants [4, 6]. The purpose of this experiment was to increase the number of shoots per explant, hence, we developed the hormone combined treatments to determine the effects of 1.5 mg/L BAP in combination with two concentrations at 0.1 and 0.3 mg/L of IBA and of NAA. Follow-up results after 6 weeks are presented in table 3.

Table 3. Effect of combination 1.5 mg/L BAP and IBA, NAA (at 0.1 mg/L, 0.3 mg/L) on *in vitro* shoot proliferation in *S. tuberosa*

Growth regulators (mg/L)			Percentage of multiple shoot formation	No. of shoots	Length of shoots (cm)	Vigor of shoots
BAP	NAA	IBA				
1.5	-	-	100	$4.58^{a} \pm 0.56$	$3.82^{a} \pm 0.43$	++
1.5	0.1		100	$4.26^{a} \pm 0.25$	$3.33^{ab} \pm 0.17$	++
1.5	0.3		86.67	$3.05^{b} \pm 0.72$	$2.82^{bc} \pm 0.53$	+
1.5		0.1	86.67	$2.78^{c} \pm 0.46$	$3.00^{b} \pm 0.31$	+
1.5		0.3	56.67	$2.62^{d} \pm 0.91$	$2.07^{c} \pm 0.14$	+
				$P < 0.05$	$P < 0.05$	

**Supplemented to MS + 30 g/L sucrose (Control medium)*

***Data indicate mean±SD; mean followed by the same letter was not significantly different by Duncan's test at 0.05% probability.*

Fifteen replicates were used per treatment and the experiment was repeated thrice.

+++: green leaves, short internodes; ++: pale green leaves, long internodes; +: small leaves, long internodes.

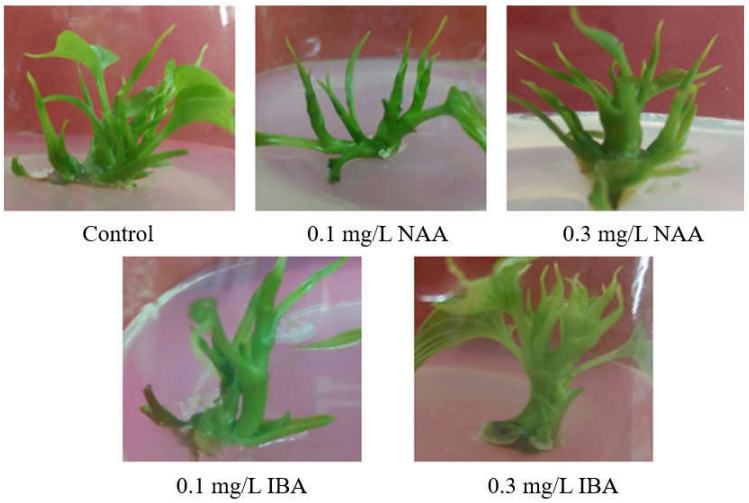

Figure 3. Effect of 1.5 mg/L BAP in combination with auxin (IBA, NAA) on *in vitro* shoot proliferation in *S. tuberosa*

From the data furnished in table 3, we observed that the combination 1.5 mg/L BAP and NAA was more effective than the combination 1.5 mg/L BAP and IBA. However, the value direction of all assessed indicators was gradually decreased with increasing concentrations of NAA and IBA, and the value of the combination 1.5 mg/L BAP and 0.3 mg/L IBA was the lowest in this experiment. The studied results of Biswas *et al.* (2011)[3] on the effect of plant growth regulators on *in vitro* shoot multiplication in *S. tuberosa*, showed that the percentage responses of nodal explants on *in vitro* shoot multiplication were just under 50% on MS medium supplemented with a range of the individual BAP concentration (1.0 - 5.0 mg/L). And they obtained the highest response percentage and the biggest number of shoots per explant, 97% and 12.7 respectively, on media fortified with 3.0 mg/L BAP + 0.5 mg/L NAA after 60 days of culture [4]. However, our results of the current study seemed opposite to these ones. MS supplemented with 1.5 mg/L BAP alone induced the best response, 100% of the cultured explants gave multiple shoots with average 4.58 shoots, the vigor of regenerated shoots was also the best on it (Figure 3). The opposition might be caused by the different ages of used explants, and our explants spent over two subcultures. In addition, it might be caused by the difference in the composition of previous culture media which were accumulated in the culture cell/tissue causing the different organogenesis.

3.4. Effects of various concentrations (g/L) of sucrose on *in vitro* shoot proliferation in *S. tuberosa*

Table 4. Effects of various concentrations of sucrose on *in vitro* shoot proliferation in *S. tuberosa*

Sucrose (g/L)	Percentage of multiple shoot formation	No. of shoots per explant	Length of shoots (cm)	Vigor of shoots
Control	-	$1.07^{c} \pm 0.31$	$2.01^{b} \pm 0.73$	+
10	76.67	$2.33^{b} \pm 0.92$	$3.50^{ab} \pm 0.07$	++
30	100	$4.73^{a} \pm 0.09$	$3.48^{ab} \pm 0.16$	+++
50	100	$4.57^{a} \pm 0.46$	$3.73^{a} \pm 0.23$	+++
		$P < 0.05$	$P > 0.05$	

** Supplemented to MS + 1.5 mg/L BAP (Control medium)*

*** Data indicate mean±SD; mean followed by the same letter was not significantly different by Duncan's test at 0.05% probability.*

Fifteen replicates were used per treatment and the experiment was repeated thrice.

+++: green leaves, short internodes; ++: pale green leaves/leafless, long internodes; +: small leaves, long internodes.

The addition of an external carbon source to the medium enhances the proliferation of cells and regeneration of green shoots [7]. The optimal sucrose concentration in a medium should be sufficient to satisfy the basic energy requirements for cell division/differentiation and not impose any negative osmotic effects on shoot formation [8]. This indicates that sucrose acts not only as a carbon energy source in a medium but also as an osmotic and that different concentrations of sucrose are one of the factors controlling the induction and growth of shoots. We found that the vigor of

regenerated shoots in all the above treatments was not well (leafless), although their number of shoots per explant was quite high. Therefore, we accomplished this further experiment with 4 treatments of sucrose concentration to study on the effect of various concentrations of sucrose on *in vitro* shoot multiplication in *S. tuberosa*. The result of this experiment after 6 culture weeks was presented in table 4 and figure 4.

No shoot multiple was formed in a medium without sucrose (Table 4). Although at least one or two axillary shoots might be regenerated in the non-sucrose medium, their length and vigor were not well. When adding sucrose to the culture media, the percentage of shoot formation, the number of shoots per explant, and the length of shoots, also shoots' vigor increased with the increase of the sucrose concentration in the medium up to 50 mg/L. However, there was statistically no significant difference in all parameters in 30 mg/L or 50 mg/L of sucrose concentration. This implied that the shoot development and proliferation of *S. tuberosa* shoots did not be affected by the osmotic level of the medium.

Figure 4. Effect of various concentrations of sucrose on *in vitro* shoot proliferation in *S. tuberosa*

On the other hand, we observed that the appearance of leaves and also the size of leaves were promoted when the sucrose concentration in the medium was greater than equal to 40 g/L (Figure 4). In addition to the propagation rate, the *in vitro* development of shoots should be considered when choosing the best medium. These observations helped us in choosing of the appropriate sucrose concentration (30 g/L) for the shoot multiplication in *S. tuberosa*.

3.5. Effects of various concentrations of coconut water on *in vitro* shoot proliferation in *S. tuberosa*

Table 5. Effects of various concentrations of coconut water in association with 1.5 mg/L BAP on *in vitro* shoot proliferation in *S. tuberosa*

Coconut water (%)	Percentage of multiple shoot formation	No. of shoots per explant	Length of shoots (cm)	Vigor of shoots
0,0	100	$4.37^{c} \pm 0.81$	$3.49^{c} \pm 0.92$	+++
5	100	$5.75^{b} \pm 1.13$	$3.76^{b} \pm 0.72$	+++
10	100	$8.87^{a} \pm 0.56$	$3.86^{a} \pm 0.69$	+++
15	100	$8.43^{a} \pm 1.16$	$3.82^{ab} \pm 0.43$	+++
		$P < 0.05$	$P < 0.05$	

**Supplemented to MS + 30 g/L sucrose + 1.5 mg/L BAP (Control medium)*

***Data indicate mean±SD; mean followed by the same letter was not significantly different by the Duncan's test at 0.05% probability.*

Fifteen replicates were used per treatment and the experiment was repeated thrice.

+++: green leaves, short internodes; ++: pale green leaves/leafless, long internodes; +: small leaves, long internodes

Coconut water (CW) is said to be complex in nature because of its indefinite composition. Efficiency of adding the appropriate concentration of coconut water to media for shoot proliferation and proved in many medicinal plants [9, 10]. Therefore, we carried out the experiment with 4 following treatments such as 0%, 5%, 10%,15% of coconut water. The goal of this experiment was to evaluate the effects of CW concentration in association with the BAP in the inoculating media to see if it had beneficial effects on the *in vitro* propagation rate and growth of the regenerated shoots in *S. tuberosa*.

Shoot multiplication of *S. tuberosa* in the presence of coconut water was significantly higher compared to the control containing only 1.5 mg/L BAP after 6 weeks of culture. When CW was augmented in the medium not only the number of shoots increased but also the shoot height was significantly different. Significant differences also existed among the various CW treatments for all parameters studied in the same time period of inoculation. Among the various levels of CW tested, 10% was found optimum as it gave rise to the maximum number of shoots per explant (8.87 shoots). Especially, besides the appearance of shoots with green leaves, the surface of the leaves mostly was also enlarged, which implied that the enlarged leaf shoots were ready for the rooting phase (Figure 5).

Figure 5. Effects of various concentrations of CW on *in vitro* shoot proliferation in *S. tuberosa*

Hence, enrichment of the culture medium with CW, which contains the natural growth regulators, sugar, some vitamins, acid amins, and enzymes, brought positive impacts on the useful shoot formation of *S. tuberosa*. The combined effect of BAP and CW has been reported in previous studies [8, 9] on the other crops which was in accordance with our results on the interaction of BAP and CW obtained on *S. tuberosa* in this study. 10% CW associated with the compatible concentration of BAP (8.9 µM) showed a synergistic effect producing a high rate of shoot multiplication in the Fig. of shoots in *Heliconia chartacea* "Sexy Pink" [9], while only 5% CW affixed to 3.0 mg/L BAP was suitable for the maximum Fig. of 6.3 multiple shoots in *Musa* cv. *Udhayam* [10].

4. CONCLUSION

Nodes of *S. tuberosa in vivo* were sterilized and regenerated shoots successfully

in vitro. The results of our study determined that the appropriate concentrations of BAP and sugar for shoot production in *S. tuberosa* were 1.5 mg/L and 30 g/L, respectively. Coconut water had a strong positive influence on *in vitro* shoot multiplication and the formation of effective shoots. MS medium supplemented with 1.5 mg/L BAP, 30 g/L sucrose and 10% CW was determined to be the optimal medium of shoot proliferation in *S. tuberosa* from the nodal explants, obtaining the maximum number of shoots per explant was 8.87 shoots.

REFERENCES

1. Xu Y., Xiong L., Yan Y., Sun D., Duan Y., Li H., Chen L. (2022), Alkaloids from *Stemona tuberosa* and their anti-inflammatory activity. *Front. Chem.*, 10, e847595

2. National Pharmacopoeia Committee (2017). "Vietnamese Pharmacopoeia V", Medical Publishing House, Ha Noi, 2, 1068-1069.

3. Bikarma S., Sashin KB., Sandhaya JPP, Bipin KS. (2012). Assessing ethnobotanical values and threat status of wild asparagus (*Stemona tuberosa* Lour.): A case study in Eastern Himalaya, India. *Int. J. Conserv. Sci.*, 3(4):319 - 324

4. Biswas A., Bari M. A, Roy M. and Bhadra S.K. (2011), *In vitro* propagation of *Stemona tuberosa* Lour. - A rare medicinal plant through high frequency shoot multiplication using nodal explants, *Plant Tissue Cult. & Biotech.*, 21(2):151-159.

5. Murthy K.S. R, Reddy M. C., Kondamudi R. and Pullaiah T. (2013). Micropropagation of *Stemona tuberosa* Lour. - An endangered and rare medicinal plant in Eastern Ghats of India, *Indian J. Biotechnol.*, 12: 420-424.

6. Munguatosha N., Emerad M., Patrick N. (2013). The effects of auxin and cytokinin on growth and development of (Musa sp.) var. "Yangambi" explants in tissue culture, *Am. J. Plant Sci.*, 4: 2174-2180

7. Praveena C. and Veeresham C. (2014). Multiple shoot regeneration and effect of sugars on growth and nitidine accumulation in shoot cultures of *Toddalia asiatica*. *Pharmacogn. Mag.*, 10 (Suppl3:) S480-S486.

8. Saiqa I., Shagufta N., Sumeera J., Kiran S., Amna T., Neelma M., Aamir A. (2013). Influence of cytokinins, sucrose and pH on adventitous shoot regeneration of *Polyscias balfouriana* (Balfour aralia). *J. Med. Plants Res.*, 7(42): 3098-3104

9. Raizer M.D. M., Martel J.H. I, Lopes M.T., Quisen R.C (2017). Effect of 6-benzylaminopurine and coconut water on shoot multiplication of *Heliconia chartacea* "Sexy pink". *Acta Hortic.*, 1155:173-176.

10. Saraswathi M.S., Praveena S., Uma S., Thangavelu R., Kannan G., Backiyarani S., Arivazhagan T. (2014). Development of an efficient micropropagation technique for Musa cv. udhayam (ABB). *Indian J. Hortic.*, 71 (4): 452-457

GENETIC DIVERSITY EVALUATION OF *Cinnamomum parthenoxylon* (Jack) MEISN IN SOME NATURE RESERVES IN NORTH VIETNAM USING SSR MARKERS

Vu Dinh Giap[1], Khuat Thi Minh Hien[2],
Pham Nhu Anh[3], Pham Mai Phuong[3, 4], Vu Dinh Duy[3, 4*]

ABSTRACT

Cinnamomum parthenoxylon (Jack) Meisn is one of the valuable wood trees indigenous to the lowland tropical forests of Vietnam, which is in danger of extinction due to habitat fragmentation and overexploitation. Furthermore, the genetic diversity of this species has not been investigated to date. This study evaluated the genetic diversity in five natural populations from 101 individuals representing the *C. parthenoxylon* distribution range in natural reserves in North Vietnam using nine SSR markers. All of the nine loci showed polymorphic. Genetic diversity in population level was moderate (*Na* = 3.82; *Ne* = 2.23; *I* = 0.9, *He* = 0.38 and *Ho* = 0.5). The lowest levels of genetic diversity were detected in the Quang Ninh population (*Ho* = 0.32, *He* = 0.0.47), and the highest levels were detected in the Vinh Phuc population (*Ho* = 0.46, *He* = 0.52). Analysis of molecular variance determined a significant 66% of genetic variation within individuals. All five populations were a positive inbreeding coefficient (*Fis* > 0). These results revealed the excess of homozygotes and deficiency of heterozygotes in all populations. Cluster analysis using the unweighted pair group method with arithmetic average (UPGMA) with genetic similarity coefficients indicated that two genetic clusters were significantly correlated with the geographical distributions. Group I included individuals collecting from two provinces (Thanh Hoa and Ninh Binh), while group II included plants from 3 areas (Phu Tho, Vinh Phuc, and Quang Ninh). Our results provide valuable information for further studies in the conservation, management, and restoration of this species.

Keywords: *Cinnamomum parthenoxylon*, genetic diversity, habitat disturbance, species conservation, SSR.

Received: 6 October 2022; revised: 2 November 2022; accepted: 30 November 2022.

1. INTRODUCTION

Cinnamomum parthenoxylon (Jack) Meisn is a species having broad evergreen leaves, which are considered a big tree, distributed on a large scale in eighteen provinces in four different ecological regions of Vietnam: Northeast (Cao Bang, Lang Son, Bac Kan, Tuyen Quang, Thai Nguyen, Phu Tho, Vinh Phuc, Bac Giang, and Quang Ninh), North Central region (Quang Binh, Quang Tri, and Thua Thien Hue), South Central Region (Da Nang, Phu Yen, and Quang Nam) and Central Highlands (Kon Tum, Gia Lai and

[1] HaUI Institute of Technology, Hanoi University of Industry (HaUI)
[2] VietNam - College of Chemical Defence Officers
[3] Graduate University of Science and Technology, Vietnam Academy of Science and Technology
[4] Join Vietnam - Russia Tropical Science and Technology Research Centre
* Corresponding author: duydinhvu87@gmail.com

Lam Dong) [1, 2]. Moreover, this species is not only economically significant within the ecosystem of the forest, but they also have a large commercial value, particularly in the fields of woodworking, plastic manufacturing, essential oil extraction, and medicinal research [3, 4, 5, 6]. In addition, studies on the species cinnamon showed biological activity in the inhibition and treatment of many diseases such as cancer, antimicrobial, anti-fungal, and anti-diabetes [6, 7, 8, 9]. However, there are only some species, such as *C. verum*, *C. cassia*, *C. zeylanicum*, and *C. camphora* were deeply researched in biological activity, ingredients, and molecular mechanisms. Unfortunately, over the past decades, many populations of *C. parthenoxylon* and *C. cambodianum* have been endangered as a result of excessive exploitation and deforestation for medicinal materials and timber. Thus, the natural populations of the two species have experienced a sharp decline. Meanwhile, these species' regeneration is not good [10]. In Vietnam, these species are listed as endangered: *C. parthenoxylon* - CR A1a,c,d [2]. They are currently protected by both the central and local governments in Vietnam and need urgent conservation and restoration. Up to now, we lack information on genetic variation at population and species levels and the mating system within populations, especially the harmful effects of human activities.

DNA molecular marker techniques have been widely applied in plants' genetic diversity studies in recent decades [11, 12]. Of these, the microsatellite markers, i. e. simple sequence repeats (SSRs), which are dispersed throughout all genomes, are codominant and multiallelic markers and are considered highly sensitive for detecting polymorphisms Investigations on plant genetic diversity, population structure, gene flow, and mating systems have benefited greatly from the application of SSRs [13, 14]. Previous studies have been undertaken to investigate the genetic variation and verify the taxonomic status of the *Cinnamomum* species at the molecular level [15, 16, 17, 18, 19, 20, 21, 22, 23, 24]. Exploration of genetic variability within and among populations of *C. parthenoxylon* is of crucial importance and priority for species conservation, management, and restoration. To date, the genetic variability of this species is unknown. Therefore, the objective of the present study was to evaluate genetic variation within and among *C. parthenoxylon* populations using SSRs as genetic markers and to provide a platform for the conservation of the endangered species in Vietnam.

2. MATERIALS AND METHODS

2.1. Plant materials

Figure 1. Adult plant of *C. parthenoxylon* species collected in Xuan Lien Nature Reserve

[Photo: Pham Mai Phuong]

The inner bars or leaves of adult trees were collected from 5 natural populations of *C. parthenoxylon,* representing the range of its geographical distribution in Vietnam (Figure 1; Table 1). A total of 101 trees were randomly sampled and preserved in marked plastic bags with silica gel in the field, then transferred to Molecular Laboratory, Join Vietnam - Russia Tropical Science and Technology Research Centre and stored at - 30°C until used for DNA extraction.

Table 1. Information of sampled populations of *C. parthenoxylon* in Northern Vietnam

Population code	Sample size	Collection locality	Altitude	Longitude
Quang Ninh	20	Yen Tu National Forest, Quang Ninh province	2336326.03	391401.64
Vinh Phuc	13	Tam Dao National Park, Vinh Phuc province	2371699.59	569664.79
Phu Tho	19	Xuan Son National Park, Phu Tho Province	2338550.91	515494.31
Hoa Binh	19	Hang Kia - Pa Co Nature Reserve, Hoa Binh province	2293578.64	389485.28
Thanh Hoa	30	Xuan Lien Nature Reserve, Thanh Hoa province	2194294.51	524572.19

2.2. DNA extraction

Total genomic DNA was isolated from the inner bars using a DNA extraction kit (Norgenbiotek, Canada). Samples were ground in liquid nitrogen using a Mixer mill MM 400 (Retsch). The total amount of DNA was checked by electrophoresis on a 1.2% agarose gel and spectrophotometer using NanoDrop 2000 (Thermo Sci., Waltham, MA, USA) and then diluted to a concentration of 10 ng/µL and stored at -20°C for microsatellite analysis.

2.3. Microsatellite amplification

A total of nine SSR primers were chosen for this analysis from *C. parthenoxylon* species was performed by polymerase chain reaction (PCR) (Table 2). Reaction mixtures of 25 µL solution volumes containing 17.5 µL of ddH_2O, 2.5 µL of 1 X PCR buffer (10 mM Tris-HCl, 50 mM KCl, pH 8.4), 1.0 µL of $MgCl_2$ (2.5 mM), 0.5 µL of dNTPs (0.2 mM each), 1.5 µL of genomic DNA (10 ng), 1.0 µL of Tag DNA polymerase at 1.25 units and 0.5 µL of each primer at 10 pmol. PCR amplification was implemented in the GeneAmp PCR System

9700 (Applied Biosystems) as follows: an initial denaturing step at 94°C for 5 min, 35 cycles of 94°C for 1 min, annealing temperature for each primer pair at 54-56°C for 30 s and 1 min extension at 72°C. After the final cycle, samples were incubated at 72°C for 10 min and held at 4°C until used for analysis. The amplification products were determined using a Sequi-Gen®GT DNA electrophoresis system with 6% polyacrylamide gels in 1 x TAE buffer and then visualized by GelRed™ Nucleic Acid Gel Stain. PCR fragment sizes were detected using Gel-Analyzer software of GenoSens1850 (Clinx Science Instruments Co., Ltd) with a 25 bp DNA ladder (Invitrogen, Carlsbad, CA, USA).

Table 2. Characteristics of nine SSR markers used in this study

Locus	Primer sequences	Tm (°C)	Size (bp)	References
SSR1	F: 5'- ACGAGTTTCCACCGATTACG -3'	55	268	[15]
	R: 5'- ACTCCTTTCAGCACCGATTG - 3'			
SSR2	F: 5'- TTGTTAAAAACACCAACCCCA - 3'	55	200	
	R: 5'- CAGTGGGCCAAGTGTATCCT - 3'			
SSR3	F: 5'- ACGTGAATGTGAATGGGGTT- 3'	55	190	
	R: 5'- TAGGCAAAGACTCCGAAGGA - 3'			
SSR4	F: 5'- ATTCGGGTCTCTCTCCCTGT - 3'	55	250	
	R: 5'- CTCTCTCGCTGTCTCTGCCT - 3'			
SSR5	F: 5'- TGGAGAACAACTTTGGGAGG - 3'	55	120	
	R: 5'- TGTTCCATGTTACAGATACAG - 3'			
SSR6	F: 5'- ATATGGTCCCAACTCCCTCC - 3'	55	200	

	R: 5'- ACCGTCACCAGATCATCCAT - 3'			
SSR7	F: 5'- TCCCAACTGGACGAAGTTCT - 3'	55	240	
	R: 5'- TTTGCTCGCTGTTATGATGC - 3'			
SSR8	F: 5'- ATCCTCCCAAGGACGCTTAT - 3'	55	130	
	R: 5'- CCTTCAAGGAAAGAAGGGCT - 3'			
SSR9	F: 5'- CACCACCTTCTCCTTCCAAA - 3'	55	230	
	R: 5'- TTGTTGGGGTCTCCAAACTC - 3'			

2.4. Genetic diversity analysis

The presence of null alleles for microsatellite data was tested using the MICRO-CHECKER v.2.2.3 [25]. We estimated genetic diversity, including the number of alleles per locus (Na), the average number of effective alleles per locus (Ne), Shannon's information index (*I*), observed heterozygosity (Ho) and expected heterozygosity (He), the inbreeding coefficient (*Fis*), an analysis of molecular variance (AMOVA), genetic distance and genetic identity using the program GenAlEx v.6.5 [26]. A UPGMA (Unweighted Pair Group Method) tree was constructed for genetic association among populations using POPTREE [27]

3. RESULTS

3.1. Evaluation of genetic diversity

Nine SSR loci were amplified consistently under standard conditions and used to assess the population's genetic structure. All primers were submitted to amplification cycles with primer annealing at 55°C and were polymorphic in *C. parthenoxylon*. Out of the nine SSR markers, five loci showed evidence for a null allele. This population is possibly in Hardy Weinberg equilibrium with loci SSR1, SSR2, SSR3, SSR4, and SSR9, indicated by signs of a null allele. The number of alleles per locus (Na) ranged from 3.33 in the Vinh Phuc population to 4.56 in the Thanh Hoa population, an average of 1.5, and the effective alleles per locus (*Ne*) within populations varied from 2.1 (Phu Tho) to 2.47 (Thanh Hoa), with an average of 2.23. The mean observed (*Ho*) and expected heterozygosity (*He*) for each population were 0.38 and 0.5, respectively. The lowest heterozygotes were found in the Quang Ninh population (*Ho* = 0.32 and *He* = 0.47), while the highest heterozygotes were observed in the Vinh Phuc population (*Ho* = 0.46 and *He* = 0.52). The inbreeding coefficient (*Fis*) varied among populations, from 0.01 in Vinh Phuc to 0.33 in Quang Ninh with an average of 0.2, suggesting a mixed breeding system of both inbreeding and outbreeding (Table 3).

Table 3. Genetic diversity estimates nine populations of *C. parthenoxylon*

Population	N	Na	Ne	I	Ho	He	Fis
Quang Ninh	20	3.89	2.24	0.93	0.32	0.47	0.33
Vinh Phuc	13	3.33	2.16	0.85	0.46	0.52	0.01
Phu Tho	19	3.44	2.10	0.83	0.35	0.47	0.26
Hoa Binh	19	3.89	2.18	0.89	0.39	0.49	0.14
Thanh Hoa	30	4.56	2.47	1.02	0.36	0.54	0.30
Mean		3.82	2.23	0.90	0.38	0.50	0.20

Note: N: sample size; I: Shannon's information index; Na: alleles per locus; Na: effective alleles; Ho and He: observed and expected heterozygosities; Fis: inbreeding coefficient.

3.2. Genetic differentiation and AMOVA

The analysis of molecular variance revealed genetic variation among and within populations of the *C. parthenoxylon* (Table 4). For *C. parthenoxylon*, the majority of the overall variance could be attributable to differences that occurred among individuals (66%, $p<0.001$), within populations (28%, $p<0.001$), and among populations (7%, $p<0.001$).

Table 4. Analysis of molecular variance of *C. parthenoxylon*

Source of variation	d.f.	Sum of squares	Variance component	Total variation (%)	P value
Among populations	4	38.34	9.59	7%	<0.001
Within populations	96	292.35	3.05	28%	<0.001
Within individuals	101	167.50	1.66	66%	<0.001
	201	498.19			

The mean value of Nei's genetic distance between the studied populations of *C. parthenoxylon* ranged from 0.03 (Phu Tho/Quang Ninh) to 0.20 (Vinh Phuc/Hoa Binh) (Table 5). Low values of Nei's genetic distance were found between population pairs of Phu Tho/Quang Ninh (0.03), Vinh Phuc/Quang Ninh (0.08), and Thanh Hoa/Phu Tho (0.08). The highest values of Nei's genetic distance were found between population pairs of Vinh Phuc/Hoa Binh (0.20). Similarly, the Genetic identity of *C. parthenoxylon* varied from 0.82 (Hoa Binh/Vinh Phuc) to 0.97 (Quang Ninh/Phu Tho).

Table 5. Nei's genetic identity (above diagonal) and genetic distance (below diagonal) within populations of *C. parthenoxylon*

	Thanh Hoa	Vinh Phuc	Phu Tho	Quang Ninh	Hoa Binh
Thanh Hoa	-	0.84	0.92	0.94	0.91
Vinh Phuc	0.18	-	0.90	0.92	0.82
Phu Tho	0.08	0.10	-	0.97	0.84
Quang Ninh	0.06	0.08	0.03	-	0.89
Hoa Binh	0.10	0.20	0.18	0.12	-

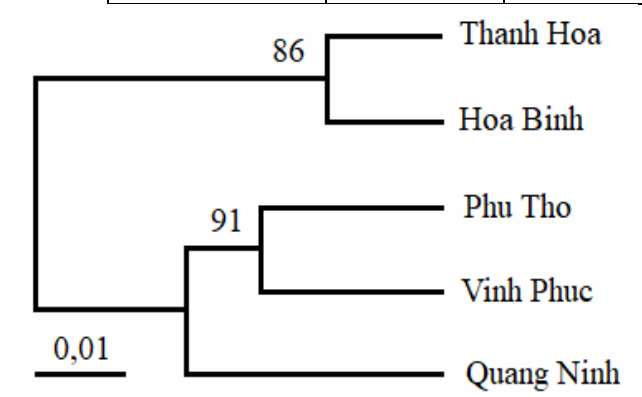

Figure 2. UPGMA dendrogram based on Nei's (1972) genetic distance among populations.

The studied populations were clustered using the UPGMA dendrogram based on pairwise genetic distances (Figure 2). The geographically closed populations were clustered together. Two different clusters were generated in the phylogenetic tree. The first cluster contained two populations (Thanh Hoa and Hoa Binh). The second included three populations (Phu Tho, Vinh Phuc, and Quang Ninh). However, the Quang Ninh population was separated clearly from geographically close populations (Phu Tho and Vinh Phuc).

4. DISCUSSION

The high level of genetic diversity within a species reflects its evolutionary history and eco-geographical environment. Species related to wide distribution patterns, large population size, long lifespan, predominantly outcrossing,

and successional stages often maintain high genetic diversity [28, 29]. Our research found that *C. parthenoxylon* (*Na* = 0.38, *Ne* = 2.23) had lower than *C. camphora* in Japan (*Na* = 13.37, *Ne* = 3.78) and in China (*Na* = 21.73, *Ne* = 9.51) [21, 22] but higher than *C. balansae* (*Na* = 1.9, *Ne* = 1.5) [15]. The results obtained in the present study indicate *C. parthenoxylon* exhibited a moderate level of genetic diversity (*Ho* = 0.38 and *He* = 0.5). High levels of genetic diversity in other *Cinnamomum* species based on SSR markers have been reported, such as *Ho* = 0.53-0.6 and *He* = 0.55-0.68 analysis from 104 adult trees of *C. camphora* collection three populations (Meiji Jingu (Shinto Shrine), Kajiya Plantation, and Manazuru Peninsula) in Japan [21], genetic diversity estimates of *C. camphora* (300 trees) in China and Taiwan with *Ho* = 0.728 and *He* = 0.878 and *C. Camphora* (504 trees) with *Ho* = 0.614 and *He* = 0.714) [22]. However, low genetic diversity has been reported in some other *cinnamomum*, such as *C. balansae* (*Ho* = 0.244, *He* = 0.264) [15], *C. camphora* (*Ho* = 0.3449, *He* = 0.4254) [30]. *Cinnamomum* species are widely distributed and have a long life. They are predominantly outcrossed via gene flow within and between populations. Pollen dispersal plays an important role in the transfer from one generation to the next. Species with a narrow distribution or endangered species tend to reduce genetic variability and maintain low genetic diversity [28, 31]. Our results indicated that *C. parthenoxylon* is endangered and has medium genetic diversity. Its habitats are degraded and isolated. Deforestation and over-exploitation of *C. parthenoxylon* may have a major impact on genetic variation and lead to low heterozygotes within populations and species while also affecting the number of alleles in all studied populations. The decrease in allelic diversity may be the result of a small population size. In this study, the two populations of Phu Tho and Quang Ninh had low genetic diversity compared to the remaining populations. These results suggested that high habitat disturbance and fragmentation had a negative effect on genetic variability within populations.

Similarly, AMOVA analysis indicated that most of the genetic variation was distributed among individuals (66%). This can be a consequence of the decrease in genetic divergence among populations. *C. parthenoxylon* is a long-living and outcrossing species. The species is insect-pollinated by insects and predominantly outcrossed. Pollen dispersal could contribute mainly to the gene flow and population structure of *C. parthenoxylon*. Moreover, its seeds can be dispersed by animals (rodents and birds). UPGMA tree showed two different groups of genetically mixed individuals of *C. parthenoxylon*. Two populations, Thanh Hoa and Hoa Binh were closed together and formed a genetic cluster. Quang Ninh population was separated from two populations (Phu Tho and Vinh Phuc) and formed one cluster by geographical distances.

Furthermore, our results showed that the inbreeding coefficient (*Fis*) was significantly positive in all populations. These factors suggested that the existence of biparental inbreeding can reduce genetic diversity within the *C. parthenoxylon* populations. This might be mainly attributed to limited pollen dispersal. To prevent inbreeding depression and gradually restore the *C. parthenoxylon* population size in the future, ex situ conservation through seed collection from natural populations into local gardens will be the material source to increase the variability of progenies in natural populations.

5. CONCLUSION

In five provinces of North Vietnam, *C. parthenoxylon* showed moderate genetic diversity. Two genetic groups connected to habitat degradation and regional separation were discovered using clustering studies.

ACKNOWLEDGEMENTS

This study was funded by Vietnam National Foundation for Science and Technology Development (NAFOSTED), project # 106.06-2021.02. We are grateful to the Institute of Tropical Ecology, Join Vietnam - Russia Tropical Science and Technology Research Centre, Graduate University of Science and Technology, Vietnam Academy of Science and Yen Tu National Park - Quang Ninh province, Tam Dao National Park - Vinh Phuc province, Xuan Son National Park - Phu Tho Province, Hang Kia - Pa Co Nature Reserve - Hoa Binh province and Xuan Lien Nature Reserve - Thanh Hoa province for support of our field work.

REFERENCES

1. Nguyen Kim Dao. 2010. Flora of Vietnam - Lauraceae. Science and Technics Publishing House. 20:22-234

2. MOST, VAST. 2007. Vietnam red data book, part II. plants. Pub Sci Tech. 289-290

3. Yan YM, Fang P, Yang MT, Li N, Lu Q, Cheng YX. 2015. Anti-diabetic nephropathy compounds from *Cinnamomum cassia*. *J Ethnopharm* 165: 141–147.

4. Chen TW, Tsai KD, Yang SM, Wong HY, Liu YH, Cherng J, Chen TW, Tsai KD, Yang SM, Wong HY, Liu YH, Cherng J, Chou KS, Wang YT, Cuizon J, Cherng JM. 2016. Discovery of a novel anti-cancer agent targeting both topoisomerase I and II as well as telomerase activities in human lung adenocarcinoma A549 cells *in vitro* and *in vivo*: *Cinnamomum verum* component cuminaldehyde. *Curr Cancer Drug Targets* 16(9): 796-806

5. Balijepalli MK, Buru AS, Sakirolla, Pichika MR. 2017. *Cinnamomum* genus: A review on its biological activities. *Int J Pharm* Pharm Sci 9(2): 1–11.

6. Lee SC, Wang SY, Li CC, Liu CT. 2018. Anti-inflammatory effect of cinnamaldehyde and linalool from the leaf essential oil of *Cinnamomum osmophloeum* Kanehira in endotoxin-induced mice. *J Food Drug Anal* 26(1): 211–220.

7. Xu S, Zhong QY, Wei Q. 2014. Anti-hepatoma effect of safrole from *Cinnamomum longepaniculatum* leaf essential oil *in vitro*. *Int J Clin Exp Pathol* 7: 2265–72.

8. Kim EC, Kim HJ, Kim TJ. 2015. Water extract of *Cinnamomum cassia* suppresses angiogenesis through inhibition of VEGF receptor 2 phosphorylation. *Biosci Biotech Bioch* 79(4): 617–624.

9. Li H, Ge Y, Luo Z, Zhou Y, Zhang X, Zhang J, Fu Q. 2017. Evaluation of the chemical composition, antioxidant and anti-inflammatory activities of distillate and residue fractions of sweet basil essential oil. *J Food Sci Technol* 54(7): 1882–1890.

10. Le Thi Dien, Pham Minh Toan, Le Phu Anh. 2010. Researching on regeneration characteristics of *Cinnamomum parthenoxylon* in Bach Ma National Park. *Hue University Journal of Science* (2): 33-41.

11. Tam NM, Trang NTP, Hoa NT. 2011. Genetic diversity of an endangered species *Fokienia hodginsii* (Cupressaceae). *Afr. J. Biotechnology* 10(71): 15838-44

12. Zhang X, chen G, Ma Y, Ge J, Sun W. 2015. Genetic diversity and population structure of Buddleja crispa Bentham in the

Himalaya-Hengduan mountains region revealed by AFLP. *Biochemical systematics and ecology* 58: 13-20.

13. Pandey M, Geburek T. 2009. Successful cross-amplification of *Shorea* microsatellites reveals genetic variation in the tropical tree, *Shorea robusta* Gaertn. *Hereditas* 146: 29-32.

14. Monteiro ER, Mangolin CA, das Neves AF, Orasmo GR, da Silva JGM, sa Siva Machado MFP. 2015. Genetic diversity and structure of populations in *Pilosocereus gounellei* (Cactaceae) in the Caatinga biome as revealed by heterologous microsatellite primers. *Biochemical Systematics and Ecology* 58: 7-12.

15. Cui B, Vu DD, Vu DG, Bui TTX, Rahman SU, Pham MP, Nguyen MT, Nguyen VS, Shah SNM, Tran VT. 2022. Genetic diversity and population structure of Cinnamomum balansae Lecomte inferred by microsatellites. *Open Life Sciences* 17: 323-332

16. Lin TP, Cheng YP, Huang SG. 1997. Allozyme variation in four geographic areas of *Cinnamomum kanehlrae. Journal of Heredity* 88: 433-438

17. Joy P, Maridass M. 2008. Inter species relationship of *Cinnamomum* species using RAPD marker analysis. *Ethnobotanical Leaflets* 12: 476-480.

18. Kuo DC, Lin CC, Ho KC, Cheng YB, Hwang SY, Lin TP. 2010. Two genetic divergence centers revealed by chloroplastic DNA variation in populations of *Cinnamomum kanehirae* Hay. *Conserv Genet* 11: 803–812.

19. Lee SC, Chiou SJ, Yen JH, Lin TY, Hsieh KT, Yang JC. 2010. DNA Barcoding *Cinnamomum osmophloeum* Kaneh. Based on the partial non-coding ITS2 region of ribosomal genes. *J Food Drug Anal* 18(2): 128-135

20. Ho KY, Hung TY. 2011. Cladistic relationships within the genus *Cinnamomum* (Lauraceae) in Taiwan based on analysis of leaf morphology and inter-simple sequence repeat (ISSR) and internal transcribed spacer (ITS) molecular markers. *African Journal of Biotechnology* 10(24): 4802-4815.

21. Kameyama Y, 2012. Development of microsatellite markers for *Cinnamomum camphora* (Lauraceae). *American Journal of Botany*: e1-e3

22. Kameyama Y, Furumichi J, Li JX, Tseng YH. 2017. Natural genetic differentiation and human-mediated gene flow: the spatiotemporal tendency observed in a long-lived *Cinnamomum camphora* (Lauraceae) tree. *Tree genet genomes* 13: 38

23. Abeysinghe PD, Samarajeewa NGCD, Li G, Wijesinghe KGG. 2014. Preliminary investigation for the identification of Sri Lankan *Cinnamomum* species using randomly amplified polymorphic DNA (RAPD) and sequence-related amplified polymorphic (SRAP) markers. *J Natn Sci Foundation Sri Lanka* 42 (3): 201-208

24. Gwari G, Bhandari U, Naik G, Haider SZ, Chauhan N. 2016. Genetic diversity in *Cinnamomum tamala* Nees. accessions through DNA fingerprinting using molecular markers. *Indian J Agric Res* 50 (5): 446-450

25. Van Oosterhout C, Hutchinson WF, Wills DPM. 2004. Micro-Checker: software for identifying and correcting genotyping errors in microsatellite data. *Mol Ecol Notes* 4: 435-538.

26. Peakall R, Smouse PE. 2012. GenAlEx 6.5: genetic analysis in excel. Population

genetic software for teaching and research an update. *Bioinformatics* 28: 2537-2539.

27. Takezaki N, Nei M, Tamura K. 2010. Software for constructing population trees from allele frequency data and computing other population statistics with Windows interface. *Mol Evol* 27: 747-752.

28. Hamrick JL, Godt MJW. 1996. Effects of history traits on genetic diversity in plant species. *Phil Trans Roy Soc Lond B Biol Sci* 351:1683-1685.

29. White TL, Adams WT, Neale DB. 2007. Forest genetics. CABI Publshing, Boston, MA, USA. 149-186.

30. Li Z, Zhong Y, Yu F, Xu M. 2018. Novel SSR marker development and genetic diversity analysis of *Cinnamomum camphora* based on transcriptome sequencing. *Plant Genetic Resources* 16(6): 568-571

31. Nyborn H. 2004. Comparison of different nuclear DNA markers for estimating intraspecific genetic diversity in plants. *Molecular Ecology* 13:1143-1155.

A SURVEY ON CATTLE LUMPY SKIN DISEASE IN SMALL SCALE HOUSEHOLD OF HO CHI MINH CITY, VIETNAM

Dang Hoang Dao[1, *]

ABSTRACT

In this study was to evaluate the prevalence of Lumpy Skin Disease (LSD), prevalence by breed, age, mortality at disease and clinical symptoms in cattle. Surveyed using a structured questionnaire used to collect information on primary data, at 120 household farms on the outskirts of Ho Chi Minh city, Vietnam, from July 2020 to July year 2021. Results showed that cows infected with LSD were 1212 cows (96%) out of the total of 1259 surveyed cows. The rates of LSD by age under 6 months, from 6 to 12 months, and over 12 months of age were 19.3 respectively; 16; 64.7%. The incidence of LSD cows according to the breeds Golden Cow, Lai Sind, Blanc Bleu Belge (BBB), Charolais, Red Angus, 3/4 Holstein Frisan (HF) such as 24.4; 22.3; 6.5; 9.9; 36.9%. The mortality rates by age under 6 months, from 6 to 12 months, and over 12 months such as 4.7; 0.5; 0%. The survey showed that severe clinical symptoms were full of symptoms in calves under 6 months including fever (100%), nodules on the skin (100%), arthritis inflammation (98%), respiratory inflammation (100%); from 6 to 12 months including fever (100%), nodules on the skin (100%), arthritis inflammation (3%), respiratory inflammation (1%); above 12 months including fever (100%), nodules on the skin (100%), arthritis inflammation (2.9%), respiratory inflammation (0%).

Keywords: *Lumpy Skin Disease (LSD), cattle, capripoxvirus, Vietnam*

Received: 9 Septembert 2022; revised: 3 November 2022; accepted: 29 November 2022.

1. INTRODUCTION

LSD is a highly infectious viral disease of cattle, caused by LSD virus (LSDV) which belongs to the genus *Capripoxvirus* of family *Poxviridae.* LSD is a poxvirus disease of cattle characterized by fever, nodules on the skin, mucous membranes and internal organs, emaciation, enlarged lymph nodes, oedema of the skin, and sometimes death [1, 2]. The disease is of economic importance as it can cause a temporary reduction in milk production, temporary or permanent sterility in bulls, damage to hides and death due to secondary bacterial infections. LSD was first seen in Zambia in 1929 then spreads into most countries limited to sub-Saharan Africa in the next decades [3], spreading into Botswana by 1943 [4], and then into South Africa, where it affected over eight million cattle causing

[1] Faculty of Veterinary Medicine – Animal Husbandry, HUTECH University, Ho Chi Minh City,Vietnam
* Corresponding author: dh.dao@hutech.edu.vn

major economic loss. The LSD virus isolated in these first outbreaks was 100% identical to viruses isolated in China (2019) based on the p32 and RP030 genes [5]. The first outbreak of LSD were reported in Lang Son Province of Vietnam, and an official documents has been submitted to Office International des Epizooties (OIE) on 1 November 2020 [5]. LSD occurred in many provinces and cities in Vietnam in 2020. That is why we conducted the study "*A survey on cattle LSD in small scale household of Ho Chi Minh city, Vietnam*".

2. MATERIALS AND METHODS

2.1. Study area and population

The survey was conducted in suburb around of Ho Chi Minh city including Binh Chanh, Hoc Mon, Cu Chi, Can Gio districts and District 9, 12 from July 2020 to July 2021. Ho Chi Minh city is located in the Southeast, a subequatorial climate with two distinct seasons: the rainy season from May to November and the dry season from December to April of the following year, it has the average temperature in range 25 - 28^{0}C, the humidity levels average 75% throughout the year but are higher during the rainy season. The environment is ideal for the reproduction and growth of blood-feeding arthropods such as mosquitoes, biting flies, ticks, and fleas. Small cattle ranches in the rural areas are often unhygienic, which accelerates the abundance of vectors. Small-scale farmers typically feed their cattle in common pastures, nearby open fields, or roadside grass, which provides cattle with opportunities to mix with other herds and thus modulate the transmission of the LSD.

2.2. Sample collection

The scale of cow breeding in Ho Chi Minh city is quite large, so the survey will use random sampling and conduct a survey of 120 households. Each household had 2 - 20 animals. Each district (Binh Chanh, Hoc Mon, Cu Chi, Can Gio districts and District 9; 12) surveyed 20 households. Suburban districts should concentrate on cow farmers. To obtain a better understanding of the epidemiology of LSD in the Ho Chi Minh city settings, data were collected in collaboration with the local veterinary services using a standard, well-structured questionnaire. The information recorded in the questionnaire is as follows: Cow infected with LSD; age of LSD: less than 6 months, from 6 to 12 months, over 1 year; breed of cow with LSD (Golden Cow breed, Lai Sind breed, BBB breed, Charolais breed, Red Angus breed, dairy cow breed); the age of cow dies of LSD. Clinical symptoms such as fever, nodules on the skin, arthritis, respiratory inflammation by age under 6 months of age, from 6 to 12 months of age, over 1 year of age.

2.3. Data analysis

Data were analyzed descriptive statistic such as percentages in the ANOVA program of the Minitab software (Minitab 2000) and software Microsoft Excel 2010.

3. RESULT AND DISCUSSION

According to a survey in 120 households with 1259 cows. After the study, we had the result and shown by table 1.

Table 1. Percentage of cow with LSD by surveyed districts

	n = 1259 (cows)	LSD (cows)	Rate (%)
Binh Chanh	107	98	92
Hoc Mon	343	343	98
Cu Chi	385	368	96
Can Gio	86	79	92
District 9	111	111	100
District 12	227	213	94
Total	1259	1212	96

Table 1 shows that a total of 1212 (96%) cows were infected with LSD out of a total of 1259 surveyed cows. In which, district 9 has an infection rate of 100%, Hoc Mon district 98%, district 12 (94%), Cu Chi district 96%, Binh Chanh district (92%), Can Gio (92%). Small cattle ranches in the rural areas are often unhygienic, which accelerates the abundance of vectors. LSD tends to have a mortality of <10% and a morbidity of 0% - 90% [6].

Table 2. Percentage of cows with LSD by age stage

	Age stage (months)			Total
	<6	6 - 12	>12	
LSD (cow)	234	194	784	1212
Rate (%)	19.3	16	64.7	100

Table 2 showed that the disease occurs at any age. The highest age of cows is over 12 months (64.7%), followed by the age of less than 6 months (19.3%) and the lowest is between 6 and 12 months (16%). Analysis of the age prevalence of LSD revealed that the highest prevalence was observed in ages of > 3 years (21.8%, n = 36). This was followed by 1–3 years (16%, n = 32) and < 1 year (11.8%, n = 10) with no statistically significant differences. The prevalence was 18% and 16.3% in females and males, respectively [7].

Table 3. Percentage of cows with LSD by breed cow

	Breed (cows)					
	Golden Cow	Lai Sind	BBB	Charolais	Red Angus	¾ HF
LSD (cow) n = 1212	0	296	271	78	120	447
Rate (%)	0	24.4	22.3	6.5	9.9	36.9

Table 3 showed that cattle breeds Lai Sind, BBB, Charolais, Red Angus, ¾ HF all infected with LSD accounted for 24.4; 22.3; 6.5; 9.9; 36.9%. Particularly for Golden Cow not infected (0%). The most susceptible to the disease was ¾ HF (36.9%). Through the survey, we found that the rate of foreign varieties infected with LSD was higher than that of domestic varieties.

Table 4. Percentage of dead cows with LSD by age stage

	Age stage (months)		
	<6	6 - 12	>12
LSD (cow)	234	194	784
Die (cow)	11	1	0
Rate, %	4.7	0.5	0

Table 4 showed that the age groups with LSD mortality rates at the age of less than 6 months, from 6 months to 12 months, and over 12 months are 4.7, respectively; 0.5; 0%. In which, the mortality rate was highest for the period under 6 months old (4.7%), the lowest for the age group over 12 months old (0%).

On July 13, 2020, Ministry of Agriculture and Rural Affairs of China officially announced 7 LSD outbreaks in 6 provinces (Fujian, Jiangxi, Guangdong, Anhui, Zhejiang) in southeast China. It was noted two independent LSD outbreaks were determined in Jiangxi. The 7 LSD outbreaks occurred between June 2 and July 7, leading to 55 infection cases and 6 death cases. On July 7, 2020, a LSD outbreak affecting 36 cattle individuals with one death case was announced in Taiwan Island. As of now, a total of 9 LSD outbreaks were reported in 7 provinces in China, infecting 156 and killing 7 cattle. The total morbidity and mortality in the 9 outbreaks were 19.5% (156/801) and 0.9% (7/801) respectively. The morbidity and mortality in each of the separate outbreaks

ranged 6.6% - 100% and 0% -16.7% respectively (http://www.xmsyj.moa.gov.cn/yqfb/202007/t20200715_6348686.htm) [8].

Table 5. Percentage of LSD with clinical symptoms of fever, nodules on the skin, arthritis inflammation, respiratory inflammation by age stage

Age stage (months)	Clinical Symptom				LSD (cows)
	Fever	Nodules on the skin	Arthritis inflammation	Respiratory inflammatiom	
<6	234 (100%)	234 (100%)	231 (98%)	236 (100%)	n = 234
6 - 12	194 (100%)	194 (100%)	6 (3%)	2 (1%)	n = 194
>12	784 (100%)	784 (100%)	7 (2.9%)	0 (0%)	n = 784

Table 5 showed that all age stages of LSD infection showed fever, nodules on the skin (100%). The clinical manifestations of arthritis were highest at the age of less than 6 months (98%), the lowest at the age of over 12 months (2.9%). For clinical symptoms of respiratory infection, the highest was in the period of less than 6 months old (100%), the lowest was in the age of over 12 months (0%). Through the survey, we found that clinical symptoms were severe in the period under 6 months of age.

Table 6. Figure clinical symptom of LSD

Figure 1. Nodules on the skin

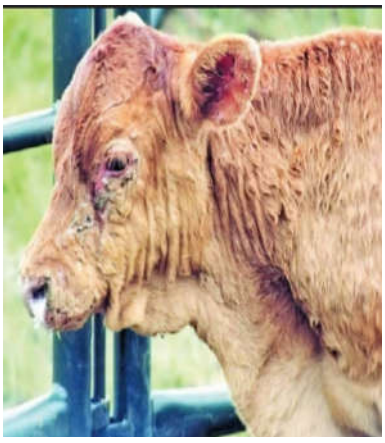

Figure 2. Respiratory inflammation

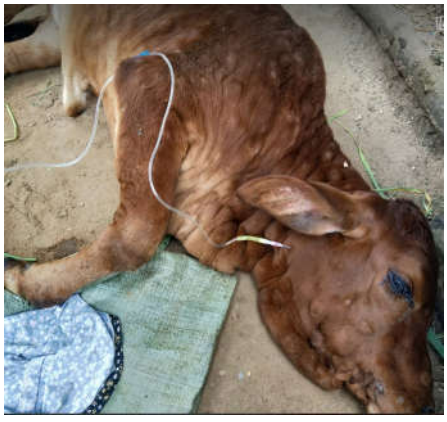

Figure 3. Arthritis inflammation

Table 6 showed the clinical symptoms in calves under 6 months of age. When calves are infected with LSD, there are all clinical symptoms such as: fever, nodules on the skin, arthritis inflammation, respiratory inflammation.

4. CONCLUSION

This study showed that it is LSD that infects all age groups. But causing severe clinical problems as well as causing death at the age of less than 6 months is 100; 4.7%.

ACKNOWLEDGMENTS

We would like to gratefully acknowledged of cow farmers in Ho Chi Minh city provided the information. This work was supported by Mr. Hoai is a Veterinary technician from the Center for Research and Transfer of Science and Technology, Nong Lam University, Ho Chi Minh city for supporting to take information.

REFERENCES

1. Abutarbush S M., Ababneh M M., Al Zoubi I G., Al Sheyab O M., Al Zoubi M G., Alekish M O., Al Gharabat R J., (2015). Lumpy Skin Disease in Jordan: Disease Emergence, Clinical Signs, Complications and Preliminary-associated Economic Losses. *Transbound Emerg Dis, 62*(5): 549-54. doi: 10.1111/tbed.12177.

2. Babiuk, S., Bowden T R., Boyle D B., Wallace D B., Kitching R P., (2008). Capripoxviruses: An emerging worldwide threat to sheep, goats and cattle. *Transbound Emerg Dis, 55*(7): 263-272. doi:10.1111/j.1865-1682.2008.01043.

3. Mercier, A., Arsevska, E., Bournez, L., Bronner, A., Calavas, D., Cauchard, J., Lancelot, R. (2018). Spread rate of lumpy skin disease in the Balkans, 2015-2016. *Transbound Emerg Dis, 65*(1), 240-243. doi:10.1111/tbed.12624.

4. Haig D. (1957). Lumpy skin disease. *Bull. Epizoot. Dis. Afr.*, 5, 421–430.

5. Ha Thi Thanh Tran, Anh Duc Truong, Anh Kieu Dang, Duc Viet Ly, Chinh Thi Nguyen, Nhu Thi Chu, Tuan Van Hoang, Huyen Thi Nguyen, Vinh The Nguyen, Hoang Vu Dang (2021). Lumpy skin disease outbreaks in Vietnam, 2020. *Transbound Emerg Dis, 68*(3): 977-980. doi: 10.1111/tbed.14022.

6. Sprygin, A., Artyuchova, E., Babin, Y., Prutnikov, P., Kostrova, E., Byadovskaya, O., & Kononov, A. (2018). Epidemiological characterization of lumpy skin disease outbreaks in Russia in 2016. *Transbound Emerg Dis, 65*(6), 1514-1521. doi:10.1111/tbed.1288.

7. Mahmoud M. Elhaig, Abdelfattah Selim, and Mohamed Mahmoud., 2017. Lumpy skin diesease in cattle: Frequency of occurrence in a dairy farm and a preliminary assessment of its possible impact on Egyptian buffaloes. 84(1): 1393.

8. http://www.xmsyj.moa.gov.cn/yqfb/202007/t20200715_6348686.htm

INFLUENCE OF HYDROLYSIS TIME ON THE FUNCTIONAL PROPERTIES OF PROTEIN HYDROLYSATES FROM SAILFISH TRIMMINGS

Nguyen Thi My Huong[1, *]

ABSTRACT

Influence of hydrolysis time on the functional properties of protein hydrolysates from sailfish trimmings was studied. Four protein hydrolysates were obtained by hydrolysis of sailfish trimmings with enzyme Flavourzyme 0.5% at the temperature of 50°C and different hydrolysis times (2 h, 4 h, 6 h, 8 h). The study results showed that the degree of hydrolysis increased with the increase of hydrolysis time. The degrees of hydrolysis of the protein hydrolysates from sailfish trimmings after 2 h, 4 h, 6 h and 8 h of hydrolysis were 18.6%, 25.8%, 29.7% and 30.5%, respectively. The protein hydrolysate from sailfish trimmings after 8 h of hydrolysis had contents of moisture 7.2%, protein 73.4%, lipid 0.6% and ash 8.6%. The sailfish trimmings protein hydrolysate had a total amino acid content of 32.87 g/100 g of protein hydrolysate and essential amino acid content of 12.32 g/100 g of protein hydrolysate. The ratio of essential amino acids to total amino acids was 37.48%. The protein hydrolysate was rich in glycine, glutamic, aspartic, proline, leucine and alanine. The solubility of sailfish trimmings protein hydrolysates increased when hydrolysis time and degree of hydrolysis increased. The sailfish trimmings protein hydrolysates had solubility in the range of 88.3 - 95.2%. The study results showed that the foaming capacity of sailfish trimmings protein hydrolysate reached a maximum value (45.8%) at hydrolysis time of 2 h and degree of hydrolysis of 18.6%. The foaming capacity of protein hydrolysates from sailfish trimmings decreased when the hydrolysis time increased from 2h to 8h of hydrolysis. The emulsifying properties of protein hydrolysates obtained after 2 h, 4 h, 6 h and 8 h of hydrolysis of sailfish trimmings were 29.2 ml/g, 24.9 ml/g, 18.8 ml/g and 17.6 ml/g, respectively. The sailfish trimmings protein hydrolysates were found to have high nutritional value and good functional properties. The study results suggested that protein hydrolysates from sailfish trimmings could be used as a protein source in food systems and were a promising potential food ingredient.

Keywords: *Fish protein hydrolysate, functional property, nutritional property, sailfish trimmings.*

Received: 6 October 2022; revised: 31 October 2022; accepted: 29 November 2022.

1. INTRODUCTION

Seafood processing industry generates up to 60% by - products including head, frames, viscera, skin, trimmings, fins, roes, and only 40% fish products for human consumption [1]. The sailfish processing industry generates a large amount of trimmings, which are a rich source of protein. High protein content in fish trimmings make them more perishable, may bring undesirable effects to environment pollution. Production of protein hydrolysate from fish by - products by enzymatic hydrolysis is one way to add value to fish by - products. Enzymatic hydrolysis is the process of breaking down the peptide bonds of the parent protein using proteases, whereas the degree of hydrolysis is the ratio of the number of peptides cleaved to the number of peptide bonds contained in the protein mass [2]. Enzymatic hydrolysis is one of the most efficient methods to recover proteins from fish by - products. Moreover, the enzymatic hydrolysis of fish proteins improved its functional properties, including solubility, foaming capacity and emulsifying capacity.

Fish protein hydrolysates have a high content of amino acids and are used as available sources of protein for humans due to their good functional properties. However, there is a little information regarding protein hydrolysates from the sailfish trimmings. Therefore, the study on influence of hydrolysis time on the functional properties of protein hydrolysates from the sailfish trimmings was necessary. The fish protein hydrolysates could be used in foods for the production of nutritional drinks and milk substitutes. In addition, they could be used as ingredients to aid in foam formation and stability in some products such as beer, fresh cream, and to aid in emulsion formation and stability in some products such as margarine and sausages. Fish protein hydrolysates have been used for incorporation into different food systems such as cereal products, fish and meat products, desserts and crackers [3].

2. MATERIALS AND METHODS

2.1. Sailfish trimmings

Sailfish (*Istiophorus platypterus*) trimmings were provided by Hoang Hai, a seafood processing company in Nha Trang, Vietnam. The sailfish trimmings were frozen and transported to the laboratory. After their arrival, they were thawed and ground in a grinder through 3 mm plate. The minced materials were packed in plastic bags (0.5 kg per unit), frozen and stored at - 20°C until use.

2.2. Enzyme Flavourzyme

Flavourzyme is a fungal protease/peptidase complex produced by submerged fermentation of a selected strain of *Aspergillus oryzae* and it contains both endoprotease and exopeptidase activities. The declared activity was 500 LAPU/g (Leucine Amino Peptidase Units per gram). This commercial enzyme was produced by Novozymes A/S (Bagsvaerd, Denmark). The optimal working conditions provided by the manufacturer for Flavourzyme are at 50°C and pH 5 - 7.

[1] Faculty of Food Technology - Nha Trang University
* Email: huongntm@ntu.edu.vn

2.3. Preparation of fish protein hydrolysate from sailfish trimmings

The four samples of sailfish trimmings was hydrolyzed with the water/trimmings ratio of 1/1 using Flavourzyme with 0.5% of the weight of sailfish trimmings (w/w) at 50°C and natural pH of substract (pH = 6) for 2 h, 4 h, 6 h and 8 h. After hydrolysis, the enzyme was inactivated by heating in a water bath at 85°C for 15 min. The mixture was centrifuged at 10000 rpm for 20 min to separate the liquid protein hydrolysate and the sludge. The liquid protein hydrolysate was then spray - dried to obtain the protein hydrolysate powder which was stored in a sealed plastic bag at 4°C until analyses.

2.4. Analysis methods

The moisture content was determined by drying the samples in an oven at 105°C until constant weight. Ash content was measured by incinerating the samples in a furnace at 600°C. Total nitrogen content was determined by the Kjeldahl method. Crude protein content was determined by multiplying total nitrogen content by 6.25. Lipid content was determined according to Folch *et al.* (1957) [4]. Amino acid composition was determined according to Kechaou *et al.* (2009) [5]. Degree of hydrolysis was determined according to Nguyen *et al.* (2011) [6].

Solubility of fish protein hydrolysate was determined according to Klompong *et al.* (2007) [7]. Each 200 mg of protein hydrolysate sample was dispersed in 20 ml of deionized water. The mixture was stirred at the room temperature for 30 min and centrifuged at 7500 rpm for 15 min. Protein content in the supernatant was determined using the biuret method. The solubility of fish protein hydrolysate, defined as the amount of soluble protein from the total protein, was calculated as follows:

Solubility = (Protein in supernatant/Total protein in sample) x 100.

Foaming capacity (FC) was determined according to Amiza *et al.* (2012) [8]. Fish protein hydrolysate (3 g) was dispersed in 100 ml of distilled water and the mixture was homogenized for 1 min using a homogenizer at high speed. The mixture was then poured into a 250 ml graduated cylinder and the total volume was read. Foaming capability was expressed as percentage of volume increase upon whipping. Foaming capability was calculated as follows:

FC% = (Volume after homogenisation - Volume before homogenisation) x 100/Volume before homogenisation.

Emulsification capacity (EC) was determined according to Diniz and Martin (1997) [9]. Protein hydrolysate samples (0.5 g) and 30 ml of vegetable oil were added to 60 ml of NaCl solution (30 g/l) and mixed using a homogenizer at 9500 rpm for 30 min. Then, another 30 ml of oil were added over 1.5 min and mixed for a further 30 seconds. The mixture was transferred to centrifuge tubes, held in a water-bath at 85°C for 15 min, and then centrifuged at 3000 rpm for 30 min. Emulsification capacity was calculated by the following equation:

EC (ml/g) = $(V_A - V_R)/W_S$ where V_A was the volume of oil added to form an emulsion (ml), V_R was the volume of oil released after centrifugation (ml), W_S was the weight of sample (g).

2.5. Statistical analysis

The experiments were carried out in triplicates. The data obtained were subjected to one way analysis of variance (ANOVA), followed by the Duncan's multiple range test to determine the significant difference between samples at $p<0.05$ level using the SPSS programme (SPSS Version 20.0).

3. RESULTS AND DISCUSSION

3.1. Proximate composition of the sailfish trimmings

The proximate composition of the sailfish trimmings is shown in table 1.

Table 1. Proximate composition of the sailfish trimmings

Proximate composition (%)	Sailfish trimmings
Moisture	75.2 ± 0.4
Protein	21.3 ± 0.2
Lipid	1.5 ± 0.1
Ash	1.2 ± 0.1

Data are expressed as mean ± standard deviation (n=3).

The study result showed that the moisture content of sailfish trimmings was 75.2%, which was higher than those of tilapia waste (66.29%) [10] and trout viscera (71.65%) [11]. The protein content of sailfish trimmings (21.3%) was far higher than those of carp meat (18.4%) [12] and eel meat (16.88%) [13]. Lipid content of sailfish trimmings (1.5%) was lower than those of carp meat (3.52%) [12] and eel meat (3.41%) [13]. Ash content (1.2%) of sailfish trimmings was higher than those of carp meat (1.07%) [12] and eel meat (0.89%) [13]. The study result showed that the sailfish trimmings was a good source of protein which can be used for production of protein hydrolysate.

3.2. Chemical composition of protein hydrolysate from sailfish trimmings

The chemical composition of the protein hydrolysate from sailfish trimmings after 8 h of hydrolysis is shown in table 2.

Table 2. Chemical composition of protein hydrolysate from sailfish trimmings

Proximate composition	Content (%)
Moisture	7.2 ± 0.1
Protein	73.4 ± 0.3
Lipid	0.6 ± 0.1
Ash	8.6 ± 0.2

Data are expressed as mean ± standard deviation (n=3).

The protein content of sailfish trimmings protein hydrolysate was 73.4%, which was higher than those of salmon head protein hydrolysates (62.3 - 64.8%) [14] but lower than those of tilapia waste protein hydrolysate

(82.19%) [10] and trout viscera protein hydrolysate (88.32%) [11]. The sailfish trimmings protein hydrolysate had protein content similar to thornback ray muscle hydrolysate (73.41%) [15]. The lipid content of protein hydrolysate from sailfish trimmings was 0.6%, which was lower than that of shortfin scad waste hydrolysate (7.55%) [16]. The low lipid content of sailfish trimmings protein hydrolysate might enhance stability of the hydrolysate towards lipid oxidation. The ash content of sailfish trimmings protein hydrolysate was 8.6%, which was lower than that of shortfin scad waste hydrolysate (10.4%) [16].

3.3. Amino acid composition of the protein hydrolysate from sailfish trimmings

The composition and content of amino acids indicated the nutritional quality of sailfish trimmings protein hydrolysate obtained after 8 h of hydrolysis.

Table 3. Amino acid composition of the protein hydrolysate from sailfish trimmings

Amino acids	Content (g/100 g protein hydrolysate)
Alanine	2.28 ± 0.14
Aspartic	3.58 ± 0.16
Glutamic	4.14 ± 0.19
Glycine	5.35 ± 0.21
Histidine	1.62 ± 0.08
Isoleucine	1.72 ± 0.07
Leucine	2.62 ± 0.12
Lysine	1.25 ± 0.07
Methionine	0.75 ± 0.02
Phenylalanine	1.27 ± 0.06
Proline	2.96 ± 0.11
Serine	1.27 ± 0.06
Threonine	1.33 ± 0.08
Tyrosine	0.97 ± 0.04
Valine	1.76 ± 0.07
Total amino acids	32.87 ± 0.35
Total essential amino acids	12.32 ± 0.28
Total essential amino acids/Total amino acids (%)	37.48 ± 0.32

Data are expressed as mean ± standard deviation (n=3).

Sailfish trimmings protein hydrolysate had a total amino acid content of 32.87 g/100 g of protein hydrolysate and total essential amino acid content of 12.32 g/100 g of protein hydrolysate. The ratio of essential amino acids to total amino acids was 37.48%. The content of essential amino acids showed the potential of hydrolysate to use as a nutrition source in food for human. Sailfish trimmings protein hydrolysate was rich in glycine, glutamic, aspartic, proline, leucine and alanine. However, the protein hydrolysate from sailfish trimmings contained low contents of methionine and tyrosin. According to Chalamaiah *et al.* (2012), aspartic acid and glutamic acid contents were found to be

higher than others amino acids in most fish protein hydrolysates [17]. The amino acid content of sailfish trimmings protein hydrolysate was higher than that of protein hydrolysate from sardine by-product (19.72 g of total amino acid /100 g and 8.2 g of essential amino acid/100 g) [18]. The present study indicated that sailfish trimmings protein hydrolysate was found to have high nutritional value and could be used in human diets.

3.4. Functional properties of the protein hydrolysate from sailfish trimmings

3.4.1. Solubility

The degree of hydrolysis and solubility of the protein hydrolysate from sailfish trimmings are displayed in figure 1. The solubility is one of the most important functional properties of fish protein hydrolysates. The high solubility of protein hydrolysates showed potential applications in food industry [8].

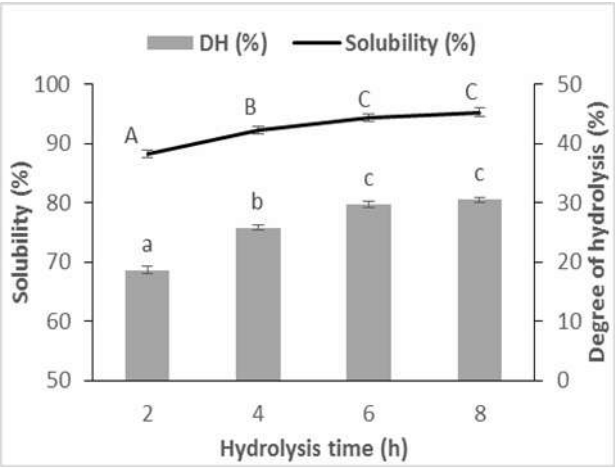

Figure 1. The degree of hydrolysis (DH) and sobubility of sailfish trimmings protein hydrolysate. Different letters show significant differences ($p < 0.05$)

The study results indicated that the degree of hydrolysis (DH) increased with increasing hydrolysis time. The degrees of hydrolysis of the protein hydrolysates from sailfish trimmings after 2 h, 4 h, 6 h and 8 h of hydrolysis were 18.6%, 25.8%, 29.7% and 30.5%, respectively. There was not a significant difference in degree of hydrolysis between hydrolysis time of 6 h and 8 h. The hydrolysis of the fish protein was characterized by an initial rapid phase, during which a large number of peptide bonds were hydrolyzed. Thereafter, the rate of enzymatic hydrolysis decreased. This result was similar to those previously reported for herring head [19] and salmon head [14].

According to results showed in figure 1, the solubility of protein hydrolysates from sailfish trimmings increased when hydrolysis time and degree of hydrolysis increased. Sailfish trimmings protein hydrolysates had solubility in the range of 88.3 - 95.2%. The fish protein hydrolysates with high degrees of hydrolysis gave higher solubility than those with low degrees of hydrolysis. The protein hydrolysate with the highest degree of hydrolysis of 30.5% at hydrolysis time of 8 h showed the highest solubility (95.2%). There was a significant difference ($p<0.05$) in solubility between hydrolysis time of 2 h and hydrolysis time of 4 h as well as between 4 h and 6 h. However, no significant difference in solubility was observed between hydrolysis

time of 6h and 8h. The similar result was also indicated in the study by Gbogouri *et al.* (2004) where the solubility of salmon by - products hydrolysates increased with the increase in degree of hydrolysis [20]. Gbogouri *et al.* (2004) showed that the solubility of salmon by - products hydrolysates was more than 90% [20] while the solubility of cobia frame hydrolysates was in the range of 85 - 86% [8].

In present study, the hydrolysis of sailfish trimmings formed a large number of hydrophilic polar group peptides when the hydrolysis time increased resulting in the high solubility of sailfish trimmings protein hydrolysate. Enzymatic breakdown of fish protein leaded to a major structural change in that the protein was gradually cleaved into smaller peptides. The increase in solubility of the hydrolysates with increased hydrolysis time may be due to the cleavage of proteins into smaller peptides that have more polar residues, with the ability to form hydrogen bonds with water and enhance solubility [2, 20].

3.4.2. Foaming capacity

The foaming capacity of protein hydrolysate from sailfish trimmings is indicated in figure 2.

When hydrolysis time increased, the sailfish trimmings protein hydrolysate displayed a lower foaming capacity. The study results showed that the foaming capacity of protein hydrolysates from sailfish trimmings decreased when the hydrolysis time increased from 2 h to 8 h. The foaming capacity of sailfish trimmings protein hydrolysate reached a maximum value (45.8%) at hydrolysis time of 2 h and degree of hydrolysis of 18.6%. The degree of hydrolysis obtained the highest value (30.5%) at hydrolysis time of 8 h but at that time the foaming capacity of sailfish trimmings protein hydrolysate was lowest (35.7%). The decrease in foaming capacity of protein hydrolysate with increased hydrolysis time may be due to the formation of smaller peptides with less surface activity and due to the reduction of hydrophobicity of protein hydrolysate during extensive hydrolysis [2].

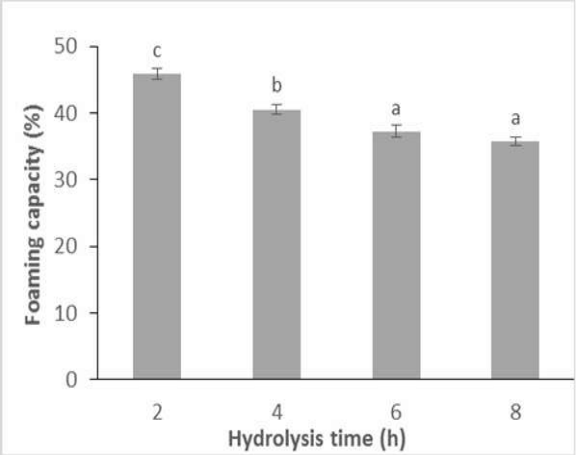

Figure 2. Foaming capacity of sailfish trimmings protein hydrolysate. Different letters show significant differences ($p < 0.05$)

Baharuddin *et al.* (2016) indicated that the foaming capacity of eel protein hydrolysate decreased significantly when the degree of hydrolysis increased from 36% to 69% [21].

The similar trend of foaming capacity was also observed for the protein hydrolysates from cobia frame [8], sardine by - product [2] and yellow stripe trevally muscle [7]. Cobia frame protein hydrolysate with the lowest degree of hydrolysis gave highest foaming capacity (122.7%) [8]. The capelin protein hydrolysate possessed the foaming capacity of 90% [22] while the protein hydrolysate from yellow stripe trevally muscle gave the foaming capacity up to 200% [7].

3.4.3. Emulsifying capacity

Emulsifying capacity of sailfish trimmings protein hydrolysate is showed in figure 3.

The study results showed that the emulsifying capacity of sailfish trimmings protein hydrolysates decreased with increasing hydrolysis time. Hydrolysates with low degree of hydrolysis had high emulsifying capacity and extensive hydrolysis resulted in a decrease in emulsifying capacity. After 2 h, 4 h, 6 h and 8 h of hydrolysis corresponding to degree of hydrolysis 18.6%, 25.8%, 29.7% and 30.5%, the emulsifying capacity of sailfish trimmings protein hydrolysates were 29.2 ml/g, 24.9 ml/g, 18.8 ml/g and 17.6 ml/g, respectively. The similar trend was also reported for protein hydrolysates from sardine by-products [2], cobia frame [8] and carp skin [23]. Souissi *et al.* (2007) indicated that the protein hydrolysates from sardine by - products with degrees of hydrolysis of 6.62%, 9.31% and 10.16% had emulsifying capacity of 20 ml/g, 15.2 ml/g and 10.8 ml/g, respectively [2]. The carp skin protein hydrolysates had emulsifying capacity in the range of 20 - 38 ml/g [23] while the cobia protein hydrolysates had emulsifying capacity in the range of 3 - 12 ml/g [8].

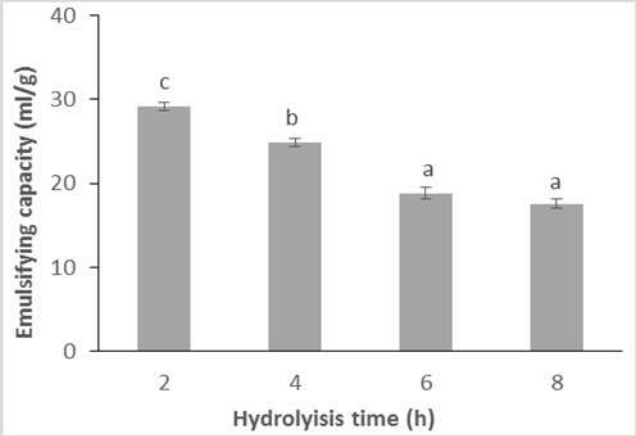

Figure 3. Emulsifying capacity of sailfish trimmings protein hydrolysate. Different letters show significant differences ($p < 0.05$)

Fish protein hydrolysates are surface active materials and promote oil - in water emulsions. The emulsifying properties of protein hydrolysis can be explained based on their surface properties. According to Foh *et al.* (2010), an increase in the number of peptide molecules and exposed hydrophobic amino acid residues due to hydrolysis of proteins contribute to an improvement in the formation of emulsions [24]. However, the hydrolysates with a higher degree of hydrolysis had poorer emulsifying capacity due to their small peptide size. Moreover, the diminishing in emulsifying capacity with an

extensive hydrolysis process is also due to the reduction of hydrophobicity of the hydrolysate during hydrolysis [2].

4. CONCLUSION

The sailfish trimmings were a rich source of protein and utilized for the production of fish protein hydrolysate. Enzymatic hydrolysis of sailfish trimmings with different hydrolysis times had a significant effect on the solubility, foaming capacity and emulsifying capacity of protein hydrolysates. The solubility of sailfish trimmings protein hydrolysates increased with increasing hydrolysis time. The sailfish trimmings protein hydrolysate at hydrolysis time of 8 h showed the highest solubility (95.2%). The protein hydrolysate after 8 h of hydrolysis had contents of moisture 7.2%, protein 73.4%, lipid 0.6% and ash 8.6%. The sailfish trimmings protein hydrolysate had a high nutritional value with total amino acid content of 32.87 g/100 g. On the contrary, the foaming capacity and emulsifying capacity decreased with increasing hydrolysis time from 2 h to 8 h. The sailfish trimmings protein hydrolysate at hydrolysis time of 2 h reached the highest foaming capacity (45.8%) and highest emulsifying capacity (29.2 ml/g). Research results suggested that sailfish trimmings protein hydrolysates had potential application as functional ingredients in different foods and could be used in food industry for human consumption.

REFERENCES

1. Dekkers E, Raghavan S, Kristinsson HG. Marshall MR. (2011). Oxidative stability of *Mahi mahi* red muscle dipped in tilapia protein hydrolysates. Food Chem. 124: 640 - 645.

2. Souissi N., Bougatef A., Triki-Ellouz Y., Nasri M. (2007). Biochemical and functional properties of Sardinella (*Sardinella aurita*) by-product hydrolysates. Food Techology Biotechnology, 45 (2): 187 - 194.

3. Kristinsson H. G., Rasco B. A. (2000). Fish protein hydrolysates: production, biochemical, and functional properties. Critical Review in Food Science and Nutrition, 40: 43 - 81.

4. Folch J., Lees N., Sloan-Stanley G. H. (1957). A simple method for the isolation and purification of total lipids from animal tissues. *J. Biol. Chem.* 226: 497 - 509.

5. Kechaou, E. S., Dumay, J., Donnay - Moreno, C., Jaouen, P., Gouygou, J. P., Bergé, J. P., Amar, R. B. (2009). Enzymatic hydrolysis of cuttlefish (*Sepia officinalis*) and sardine (*Sardina pilchardus*) viscera using commercial proteases: Effects on lipid distribution and amino acid composition. *Journal of Bioscience and Bioengineering*, 107, 158 - 164.

6. Nguyen T. M. H, Sylla K. S. B., Randriamahatody Z., Donnay - Moreno C., Moreau. J., Tran T, L, Bergé J. P. (2011). Enzymatic hydrolysis of yellowfin tuna (*Thunnus albacares*) by - products using

Protamex protease. *Food Technology and Biotechnology*, 49 (1): 48 - 55.

7. Klompong V., Benjakul S., Kantachote D., Shahidi F., (2007). Antioxidative activity and functional properties of protein hydrolysate of yellow stripe trevally (*Selaroides leptolepis*) as influenced by the degree of hydrolysis and enzyme type. Food Chemistry, 102: 1317 - 1327.

8. Amiza M. A., Kong Y. L., Faazaz A. L. (2012). Effects of degree of hydrolysis on physicochemical properties of Cobia *(Rachycentron canadum)* frame hydrolysate, *International Food Research Journal*, 19 (1): 199 - 206.

9. Diniz F. M., Martin A. M. (1997). Effects of the extent of enzymatic hydrolysis on functional properties of shark protein hydrolysate, Lebensm. - Wiss. U. - Technol., 30: 266 - 272.

10. Srikanya, A., Dhanapal, K., Sravani1, K., Madhavi K., and Kumar, P G. (2017). A study on optimization of fish protein hydrolysate preparation by enzymatic hydrolysis from tilapia fish waste mince. *International Journal of Current Microbiology and Applied Sciences*, 6 (12) pp. 3220 - 3229.

11. Taheri, A, Anvar, S. A. A, Ahari H , Fogliano, V. (2013). Comparison the functional properties of protein hydrolysates from poultry byproducts and rainbow trout (*Onchorhynchus mykiss*) viscera. *Iranian Journal of Fisheries Sciences*, 12 (1) 154 - 169.

12. Saputra, D., Nurhayati, T. (2016). Production of fish hydrolysate protein from waste of fish carp (*Cyprinus carpio*) by enzymatic hydrolysis. Com Tech, 7 (1): 11 - 18.

13. Halim, N. R. A., Sarbon, N. M. (2017). A response surface approach on hydrolysis condition of eel (*Monopterus* sp.) protein hydrolysate with antioxidant activity. *International Food Research Journal,* 24 (3) 1081 - 1093.

14. Sathivel S., Smiley S., Prinyawiwatkui W., Bechtel P. J. (2005). Functional and nutritional properties of red salmon (*Oncorhynchus nerka*) enzymatic hydrolysates. *Journal of Food Science*, 70 (6): 401 - 406.

15. Lassoued, I., Mora, L., Nasri, R., Aydi, M., Toldrá, F., Aristoy, M. C., Barkia, A. and Nasri, M. (2015). Characterization, antioxidative and ACE inhibitory properties of hydrolysates obtained from thornback ray *(Raja clavata)* muscle. *Journal of Proteomics,* 128: 458 - 468.

16. Ishak, N. H; *Sarbon, N. M. (2018). Physicochemical characterization of enzymatically prepared fish protein hydrolysate from waste of shortfin scad *(Decapterus macrosoma). International Food Research Journal*, 25 (6): 2593 - 2600.

17. Chalamaiah M., Dinesh kumar B., Hemalatha R., Jyothirmayi T. (2012). Fish protein hydrolysates: Proximate composition,

amino acid composition, antioxidant activities and applications: A review. Food Chemistry, 135: 3020 - 3038.

18. Batista I., Pires C. (2011). Feasibility study - Production of protein hydrolysates from sardine byproducts. Atlantic Area Programme.

19. Sathivel S., Bechtel P. J., Babbitt J., Smiley S., Crapo C., Reppond K. D., Prinyawiwatkul W. (2003). Biochemical and functional properties of herring (*Clupea harengus*) byproduct hydrolysates. Food Science, 68: 2196 - 2200.

20. Gbogouri G. A., Linder M., Fanni J., Paramentier M. (2004). Influence of hydrolysis degree on the functional properties of salmon byproducts hydrolysates. *Journal of Food Science*, 69 (8): 615 - 622.

21. Baharuddin, N. A., Halim, N. R. A., Sarbon, N. M. (2016). Effect of degree of hydrolysis (DH) on the functional properties and angiotensin I - converting enzyme (ACE) inhibitory activity of eel (*Monopterus* sp.) protein hydrolysate. *International Food Research Journal*, 23 (4), 1424 -1431.

22. Shahidi F., Han X. Q, Synowieck J. (1995). Production and characteristics of protein hydrolysates from capelin (*Mallotus villosus*). Food Chem, 53: 285 - 293.

23. Wasswa J., Tang J., Gu X., Yuan X. (2007). Influence of the extent of enzymatic hydrolysis on the functional properties of protein hydrolysate from grass carp (*Ctenopharyngodon idella*) skin. Food Chemistry, 104: 1698 - 1704.

24. Foh, M. B. K., Amadou I., Foh, B. M., Kamara, M. T., Xia, W. (2010). Functionality and antioxidant properties of Tilapia (*Oreochromis niloticus*) as influenced by the degree of hydrolysis. *International Journal of Molecular Sciences*., 11, 1851 - 1869.

CHARACTERISTICS OF HABITAT OF TONKIN SNUB-NOSED MONKEY IN QUAN BA WATERSHED FOREST, HA GIANG PROVINCE

Nguyen Xuan Dang[1,*], Nguyen Tien Dat[2],
Nguyen Xuan Nghia[1], Pham Van The[3], Trinh Ngoc Bon[4]

ABSTRACT

The forest habitat of the Tonkin Snub-nosed Monkey (TSM) population in Cao Ma Po, Ta Van and Tung Vai communes (Quan Ba district, Ha Giang province) was surveyed in 2019 – 2022 using line transects and sampling plot methods. The study results show that the habitat includes 4,213.16 ha of natural forest with two forest types: Montane evergreen broad-leaf forest and Limestone evergreen forest. Each forest type has 4 states (rich, medium, poor and rehabilitation) of which 2 states (rich and medium forests) can support the activity of TSM and have an area of 2,560 ha, accounting for 61.48% of the forest area in the study area. Key characteristics of forests in the study area are highlighted including plant species composition (647 species of 364 genera and 129 families), list of TSM food plant species (19 species), the density of trees of $D_{1.3} \geq 5$ cm (1491.3 trees/ha), $D_{1.3}$ size (mean 14.97), basal area (BA) of tree species (average 275.17 cm^2/tree and total BA = 41.04 m^2/ha) and dominant families and species. In comparison with Khau Ca TSM Conservation Area, the ecological indicators of forests in the study area are lower indicating the forest in the study area was more degraded. It is necessary to have management solutions and sylvicultural interventions to improve the forest quality in the study area for the long-term conservation of Quan Ba TSM population.

Keywords: *Habitat, primate, Quan Ba forest, Rhinopithecus avunculus.*

Received: 22 September 2022; revised: 14 October 2022; accepted: 24 November 2022.

1. INTRODUCTION

The Tonkin Snub-nosed Monkey (TSM) *Rhinopithecus avunculus* is an endemic primate species of North Vietnam. Historically, the species occurred in five provinces including Yen Bai, Ha Giang, Tuyen Quang, Thai Nguyen and Bac Kan provinces [1]. However, due to excessive illegal hunting and massive habitat loss and degradation, the species is now found only in a few forest areas

[1] Institute of Ecology and Biological Resources, VAST

[2] Centre for Resources, Environment and Climate Change

[3] Laboratory of Ecology and Environmental Management, Science and Technology Advanced Institute, Van Lang University, Ho Chi Minh city, Vietnam.

[4] Silvicultural Research Institute, Vietnamese Academy of Forest Sciences

*Corresponding author: dangiebr@gmail.com

in Ha Giang and Tuyen Quang provinces, with a total number not exceeding 250 individuals [2], [3]. The species was listed as "Critically endangered" (CR) in both the Red Data Book of Vietnam [4] and the IUCN Red List [5]. Quan Ba watershed forest in Ha Giang Province harbors a small population of TSM (about 30 - 35 individuals [6]. It is the second largest population of TSM after the largest population of about 120 individuals found in the Khau Ca TSM Conservation Area, Ha Giang province. This population is highly vulnerable due to illegal wildlife hunting and forest degradation by illegal timber cutting, non-timber product harvesting, and especially, the excessive forest farming of the Cardamon plant Amomum tsao [7].

As an arboreal and plant-eating monkey [8], [9], the survival of TSM depends much on the quality of the forest in which they live. Thus, understanding the characteristics of the forest where the TSM population is living is very important for the species conservation. The habitat of TSM in Khau Ca TSM Conservation Area was well studied in many aspects including forest types/states, structure, floral composition, plant community ecological characteristics, TSM food plant species, reserves and phenology, etc. [10], [8], [9]. While the TSM habitat in Quan Ba watershed forest is still poorly studied except for some general information on forest types and the impacts of the forest farming of Cardamon on the habitat quality [7]. Thus, during 2019-2022, we conducted field studies of TSM habitat in Quan Ba watershed forest, intending to better understand the forest characteristics.

2. METHODS

Study area: This study is focused on an area of about 5,000 ha of natural forests that the TSM population is inhabiting (the study area). The study area is located within the eastern part of Quan Ba district, Ha Giang province, sharing 3 communes (Cao Ma Po, Ta Van and Tung Vai) and a national border with Malipo district of China. The terrain of the study area is characterized by steep limestone mountains with deep narrow valleys, and the altitude ranges from 900 to 1,700 m above sea level. The study area has a humid tropical climate, influenced by monsoon (Quan Ba district statistical Yearbook 2017). There are two distinct seasons: the rainy season from May to October, with the heaviest rain in July and August, with the average rainfall of 246 mm/month. In the dry season from November to April next year, the average rainfall is 44.8 mm/month. The average annual rainfall is 1,768 mm.

Line transect method: We followed Buckland *et al.* (2007) [11]. In each habitat type, transects with a length of 500 m or more were established, depending on the topography and habitat size. The information/data collected on the transects were canopy structure, tree species name and tree photography. The width of survey transects varied from 5 to 20 m depending the

thickness of forests. A total of 15 transects with a total length of 30.7 km were carried out (Figure 1).

Sampling plot method: According to Brockelman (1987) [12], when studying the habitat of primates, the plots are arranged scattered in the habitat but must be in the most concentrated distribution area of the studied species. Due to the very steep and rugged terrain of the study area, plots of size 10 x 10 m (100 m^2) were used. The plots were randomly established on survey transects in different habitat types and at least 500 m apart. In each plot, one sub - plot of size 5 x 5 m was established to survey shrubs and regenerated trees and one sub - plot of size 1 x 1 m to survey herbaceous plants. In the plots, data were collected on trees with breast circumference C1.3 ≥ 19 cm and height Hvn ≥ 5 m, including common names or local names, breast girth (C1.3) and height (Hvn). At the same time, the names of extra-layer plant species were also recorded. In the 5 x 5 m sub-plots, collected data included species names and the height Hvn of all trees having C1.3 < 19 cm and Hvn < 5 m. In the herbaceous sub-plots, we identified the species' names and counted the number of plants of each species. A total of 23 sampling plots were established (Figure 1).

Plant species identification and data analysis: Species identification was carried out mostly in the field. For plants that could not be identified in the field, specimens were collected for later identification at the laboratories (Institute of Ecology and Biological Resources). Key documents used for the species identification include [13], the Flora of Vietnam (MoST and the VAS, multi-volumes) and the Flora of China [14].

The obtained data were stored and analyzed using Word, Excel, MapInfor 10.5 programs. The ecological indicators of the forest are determined according to Bhadra *et al.* (2016) [15]: Plant density (stem/ha) = total number of trees of considered species in all plots/total area of all plots implemented. Dominance of species (cm^2) = total basal area (BA) of all trees of considered species in the plots. The basal area of the stem BA (cm^2) = 3.1416 x $(D_{1.3}/2)^2$, where $D_{1.3}$ is the diameter at the breast height of the tree. Sorensen similarity index between 2 areas SI = 2C/(A+B). In which: C - number of species occurring in both areas A & B, A - number of species of area A; B - the number of species of area B. Important Value Index IV(%) = (RF% + RDe% + RDo%)/3 [16]. In which, RF(%) - relative frequency, RDe (%) - relative density, RDo(%) - Relative dominance, while RF (%) = (number of plots with the considered species/total number of plots with occurrence of all species) x 100; RDe(%) = (total number of plants of considered species/total number of plants of all species) x 100; and RDo(%)= (total BA of considered species/sum of BA of all species) x 100.

3. RESULTS AND DISCUSSION

3.1. Forest cover

Out of the total 4,563.46 ha of the survey area, 4,213.16 ha (92.3%) is covered by natural forests, and the rest 350.3 ha (7.7%) is non-forest land. There are two main forests including: Montane evergreen broad-leaf forest and Limestone evergreen forest. Due to the long-term impact of human livelihood activities, these main types of forest have been converted into sub-categories as a rich, medium, poor and rehabilitation forest (Figure 1).

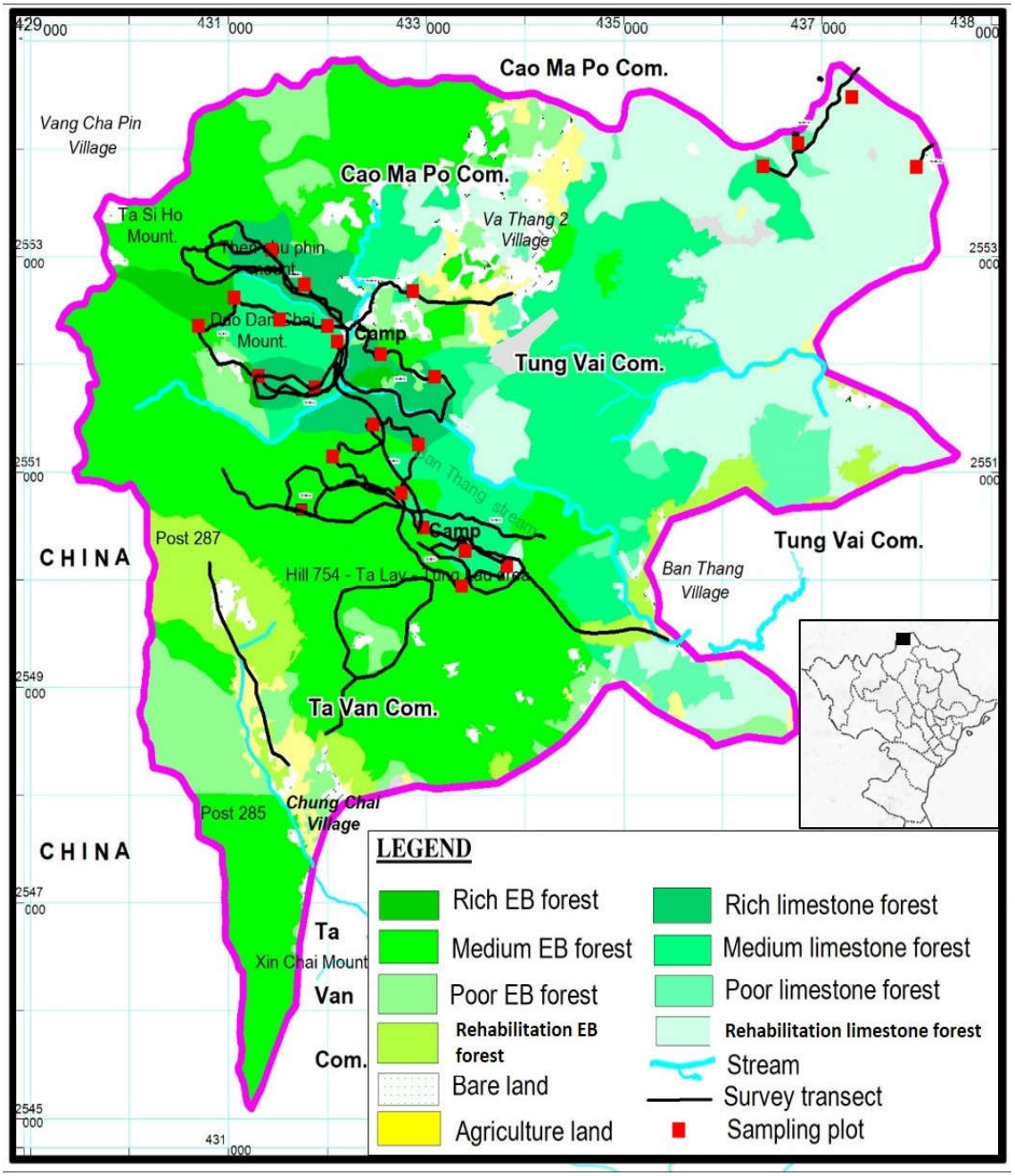

Figure 1. Land-use map of watershed forest in Quan Ba

(EB – evergreen broad-leaf)

The Montane evergreen broad-leaf forest includes rich montane evergreen broad-leaf forest (49.7 ha), medium montane evergreen broad-leaf forest (1,619.99 ha), poor montane evergreen broad-leaf forest (360.03 ha) and rehabilitation montane evergreen broad-leaf forest (250.63 ha). The limestone evergreen forest includes the rich limestone evergreen forest (173.42 ha), medium limestone evergreen forest (746.67 ha), poor limestone evergreen forest (141.98 ha), and rehabilitation limestone evergreen forest (860.74 ha) (Figure 1).

Rich forests remain only on very steep slopes and limestone mountains. The forests have the typical structure of tropical rainforest with 4 canopy layers and forest canopy coverage of more than 70%. Trees have a diameter at breast height ($D_{1.3}$) of 40-60 cm, and a height of 20-40 m. Medium forests has no superior layer (A1 layer) in some places, and the forest canopy has been disrupted in many places due to many tall trees having been removed.

The structure of poor and rehabilitation forests was severely altered due to the falling of large trees. The superior layer (A1 layer) has been removed; the main canopy layer (A2 layer) and lowest woody tree layer (A3 layer) are also strongly impacted, and almost absent in some limestone areas. According to Le Khac Quyet *et al.* (2010) [6] and Nguyen Xuan Dang *et al.* (2019) [7], in the limestone evergreen forests, the TSM is found in rich, medium forests and occasionally in the poor forest, while in montane evergreen broad-leaf forest, the animals found only in rich and medium forests. Thus, out of a total of 4213.16 ha of natural forest in the study area, the area of habitats suitable for TSM activity is about 2590 ha, accounting for 61.48% of the total forest area. This is much larger than the current activity area of the TSM population (about 1000 ha). In other words, the study area can support the TSN population here to be increased many times more. This is comparable with the fact that in Khau Ca area, the total area of forests suitable for the TSM population is only 816.5 ha [9]) which harbors a TSM population of about 120 individuals.

3.2. Species richness

A total of 647 species of vascular plants belonging to 364 genera, 129 families and 5 phyla have been recorded in the study area. The Magnoliophyta is the most diverse phylum with 106 families, 582 species, accounting for 82.17% of the total families and 89.95% of the total species. The second most diverse Pteridophyta includes 17 families, 52 species (13.18% and 8.04%, respectively). The Pinophyta has 3 families and 7 species, the Lycopodiophyta has 2 families and 5 species, and the Gnetophyta has only one family and one species. Among the families, the species-richest are Orchidaceae (53 species), followed by Lauraceae (36 species), Rubiaceae (31 species), Urticaceae (22 species), Gesneriaceae (19 species), Primulaceae (19

species), Asteraceae (17 species), Fagaceae (16 species), Moraceae (16 species), Rosaceae (13 species), Araceae (12 species), Polypodiaceae (11 species), Asparagaceae (11 species), Apocynaceae (10 species) and Rutaceae (10 species). There are 5 families with 9 species each, 3 families with 8 species each, 3 families with 7 species each, 8 families with 6 species each, 4 families with 5 species each, 16 families with 4 species each, 18 families with 3 species each, 20 families with 2 species each and 36 families with one species each.

There has been no study on the food plants of TSM in the study area. However, based on the list of TSM food plants known in previous studies in Vietnam [1], [10], [8], [9] and our list of 647 plant species found in the study area we have identified 19 species belonging to 11 families are food plant species of TSM in the study area. They are *Litsea baviensis* Lec., *Litsea yunnanensis* Yen C. Yang & P.H. Huang, *Machilus bonii* Lecomte, *Archidendron robinsonii* (Gagn.) L. Niels., *Brassaiopsis stellata* Fang, *Toona sinensis* (Juss.) M. Roem, *Ficus auriculata* Lour, *Ficus hispida* L.f., *Broussonetia papyrifera* (L.) L' Hér. ex Vent., *Canarium album* (Lour.) DC., *Canarium pimela* K. D. Koenig, *Garcinia oblongifolia* Champ. ex Benth., *Caryota urens* L., *Castanopsis tonkinensis* Seemen, *Castanopsis chinensis* (Spreng.) Hance, *Quercus platycalyx* Hickel & A.Camus, *Gnetum montanum* Markgr., *Musa acuminata* Colla, *Phyllostachys bambusoides* Sieb. & Zucc.

3.3. Physical structure of forests

A total of 612 trees were counted in the 23 plots of the study area. The total plot area covered 0.23 ha, and the density of trees of $D_{1.3} \geq 5$ cm was 1491.3 per hectare. Most of the trees have a D1.3 from 5 to 20 cm, accounting for 80.11% of the total number of trees sampled. Species with $D_{1.3}$ from 5 to 9.0 cm accounted for the largest proportion (41.81%) and only 7.61% of the total trees with D1.3 ≥ 40 cm. The highest $D_{1.3}$ value of 91.4 cm was recorded in the *Lithocarpus garrettianus* (Craib) A.Camus. The mean value of $D_{1.3}$ of the trees in the plots is 14.97 cm.

Out of a total of 343 sampled timber trees, 131 species belonging to 79 genera and 48 families have been identified for a ratio of about 2.6 plants per species and 2.7 species per family. The largest BA area of 8869.19 cm^2 was recorded in *Castanopsis chinensis* (Spreng.) Hance and the average BA area for all trees was 275.17 cm^2. The area of plots sampled is 23,000 m^2, a total BA of all species is 9.44 m^2. Therefore, the total BA per hectare is 41.04 m^2.

Out of 48 sampled families, the family Fagaceae has the highest number of trees (37 trees, accounting for 10.82% of the total number of trees), followed by Lauraceae (26 plants, 7.60%), Fabaceae (23 trees, 6.73%),

Araliaceae (22 trees, 6.43%), Illiciaceae (22 trees, 6.43%), Icacinaceae (20 trees, 5.85%), Taxaceae (20 trees, 3.51%). These seven (7) families have 170 trees, accounting for 47.37% of the total sampled trees. In terms of BA area, Fagaceae has the largest BA (30035.83 cm^2), accounting for 31.82% of the total BA of sampled trees. Next are the Magnoliaceae (7884.12 cm^2, 8.35%), Elaeocarpaceae (7141.31 cm^2, 7.57%), Araliaceae (5493.40 cm^2, 5.82%), Lauraceae (4943.02 cm^2, 5.24%), Fabaceae (4846.06 cm^2, 5.13%), Theaceae (4265.66 cm^2, 4.52%). These seven families have a total BA accounting for 68.45% of the total BA of all sampled trees.

Species *Archidendron robinsonii* (Gagnep) I. Nielsen was the most common species in terms of number of trees (21 trees, accounting for 6.14% of the total number of trees). Followed by the *Gomphandra mollis* Merr (20 trees, 5.85%), *Machilus bonii* Lecomte (16 trees, 4.68%), *Castanopsis tonkinensis* Seemen (11 trees, 3.22%), *Garcinia gracilis* Pierre (11 trees, 3.22%), *Amentotaxus yunnanensis* H. L. Li (10 trees, 2.92%). In terms of BA area, *Castanopsis chinensis* (Spreng.) Hance was the most common species (8869.19 cm^2, accounting for 9.4% of the total BA of the species). Next are the *Castanopsis tonkinensis* Seemen (6548.16; 6.94%), and *Archidendron robinsonii* (Gagnep) I. Nielsen (4751.16; 5.03%). In the sampled plots, there are no species with IV≥5%, there are 4 species with IV≥4%, namely *Archidendron robinsonii* (Gagnep) I. Nielsen (4.65%), *Castanopsis chinensis (Spreng.)* Hance (4.53%), *Castanopsis tonkinensis* Seemen (4.51%) and *Gomphandra mollis* Merr. (4.44%).

Khau Ca TSM Conservation Area in Vi Xuyen district, Ha Giang province is home of the largest population of TSM today [7]. Therefore, comparing the forest factors of study area with those of Khau Ca area will have suggestions for the management solutions to protect the habitats of TSM in Quan Ba watershed forest. The key forest ecological factors of tree communities between the two areas are listed in table 1 and figure 2.

Table 1. Comparison of factors of two tree communities in the study area and Khau Ca TSM Conservation Area

Factor	Study area	Khau Ca area*
Species composition	131 species, 48 families	136 species, 49 families
Ratio of tree per species and species per family	2.6 trees/species; 2.7 species/ family	3.7 tree/species; 2.8 species/family.

Tree density	1491 trees / ha	882 trees /ha
Maximum $D_{1.3}$ t	91.4 cm	134.3 cm
Trees of $D_{1.3}$ from 6 to 40 cm	97.24% total tree number	95.7% total tree number
Trees of $D_{1.3}$ from 6 to <10 cm	41.98% total tree number	34.4% total tree number
Trees of $D_{1.3}$ ≥ 40 cm	2.76% total tree number	4.3% total tree number
Mean $D_{1.3}$	15.0 cm	17.4 cm
Maximum BA	8869.19 cm^2	15546.54 cm^2
Mean BA per tree	275.17 cm^2/tree	393.90 cm^2/tree
Total BA per hectare	41.04 m^2/ha	34.77m^2/ha

*Notes: *After Dong Thanh Hai (2011)*

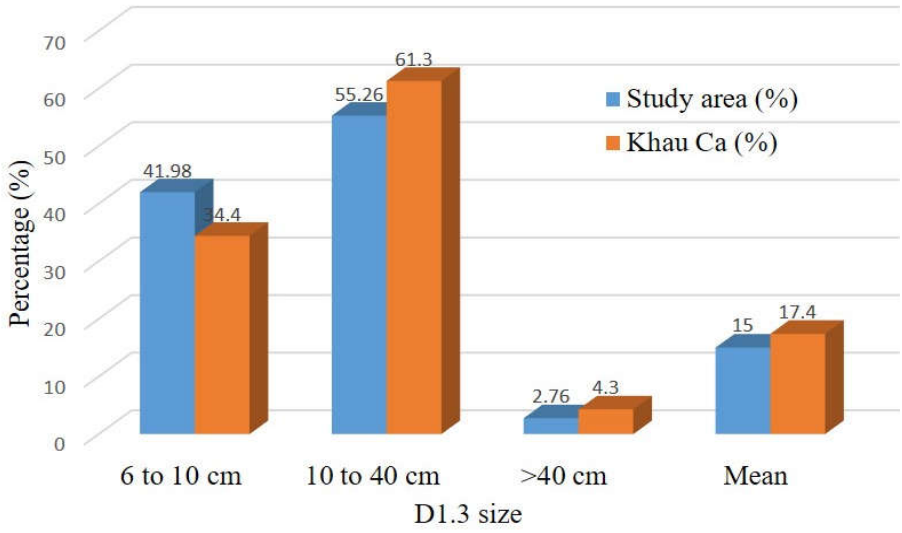

Figure 2. Percentage of trees by $D_{1.3}$ size in study area and Khau Ca area

In table 2, data on tree species composition and species/family ratios did not differ much between the two regions. However, taking into account that the number of sampling plots in study area is much less than in Khau Ca area (23 plots versus 58 plots), it is possible to predict a more diverse tree species composition in the study area. This is also consistent with the data on density and $D_{1.3}$ size of the trees. In general, tree

density in study area was higher (1491.3 trees/ha compared with 882 trees/ha) and $D_{1.3}$ of trees in study area was smaller than in Khau Ca (average $D_{1.3}$ in study area was 14.97 cm compared to 17.4 cm in Khau Ca area). The average and maximum BA values per tree were lower in study area than in Khau Ca area. However, total BA per ha of the study area is larger those in Khau Ca (41.04 m^2/ha compared to 34.77 m^2/ha). This is due to higher tree density in study area than in Khau Ca (1491.3 trees/ha versus 882 trees/ha). In general, the ecological indicators of plant communities in study area were lower than in Khau Ca area indicating the forest in study area was more degraded than in Khau Ca area (fewer large trees). Therefore, in order to ensure long-term conservation of TSM populations in the study area, it is necessary to have management solutions and sylvicultural interventions to improve the forest quality in study area.

4. CONCLUSION

The forest habitat of TSM in Quan Ba district includes 4,213.16 ha of natural forest with two forest types: Montane evergreen broad-leaf forest and Limestone evergreen forest. Each forest type has 4 states: rich, medium, poor and rehabilitation. The forests that are suitable for TSM activity (rich and medium forests of both types) cover an area of about 2560 ha, accounting for 61.48% of the total forest area in the study area.

Key characteristics of forests in study area include plant species composition (647 species of 364 genera and 129 families), list of TSM food plant species (19 species), the density of trees of $D_{1.3} \geq$ cm (1491.3 trees/ha), $D_{1.3}$ size (mean 14.97), basal area (BA) of tree species (average 275.17 cm^2/tree and total BA = 41.04 m^2/ha) and dominant families and species.

In comparison with Khau Ca TSM Conservation Area, the ecological indicators of forests in the study area are lower indicating the forests in the study area was more degraded. It is necessary to have management solutions and sylvicultural interventions to improve the forest quality in study area for the long-term conservation of the TSM population here.

ACKNOWLEDGEMENTS

This study was funded by FFI – Vietnam, US WWF Russell E. Train Education for Nature Program, The Mohamed bin Zayed Species Conservation Fund and Ostrava Zoo (Czech Republic). The authors also would like to express their sincerely thanks to Quan Ba Forest Protection Department, authorities and people of Cao Ma Po, Ta Van and Tung Vai communes for their kindly supporting during the field survey.

REFERENCES

1. Pham Nhat (2002). *Primates of Vietnam*. Agriculture Publishing, Ha Noi, 111 pp.

2. Covert H., Le Khac Quyet and B. W. Wright (2008). On the Brink of Extinction: Research for the Conservation of the Tonkin Snub-nosed Monkey *Rhinopithecus avunculus*. In J. G. Fleagle, C. C. Gilbert (eds.), Elwyn Simons: *A Search for Origins*. Springer 2008: 409–427.

3. Schwitzer C., Mittermeier R. A., Rylands A. B., Chiozza F., Williamson E. A., Wallis J. and Cotton A. (eds.). (2015). Primates in Peril: The World's 25 Most Endangered Primates 2014–2016. IUCN SSC Primate Specialist Group (PSG), International Primatological Society (IPS), Conservation International (CI), and Bristol Zoological Society, Arlington, VA. iv+93pp.

4. MoST & VIST. (2007). *Vietnam Red Book. Part I. Animals*. Natural Science and Technology Publishing, Hanoi, 315 pp.

5. IUCN. (2022). The IUCN Red List of Threatened Species. Version 2022-1.

https://www.iucnredlist.org, Downloaded on 05 September 2022

6. Le Khac Quyet and Covert H. H. (2010). Another population of the Tonkin Snub-nosed Monkey *Rhinopithecus avunculus* discovered in Ha Giang province, Vietnam. *Vietnamese Journal of Primatology* 4: 19-25.

7. Nguyen Xuan Dang, Nguyen Xuan Nghia, Pham Van The. (2019). The Tonkin Snub-nosed Monkey *Rhinopithecus avunculus* population in the Quan Ba forest, North-east Vietnam: An identification of priority habitat for conservation. *Academia Journal of Biology* 41(3): 47–54. doi: 10.15625/2615-0923/v41n3.13799.

8. Dong Thanh Hai. (2011). Ecology, behavior and conservation of the Tonkin Sub-nosed Monkey (*Rhinopithecus acunculus*) in Vietnam. A thesis submitted for the degree of Doctor of Philosophy of The Australian National University, 278 pp.

9. Nguyen Thi Lan Anh, Nguyen Xuan Dang, Nguyen Xuan Huan, Nguyen Anh Duc. (2017). Nutritional ecology of the Tonkin Snub-nosed Monkey (*Rhinopithecus avunculus*) in Ha Giang province, Vietnam. Ha Noi National University Publishing, 283 pp.

10. Le Khac Quyet, Nguyen Anh Duc, Vu Anh Tai, Covert, H.H., and Wright, B.W. (2007). Diet of the Tonkin snub-nosed monkey (*Rhinopithecus avunculus*) in the Khau Ca area, Ha Giang province, Northeastern Vietnam. *Vietnamese Journal of Primatology* pp. 75-83.

11. Buckland S. T., Borchers D. L., Johnston A., Henrys P. A., & Marques T. A.

(2007). Line transect methods for plant surveys. *Biometrics*, 63(4), 989-998.

12. Brockelman, W.Y. & Ali, R. (1987). Methods of surveying and sampling forest primate populations. In: Marsh CW, Mittermeier RA, eds. *Primate conservation in the Tropical Rain Forest*. New York: Alan R. Liss Inc., 23-62.

13. Pham Hoang Ho. (1999, 2000, 2003). Flora of Vietnam - An Illustrated Flora of Vietnam, vol. 1, 2, 3. Young Publishing, Ho Chi Minh city.

14. Chen J., and Gilbert M. G. (2006). Flora of China. Science, Beijing and Missouri Botanical Garden Press, St Louis.

15. Bhadra A.K. and S.K. Pattanayak. (2016). Abundance or dominance: which is more justified to calculate importance value index (IVI) of plant species? *Asian Journal of Science and Technology.* Vol. 07 (09):3577-3601.

16. Pham Van Dien, Pham Xuan Hoan. (2016). Forest Ecology Textbook. Agriculture Publishing, 268 pp.

SURFACE WATER QUALITY IN A RURAL AREA OF HAU GIANG PROVINCE, VIETNAM

Nguyen Van Cong[1,*], Huynh Van Thao[1],
Huynh Cong Khanh[1], Nguyen Thanh Giao[1]

ABSTRACT

This study investigates the surface water quality of rural areas in Hau Giang province, Vietnam using multivariate statistical analysis. Surface water samples were collected at 24 separate locations during the period from November 28 to December 3, 2019, and were measured for temperature (T), pH, dissolved oxygen (DO), biochemical oxygen demand (BOD), chemical oxygen demand (COD), total suspended solids (TSS), ammonium (NH_4^+-N), nitrite (NO_2^--N), nitrate (NO_3^--N), orthophosphate (PO_4^{3-}-P), Fe, As, Cd and coliform. Surface water quality was assessed using national technical regulations (QCVN 08-MT: 2015/BTNMT). The results showed that surface water in the study area was polluted with organic matter, nutrients, coliform, and Fe. BOD, COD, DO, TSS, NH_4^+-N, NO_2^--N, NO_3^--N, PO_4^{3-}-P are well correlated, which could be used to predict the concentration of correlated water parameters. Principal component analysis showed that 14 water quality variables affect surface water quality and therefore should be included and emphasized in monitoring programs. Water quality in the study area was divided into three groups with common pollution concerns of organic matter, microbes, and Fe. Particularly, group I had a high concentration of NO_2^--N, while groups II and III had high coliform density. The findings highlight that surface water quality in the rural areas of Hau Giang province is heavily polluted and unsuitable for water supply. Urgent solutions are needed to protect water quality for local population usage needs.

Keywords: *Surface water pollution, coliform, rural, Hau Giang province, Vietnam.*

Received: 23 September 2022; revised: 14 October 2022; accepted: 24 November 2022.

1. INTRODUCTION

An essential component of life and the environment, water resources play a crucial role in a country's existence and sustainable development. In recent years, Vietnam's strong economic growth has led to this finite and important natural resource increasing at risk of pollution and depletion, especially surface water resources. The quality of surface water is influenced by both natural and human activities, including weather conditions, erosion conditions, hydrological characteristics, effects of climate change, precipitation, industrial activities, agricultural land use, wastewater discharge and water resource exploitation [1, 2]. Domestic, agricultural, industrial and aquaculture

[1]College of Environment and Natural Resources, Can Tho University

[*]Correspondence author: nvcong@ctu.edu.vn

activities that generate an equivalent amount of wastewater directly or indirectly impact the water quality of ponds, lakes, rivers, streams, and receiving sources [1, 3].

The rural areas of Hau Giang province account for over 74.2% of the total population of 774,350. While the population density varies greatly between districts, towns, and cities. As rural production activities such as rice cultivation, husbandry and fisheries are not concentrated, it is challenging to implement and monitor environmental management solutions in general and waste management standards. Therefore, the surface water of rural areas is at high risk of pollution. Rural people in Hau Giang province depend much on surface water for daily activities, including water supply. Therefore, investigating the quality of this water is important for providing early warning for the human health of rural people.

In Vietnam, several studies on surface water quality assessment have been carried out. Truc *et al.* (2019) [4] studied the surface water quality of the Tien River flow through Tan Chau, An Giang province, to assess the water quality from upstream of the Mekong River affected by agricultural processing activities, hydropower projects and activities of the people. Moreover, Lien *et al.* (2016) [5] investigated the water quality of the main and tributary rivers of the Hau River, which is influenced by aquaculture and agricultural production. Surface water quality is often assessed using physio-chemical and biological factors, including temperature, pH, total suspended solids, dissolved oxygen, biochemical oxygen demand, chemical oxygen demand, nitrogen and phosphorus compounds, heavy metals, pesticides, *E. coli* and coliforms [6, 7, 8, 9]. In Vietnam, water quality is evaluated by comparing the measured values of parameters with the current national technical regulation on surface water quality. In addition, surface water quality is also evaluated using the water quality index (WQI). This study aims to assess surface water quality in the rural areas of Hau Giang province using multivariate statistical approaches, including Pearson's correlation, cluster analysis (CA), and principal component analysis (PCA). The study elaborates on the spatial variation of surface water quality, which helps design surface water quality monitoring systems in the rural areas of Hau Giang province and provides a more accurate overview of the state of surface water quality.

2. MATERIALS AND METHODS

2.1. Study area

Hau Giang province has administrative boundaries bordering Can Tho city to the North, Soc Trang province to the South, Kien Giang and Bac Lieu provinces to the West and Vinh Long and Song Hau provinces to the East (Figure 1). The province's natural area is 1,621.70 km^2, divided into eight administrative units. The geographical position of Hau Giang province shows that the section is influenced by both the East Sea tide and the West Sea tide regime. Therefore, the region is a water-bordered area and a water junction between the East and West Sea tides. Hau Giang province is interlaced rivers and canals with a total length of about 2,300 km. The topography is relatively flat, with gradually lower elevation from North to South and East

to West, with three distinct regions. The tidal zone is bordered by the Hau river with an area of 19,200 ha, with a developing orchard, agriculture, forestry, and fishery economy. The tidal flood zone is adjacent to the tidal zone with an area of about 16,800 ha; here, rice cultivation with industrial and service potentials is thriving. The flooded area is deep in the inner field for diversified agricultural development.

According to Hau Giang Statistical Yearbook (2018), the population in rural areas of the province does not fluctuate significantly from 573,462 - 583,848 people. However, the population has recently decreased, possibly due to the migration of people to urban areas in search of work. The population is related to resource use, domestic wastewater generation, and solid waste. Therefore, localities with higher population densities place more pressure on wastewater and solid waste management. Most of the wastewater from residential areas or communities is typically not collected or treated but solely passed or not through septic tanks and then discharged to infiltrate into the soil or discharged into ponds, ditches, rivers, and canals. There are many diverse types of production and husbandry activities in the area, including rice cultivation, livestock raising, aquaculture and the activities of craft villages and industries, creating a quantity of waste that contributes to environmental pollution.

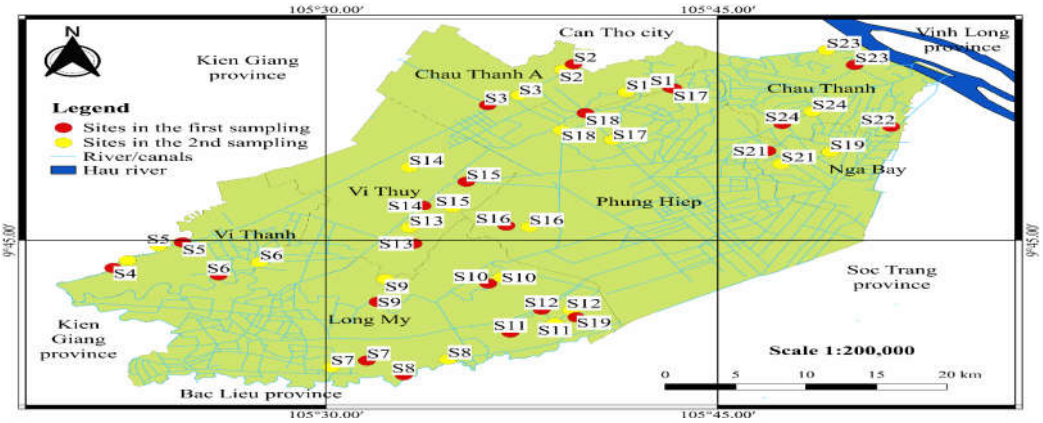

Figure 1. Map of the sampling sites in the rural areas of Hau Giang province

2.2. Water sampling and analysis

Water samples were collected at 24 locations (S1-S24) in Hau Giang province (HG1-HG8) in the dry season during the period from November 28 to December 3, 2019 (Figure 1).

The fields of HG1, HG2, HG3, HG4, HG5, HG6, HG7, and HG8 were Chau Thanh district, Chau Thanh A district, Vi Thanh city, Vi Thuy district, Long My district, Long My town, Nga Bay town, Phung Hiep district, respectively. The sampling sites were selected outside the towns or city centres with low population density. Fourteen parameters were checked to evaluate the quality of these water samples (Table 1). Water temperature, pH and dissolved oxygen (DO) were onsite detected while other parameters were analyzed as standard methods (Table 1). The limited values of surface water quality and methods for water quality analysis are presented in table 1.

Table 1. Analytical methods water quality parameters

No.	Parameters	Unit	Analytical methods	QCVN 08-MT: 2015/BTNMT, Column A1
1	Temperature	^{0}C	SMEWW 2550B: 2012	-
2	pH	-	TCVN 6492: 2011	6-8.5
3	DO	mg/L	TCVN 7325: 2004	≥6
4	BOD	mg/L	SMEWW 5210B: 2012	4
5	COD	mg/L	SMEWW 5220B: 2012	10
6	TSS	mg/L	TCVN 6625: 2000	20
7	NH_4^+-N	mg/L	TCVN 6179-1: 1996	0.3
8	NO_2^--N	mg/L	TCVN 6178: 1996	0.05
9	NO_3^--N	mg/L	TCVN 6180: 1996	2
10	PO_4^{3-}-P	mg/L	TCVN 6202: 2008	0.1
11	Fe	mg/L	TCVN 6177: 1996	0.5
12	As	µg/L	SMEWW 3114.C: 2012	10
13	Cd	µg/L	SMEWW 3113.B: 2012	5
14	Coliform	MPN/100 ml	TCVN 6187-2: 1996	2500

2.3. Data analysis

Data on surface water quality was assessed through comparison with the threshold values of national technical regulation QCVN 08-MT: 2015/BTNMT [11], column A1 (Table 1). Water quality index of Vietnam (VN_WQI) (1460/QD-TCMT dated November 12th, 2019) was used to evaluate the water quality for 8 units (H1-H8), including Group I (pH), Group III (As and Cd), Group 4 (DO, BOD_5, COD, N-NH_4^+, N-NO_3^-, N-NO_2^- and P-PO_4^{3-}) and Group V (Coliform). Correlation analysis (Pearson) was used to describe the relationship and interdependence among the analyzed water quality variables. A positive correlation means that the two variables increase or decrease together, while the negative correlation is a decreasing variable and one increasing variable [8]. Water parameter values of greater than 0.5 show a statistically significant correlation ($p<0.05$) between the water quality indicators [12]. Correlation analysis was performed using the statistical software IBM SPSS 20.0 for Windows. Principal Component Analysis (PCA) was used to reduce the quantity of features from many variables to a smaller number of factors in order to select a small set of variables that are highly correlated with the main component. The PCA result produces a new set of variables called the major component or factor (PC). The eigenvalue coefficients were used to evaluate the main components. The larger this coefficient, the greater the major component that contributes to the explanation of the variation of the original data set. Correlation between the main component and the primary data variables is explained by the weighted correlation data [12]. An absolute value of the

weighted correlation coefficient greater than 0.75 means that the correlation between the main component and the water quality parameter is strong, 0.5 - 0.75 is a moderate correlation and less than 0.5 is a weak correlation [13]. Cluster analysis (CA) was applied to the site group based on physical, chemical, and biological parameters of surface water quality. Sampling points were clustered on the basis of similarities. PCA and CA analysis were analyzed using Primer 5.2 for Windows software (PRIMER-E Ltd, Plymouth, UK).

3. RESULTS AND DISCUSSION

3.1. Evolution of surface water quality in rural Hau Giang province in 2019

3.1.1. Water pH

pH of surface water in rural areas of Hau Giang province ranged from 6.13 to 7.13 with an average of 6.54 ± 0.17 - 6.93 ± 0.17 (Table 2). Compared with the study results in the main river and tributaries of the Hau River, where the pH had a relatively higher value ranging from 6.3 to 8.0 with an average of 7.1 ± 0.32 [5]. In summary, the pH in the Hau Giang province study area, although lower than other study areas, is still within the permissible limit of column A1 of QCVN 08-MT: 2015/BTNMT. The results show that temperature and pH were in suitable ranges for aquatic life, fluctuating in water bodies in Hau Giang province, consistent with changes in the tropics [9].

3.1.2. Oxygenation compounds

DO in the rural Hau Giang province was seen to be relatively low, ranging from 0.17 to 4 mg/L with an average of 1.73 ± 0.94-3.72 ± 0.29 mg/L (Table 2). This low DO is due to the water environment with many organic substances that increase oxidation and oxygen consumption leading to oxygen depletion. Furthermore, the accumulation of organic humus in the areas affects the flow circulation and diffuses oxygen from the air into the water [15]. According to Lien *et al.* (2016) [5], wastewater from agricultural production, as well as domestic wastewater contains a lot of organic matter, so the decomposition of organic matter consumes dissolved oxygen, and DO is low. The results showed DO in rural areas of Hau Giang province have a value lower than the permissible limit for the column A1 of QCVN 08-MT: 2015/BTNMT, and the area shows signs of organic matter pollution.

Table 2. Water quality in rural areas of Hau Giang province

Parameter	HG1	HG2	HG3	HG4	HG5	HG6	HG7	HG8	QCVN‡
Temp. (°C)	28.9±0.43	30.0±0.99	28.8±0.42	29.5±0.15	29.5±0.12	29.2±0.27	29.6±0.16	29.5±0.22	-
pH	6.93±0.17	6.54±0.33	6.54±0.17	6.61±0.25	6.67±0.24	6.37±0.26	6.56±0.33	6.76±0.21	6-8.5
DO (mg/L)	2.50±1.16	2.95±1.34	2.2±1.63	1.73±0.94	2.11±1.38	2.25±1.07	2.97±0.66	3.72±0.29	≥6
BOD (mg/L)	11.0±4.38	16.5±2.07	17.2±3.97	17.7±4.18	18.8±2.86	9.17±0.98	9.00±0.89	11.2±3.25	4
COD (mg/L)	20.0± 8.1	29.5±4.59	31.5±7.87	33.0±8.76	33.2±5.42	15.8±1.94	15.00±2.1	19.3±5.35	10
TSS (mg/L)	52.8±9.37	154±98.2	89.7±16.8	106±76.4	148±58.7	65.2±19.3	64.3±23.4	46.0±14.8	20
NH_4^+-N (mg/L)	0.31±0.31	0.83±0.33	1.29±0.25	0.70±0.21	0.79±0.32	0.50±0.33	0.27±0.26	0.32±0.17	0.3
NO_2^-N	0.01±0.01	0.05±0.02	0.06±0.02	0.11±0.11	0.06±0.01	0.04±0.01	0.03±0.02	0.01±0.00	0.05

(mg/L)									
NO_3^-N (mg/L)	0.21±0.05	0.38±014	0.27±0.12	0.39±0.15	0.38±0.17	0.20±0.07	0.21±0.09	0.1±0.03	2
$PO_4^{3-}P$ (mg/L)	0.1±0.02	0.15±0.06	0.17±0.01	0.19±0.09	0.17±0.1	0.09±0.01	0.12±0.05	0.07±0.01	0.1
Fe (mg/L)	1.13±0.32	2.11±0.65	2.21±0.46	1.87±0.39	1.90±0.14	2.42±0.79	1.3±0.47	0.87±0.39	0.5
As (µg/L)	2.31±0.16	3.74±2.34	3.46±0.67	2.52±0.58	2.27±0.06	1.69±0.60	1.96±0.01	2.21±0.39	10
Cd (µg/L)	0.12±0.00	0.12±0.01	0.14±0.06	0.12±0.00	0.12±0.00	1.41±3.16	0.12±0.00	0.12±0.00	5
Coliform†	28.6±19.2	45.7±52.5	44.2±34.7	20.3±14.5	28.2±32.6	60.0±37.0	13.7±68.8	57.8±57.4	2.5
VN-WQI	28	26	22	22	22	28	29	28	-

"†" indicates the unit presented by 10^3 MPN/100 mL; "♯" denotes the technical standard (QCVN 08-MT: 2015/BTNMT, A1 column)

The BOD ranged from 7 to 25 mg/L, exceeding the permitted limit by 1.8-6.3 times (Table 2). The high BOD is consistent with low DO results. BOD in the study area exceeds column A1 of QCVN 08-MT: 2015/BTNMT. According to Nga and Thu [15], the source of organic pollution is the indiscriminate waste of the rural people, and the wastewater of households living and production activities in the area. The amount of organic humus has accumulated over time, increasingly obstructing the flow of water, which has reduced the ventilation and self-cleaning ability of the water bodies.

The COD ranged from 12 to 48 mg/L, averaging 15.00 ± 2.1-33.17 ± 5.42 mg/L (Table 2). The COD water quality in the Hau River was measured to be about 11.68 ± 3.76-13.54 ± 4.71 mg/L, while Ba Lua canal had a COD ranging from 14.7 ± 3.3 to 212.2 ± 37.4 mg/L, Phu Thinh commune (Hung Yen) has a COD of 152 mg/L [16]. If COD is <5 mg/L, the environment is classed as nutrient-poor, 20-30 mg/L is rich in nutrients and > 30 mg/L is polluted. In general, the COD in the study area exceeds the permissible limit of the standard of QCVN 08-MT: 2015/BTNMT, indicating that the water is organically polluted. The source of organic matter generation can be waste from farming, livestock, landfills, domestic activities, and services that discharge untreated waste into surface water [17, 18].

3.1.3. Total suspended solids

Measured TSS ranged from 32 to 290 mg/L, exceeding the QCVN 08-MT: 2015/BTNMT, column A1 by a magnitude of 1.6 - 10.5 times (Table 2). This is consistent with the result of low DO, as a high amount of TSS can increase surface water temperature and reduce dissolved oxygen. In the main rivers and tributaries of the Hau River, TSS ranged from 41.2 ± 33.7 to 89.57 ± 31.31 mg/L [5], while on the canals of An Giang province in the period 2009 - 2016, TSS ranged from 25.0 ± 11.5 mg/L to 93.7 ± 28.3 mg/L [5]; In canals in Soc Trang province, TSS ranges from 16 to 176 mg/L [19]. TSS exceeding the standard may be due to the characteristics of water, sediment, and storm water runoff, in addition to the water flowing from agriculture, aquaculture, industry and human activities in the area. TSS increases the cost of water treatment and affects aquatic life. TSS is also a

carrier that helps transport pollutants such as microorganisms, pesticides, and antibiotics, increasing exposure to adverse environmental factors.

3.1.4. Nutrients

NH_4^+-N ranged from 0.06 to 1.65 mg/L, with an average of 0.27 ± 0.26 - 1.29 ± 0.25 mg/L (Table 2). Chau Thanh A district and Nga Bay town had two sampling points with NH_4^+-N exceeding the allowed limit. Chau Thanh district had three points exceeding the permissible limit, while Phung Hiep District had four points exceeding the standard, while the remaining four areas all had six points exceeding the allowed limit in column A1 of QCVN 08-MT: 2015/BTNMT. The results indicated that NH_4^+-N is a serious problem of water quality in the study area. The NH_4^+-N value specified in QCVN 08-MT: 2015/BTNMT in columns A1 and A2 is 0.3 mg/L for domestic water supply and 0.9 mg/L for columns B1 and B2 used for irrigation and navigation purposes. NH_4^+-N is present in water due to the product of the decomposition of organic substances (especially proteins). The ammonium in the nitrogen cycle in nature or the water is contaminated with domestic wastewater and agricultural wastewater. Nitrite oxidises haemoglobin in red blood cells to form methemoglobin that cannot transport oxygen in the blood. Nitrite is toxic to aquatic organisms at a concentration of 0.1 mg/L and causes brown blood when the nitrite concentrations are about 0.5 mg/L. The results showed that the NO_2^--N concentration ranged from 0.005 to 0.247 mg/L with an average of 0.01 ± 0.01-0.11 Ơ 0.11 mg/L (Table 3). NO_2^--N concentration in the study area were relatively high, especially in Long Phu commune, Long My town, which had a very high NO_2^--N, exceeding 4.6-4.9 times compared with the QCVN 08-MT: 2015/BTNMT.

Nitrate is the end product of the mineralization of nitrogen-containing organic substances and is one of the most easily absorbed forms of protein by plants and is not toxic to aquatic organisms. But too high concentrations of nitrate in water environments affect aquatic animals. NO_3^--N in the study area ranged from 0.07 to 0.6 mg/L with the average ranging from 0.1 ± 0.03 to 0.39 ± 0.15 mg/L (Table 2). NO_3^--N concentration in rural areas of Hau Giang province in 2019 was still within the permissible limit of column A1 of QCVN 08-MT: 2015/BTNMT. PO_4^{3-}-P concentrations in the study area ranged from 0.05 to 0.33 mg/L with an average of 0.07 ± 0.01-0.19 ± 0.09 mg/L (Table 2). The results showed that there were 28/48 monitoring points exceeding the allowable limit by 1.1-3.3 times when compared with the column A1 of QCVN 08-MT: 2015/BTNMT. The localities with very high PO_4^{3-}-P concentration were Hoa Luu commune - Vi Thanh city (exceedence1.4-2.6 times), Long Phu commune - Long My town (exceedance 2.7-3.2 times). PO_4^{3-}-P in the canals in Soc Trang province was measured to be 0.05-0.90 mg/L [19], and in the Tien River, a section flows through Tan Chau (An Giang) 0.02-8 mg/L [4]. In some locations, the high concentration of PO_4^{3-}- P is due to the excessive number of organic fertilizers, pesticides, livestock farming activities, and household detergents [4]. Binh *et al.* (2020) [20] revealed that nutrient oxyanions were

affected by seasons, of which higher concentrations were identified in the dry season. This result is in line with the current study.

3.1.5. Heavy metals (Fe, As, Cd)

Fe concentration in rural areas of Hau Giang province in 2019 had values ranging from 0.54 to 3.49 mg/L, exceeding 1.08-6.98 times the permitted limit, with the average value fluctuating from 1.3 ± 0.47 to 2.42 ± 0.79 mg/L (Table 2). The concentration of As in the study area was in the range of 0.98-7.03 µg/L with the average ranging from 1.69 ± 0.60 to 3.74 ± 2.34 µg/L (Table 2). This value of As in the study area was still within the permissible limit for column A1 of QCVN 08-MT: 2015/BTNMT. Cd value was in the range of 0.12-7.86 µg/L, with the average ranging from 0.12 to 1.41 µg/L (Table 2). Cd value was also still within the permissible limit of column A1 of QCVN 08-MT: 2015/BTNMT.

3.1.6. Coliform

The coliform density in rural Hau Giang province in 2019 ranged from 9,300 to 150,000 MPN/100 mL, exceeding the limit threshold by 3.72-60 times (Table 2). Former studies have also previously reported high densities of coliform in surface waters. In the Can Tho River in 2010-2014, coliform density was from 3,448 to 27,327 MPN/100 mL [21]. Coliform density in the study area was high and exceeded the permissible limit in column A1 of QCVN 08-MT: 2015/BTNMT. The water source was polluted with microorganisms, and surface water must be properly treated before use. The presence of coliforms shows that the environment is receiving secretions from humans and animals (livestock, poultry, and aquaculture in Hau Giang province).

3.1.7. VN_WQI index

Table 2 shows that VN_WQI indexes varied between 22 and 29. It means that the water quality ranged between poor and very poor. Higher pollution was identified in sites HG3, HG4, and HG5, where VN_WQI was below 25 (very poor), recommended suitable water treatment methods for further use. While the VN_WQI of HG1, HG2, HG6, HG7 and HG8 fluctuated from 26 to 28. The water quality was poor and appropriate for waterway transportation and other analogous purposes.

3.2. Correlation between surface water quality variables

Correlation analysis (Pearson) was used to describe the positive and negative relationships and interdependence between the analyzed criteria (Figure 2). BOD correlated positively with COD, TSS, NH_4^+-N, NO_2^--N, NO_3^--N, PO_4^{3-}-P with correlations of (0.992), (0.663), (0.563), (0.565), (0.725) and (0.667). COD was also correlated with TSS (0.659), NH_4^+-N (0.579), NO_2^--N (0.588), NO_3^--N (0.738) and PO_4^{3-}-P (0.683). TSS was found to be positively correlated with NH_4^+-N (0.531), NO_2^--N (0.611), NO_3^--N (0.761) and PO_4^{3-}-P (0.715). Moreover, the nitrogen and phosphorus compounds were positively correlated. Specifically, NH_4^+-N correlates with PO_4^{3-}-P with a high correlation (0.606); NO_2^--N correlated positively with NO_3^--N (0.564) and PO_4^{3-}-P (0.744); NO_3^--N is positively correlated with PO_4^{3-}-P (0.708). In general, organic matter and nutrients in surface water were positively correlated and can help predict the correlated

pollutants, thereby reducing the number of analysis criteria to save time and money.

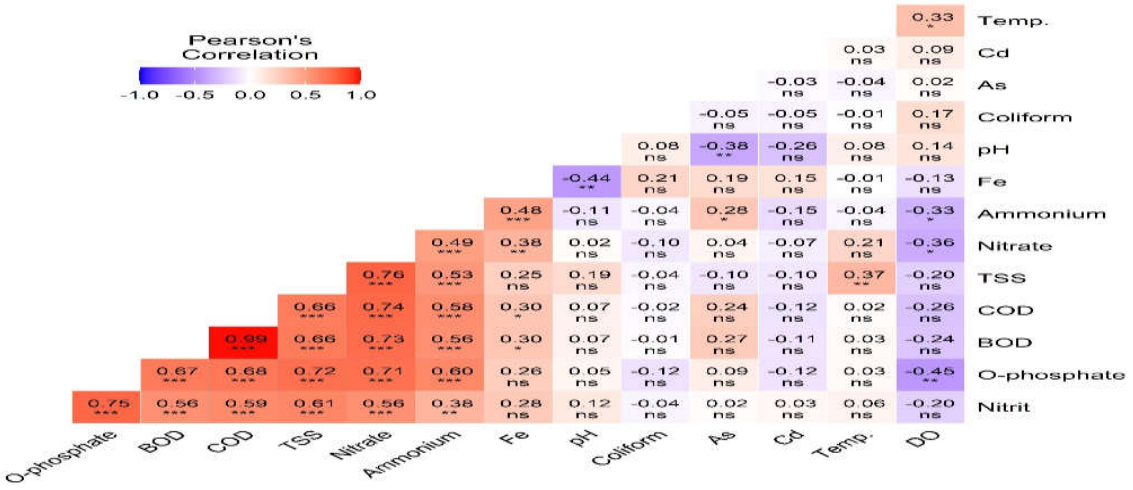

Figure 2. Pearson correlation heat map between surface water quality variables

"ns", P≥ 0.05; "", P<0.05; "**", P<0.01; "***", P<0.001.*

3.3. Key parameters affecting surface water quality

The principal component analysis (PCA) results showed that four main factors explained 92.7% of the variation in surface water quality in the study area of rural Hau Giang province (Table 3). As reported by Shrestha and Kazama (2007) [22], a PC with eigenvalues values greater than 1 is considered significant. PC1 accounts for 50.9% of the total variation in the data. PC1 is affected by positive coefficients that correlate weakly with indicators BOD (0.348), COD (0.349), TSS (0.32), NH_4^+-N (0.305), NO_2^--N (0.32), NO_3^--N (0.35) and PO_4^{3-}-P (0.359). The results are similar to those reported by [5], in which the variables pH, NO_3^--N, TN, TP and COD were highly correlated, and the nutrient content and organic matter existed in the water. This is also consistent with the results of the correlation analysis discussed in the previous section. PC1 can be the decentralized source of impacts due to the daily domestic wastewater of households, farming activities, fertilization, animal husbandry and aquaculture in the area. PC2 explained 19.5% of the total variation of the obtained data, which correlated weakly with pH (0.496), Fe (-0.452), coliform (-0.342), and the average correlation with Cd (-0.554). PC2 is mainly affected by industrial production and trade villages and waste excreted from humans and animals. Furthermore, PC3 explained 12% of the variation in surface water quality. PC3 is affected by a positive coefficient with a weak correlation to temperature (0.341), As (0.453), and coliform (0.481), which had an average correlation with DO (0.511), affected by industrial activities, human and animal waste.

According to Nga *et al.* (2005) [15], this appears in areas with many suspended materials, and agricultural and industrial wastewater. PC4 explains 10.4% of the variation in surface water quality within the study area, at a high correlation with temperature (0.7) affected by natural environmental conditions and a weak correlation with NH_4^+-N (0.365). The PCA results show that the 14 initially selected indicators all have a significant impact on

surface water quality and should therefore be included in a periodic monitoring program to monitor the changes in surface water quality. However, it can be possible to select BOD or COD to represent organic matter; among the nitrogen species, NH_4^+-N should be selected since NO_2^--N and NO_3^--N could be predicted using the relationship among NH_4^+-N, NO_2^--N, NO_3^--N and DO. The possible polluting sources of water quality in the study area come from domestic activities, cultivation, husbandry, fisheries, industrial production, and hydrology.

Table 3. Key variables influencing water quality in the rural areas of Hau Giang province

Variable	PC1	PC2	PC3	PC4
Temp.	0.077	0.122	0.341	-0.700
pH	-0.074	0.496	-0.125	0.257
DO	-0.245	0.187	0.511	-0.094
BOD	0.348	0.125	0.076	0.136
COD	0.349	0.12	0.052	0.163
TSS	0.320	0.043	0.209	-0.237
NH_4^+-N	0.305	-0.142	0.170	0.365
NO_2^-N	0.32	-0.095	-0.231	-0.145
NO_3^-N	0.35	0.049	-0.063	-0.219
PO_4^{3-}P	0.359	0.070	-0.152	-0.014
Fe	0.241	-0.452	0.028	-0.017
As	0.238	0.089	0.453	0.237
Cd	-0.106	-0.554	-0.095	-0.101
Coliform	-0.1	-0.342	0.481	0.253
Eigenvalues	7.12	2.72	1.68	1.45
%Variation	50.9	19.5	12	10.4
Cum. %Variation	50.9	70.3	82.3	92.7

3.4. Spatial variation of surface water quality in rural areas of Hau Giang province

The results of cluster analysis (CA) in rural Hau Giang province in 2019 showed that water quality was divided into three clusters (Figure 3). Cluster I consist of 4 sampling sites (S10, S13, S14, S19), Cluster II includes 10 sampling sites (S2, S4, S8, S9, S15, S16, S17, S18, S23, S24), and group III includes the remaining 10 sampling locations (S1, S3, S5, S6, S7, S11, S12, S20, S21, S22).

All three groups showed water sources polluted with organic matter, microorganisms and heavy metals (Table 4). However, Cluster I showed the presence of NO_2^--N in the water in concentrations exceeding the permitted standard by1.2 times. Whereas Clusters II and III, although located in a large branch, the density of coliform in Cluster II is relatively higher than that of Cluster III (2.66 times), and higher than that in the standard by 24.51 times.

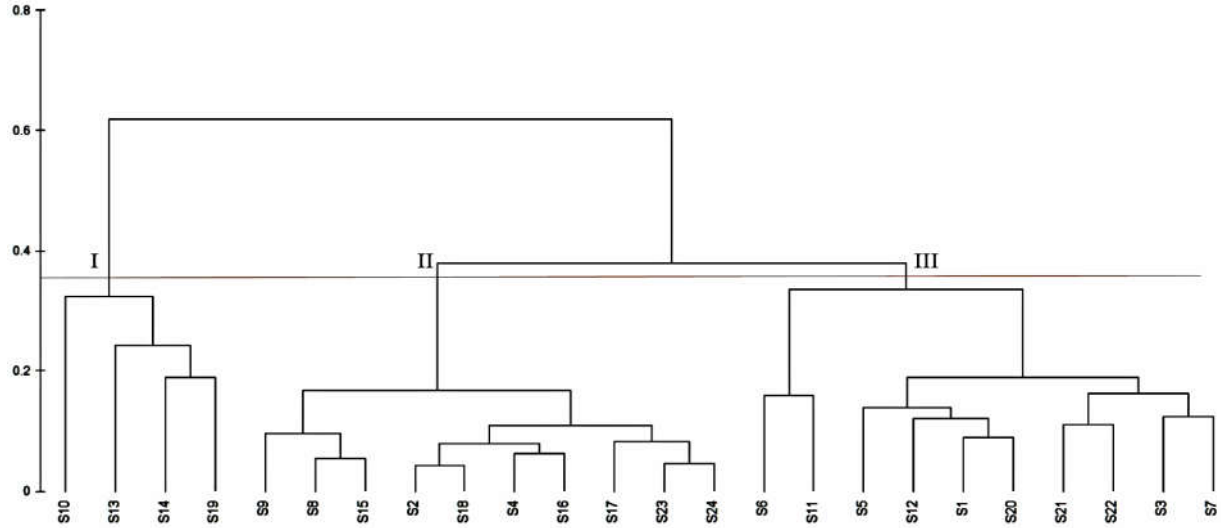

Figure 3. Spatial variation of surface water quality

Table 4. Characteristics of water quality in the group

Parameter	Units	Cluster			
		Cluster I	Cluster II	Cluster III	QCVN
Temp	°C	29.46	29.34	29.39	-
pH	-	6.69	6.66	6.58	6-8.5
DO	mg/L	1.84	3.02	2.37	≥6
BOD	mg/L	16.25	12.70	13.95	4
COD	mg/L	28.74	22.48	25.39	10
TSS	mg/L	123.50	72.00	96.25	20
NH_4^+-N	mg/L	0.69	0.65	0.57	0.3
NO_2^--N	mg/L	0.06	0.04	0.05	0.05
NO_3^--N	mg/L	0.33	0.21	0.30	2
PO_4^{3-}-P	mg/L	0.18	0.11	0.13	0.1
Fe	mg/L	1.55	1.93	1.59	0.5
As	µg/L	2.23	2.40	2.76	10
Cd	µg/L	0.12	0.51	0.13	5
Coliform	MPN/100mL	*12975.00*	*61280.00*	*23075.00*	2500

4. CONCLUSIONS

This study on the surface water quality in the rural areas of Hau Giang province showed that the pH, NO_3^--N, As and Cd were within the allowable limits, while the indicators NO_2^--N, PO_4^{3-}-P, NH_4^+-N exceeded the corresponding permitted thresholds of QCVN 08-MT: 2015/BTNMT, column A1. DO was below the allowable threshold, while BOD, COD, TSS, Fe, and coliform at all sampling locations exceeded the permitted threshold limits. The results show that the surface water environment in the study area is polluted with organic matter, nutrients, microorganisms, and Fe. The parameters of organic matter (BOD, COD, DO, TSS), and nutrients (NH_4^+-N, NO_2^--N, NO_3^--N, PO_4^{3-}-P) were positively correlated and can be used for prediction of the correlated water pollutants and, thus reduce water sample analysis criteria. PCA

results showed that all water quality parameters need to be monitored. The cluster analysis results divided the surface water quality in the study area into three clusters with common pollution problems, including organic matter, microbes, and Fe. The pollution of Cluster I was characterized by high NO_2^-N, while Clusters II and III were characterized by coliform. The sources of surface water pollution are mainly from daily activities, cultivation, animal husbandry, fisheries, industrial production, soil conditions and the hydrological regime. The results of the current study provide important information on the current state of surface water quality, serving as a scientific basis for establishing a much-needed water monitoring network.

ACKNOWLEDGEMENT

This study was funded by the Department of Natural Resources and Environment of Hau Giang province, Vietnam. The authors would like to thank Nigel K. Downes-Researcher for Integrated Water Resource Management (IWRM), for proofreading the article.

AUTHOR CONTRIBUTIONS

All authors contributed to the study's conception and design. Material preparation, data collection and analysis were performed by Nguyen Van Cong, Huynh Van Thao, Huynh Cong Khanh. The first draft of the manuscript was written by Nguyen Thanh Giao and authors commented on the previous versions of the manuscript. All authors read and approved the final version.

REFERENCES

1. Jarvie, H. P., Whitton, B. A., Neal, C. (1998). Nitrogen and phosphorus in east coast British rivers: Speciation, sources and biological significance. Science of the Total Environment, 1998, 210-211: 79-109.

2. Arain, M. B., Kazi, T. G., Jamali, M. K., Jalbani, N., Afridi, H.I., Shah, A. (2008). Total dissolved and bioavailable elements in water and sediment samples and their accumulation in Oreochromis mossambicus of polluted Manchar Lake. Chemosphere, 70 (10), 1845-1856.

3. Carpenter, A.S. R., Caraco, N. F., Correll, D. L., Howarth, R. W., Sharpley, A. N., Applications, S. E., Aug, N. (2016). Non-point Pollution of surface waters with phosphorus and nitrogen. Wiley Stable, 8 (3), 559-568.

4. Truc, D. T., Phat, P. H., Nam, N.D. G., Toan, P. V., Tri, V.P.D. (2019). Surface water quality of Tien River flows through Tan Chau, An Giang province. *Can Tho University Journal of Science*, 2, 53 - 60 (in Vietnamese)

5. Lien, N. T. K., Huy, L. Q., Oanh, D. T. H., Phu, T. Q., Ut, V.N. (2016). Water quality in mainstream and tributaries of Hau River. *Can Tho University Journal of Science*, 43, 68-79 (in Vietnamese).

6. Helena, B., Pardo, R., Vega, M., Barrado, E., Fernandez, J. M., Fernandez, L. (2000). Temporal evolution of groundwater composition in an alluvial aquifer (Pisuerga River, Spain) by principal component analysis. Water Research, 34(3), 807 - 816.

7. Singh, K. P., Malik, A., Mohan, D., Sinha, S. (2004). Multivariate statistical techniques for the evaluation of spatial and temporal variations in water quality of Gomti River (India) - A case study. Water Research, 38(18), 3980–3992.

8. Gazzaz, N. M., Yusoff, M. K., Ramli, M. F., Aris, A. Z., Juahir, H. (2012). Characterization of spatial patterns in river water quality using chemometric pattern recognition techniques. Marine Pollution Bulletin, 64(4), 688-698.

9. Chounlamany, V., Tanchuling, M. A., Inoue, T. (2017). Spatial and temporal variation of water quality of a segment of Marikina River using multivariate statistical methods. Water Science and Technology, 76(6), 1510-522.

10. American Public Health Association (APHA). (2012). Standard Methods for the Examination of Water and Wastewater, 20th edition, Washington DC, USA.

11. Vietnam Environmental Protection Agency. (2015). National technical regulation on surface water quality (QCVN 08 - MT: 2015/BTNMT); Vietnam Environmental Protection Agency: Ha Noi, Vietnam. (in Vietnamese).

12. Feher, I. C., Moldovan, Z., Oprean, I. (2016). Spatial and seasonal variation of organic pollutants in surface water using multivariate statistical techniques. Water Science and Technology, 74 (7), 1726-1735.

13. Liu, C. W., Lin, K. H., Kuo, Y. M. (2003). Application of factor analysis in the assessment of groundwater quality in a blackfoot disease area in Taiwan. Science of the total Environment, 313 (1 - 3), 77 - 89.

14. Ongley, E. D. (2009). Water quality of the lower Mekong River. 4951 Connaught Ave., Montreal, QC, Canada H4V 1X4, 297-320.

15. Nga, B. T., Thu, B. A. (2005). Surface water quality and domestic waste management in Rach Ban canal, Can Tho city. *Can Tho University Journal of Science*, 4:26-35 (in Vietnamese).

16. Hung, T., Kien, P. Đ., Chuong, V. H., Loan, N. T., Tra, V. T., Duc, N. M., Tuan, T. D., Dung, N. T. P. (2017). Collection and treatment of domestic wastewater in rural areas of the Mekong River Delta. *Journal of Science and Technology Activities Safety, Health and Working Environment,* 91–96.

17. Mekong River Commission, (2015). Lower Mekong regional water quality monitoring report. ISSN: 1683-1489. MRC Technical Paper No.51.

18. Chea, R., Grenouillet, G., Lek, S. (2016). Evidence of Water quality degradation in Lower Mekong Basin Revealed by Self-Organizing Map, https://doi.org/10.1371/journal.pone.0145527

19. Tuan, D. D. A., Thu, B. A., Trung, N. H. (2019). Assessing quality of surface water for urban water supply source for Soc Trang city. *Can Tho University Journal of Science*, 4A, 61-70 (in Vietnamese).

20. Binh, T. N., Long, D. V., Tong, X. N., Quang, N. X. (2020). The interactive effects of natural factor and pollution sources on surface water quality in the lower Mekong River Basin, Southwestern Vietnam. Water Resources, 47 (5), 865 – 876.

21. Giau, V. T. N., Tuyen, P. T. B., Trung, N. H. (2019). Assessment of changes in surface water quality of Can Tho River in the period 2010-2014 by calculation method of water quality index (WQI). *Can Tho University Journal of Science*, 55(2), 105-113 (in Vietnamese)

22. Shrestha, S., Kazama, F. (2007). Assessment of surface water quality using ultivariate statistical techniques: A Case Study of the Fuji River Basin, Japan. Environmental Modelling and Software, 22(4), 464-475.

SYNTHESIS OF HYBRID SPONGY NANOCOMPOSITE MATERIALS BASED ON Al_2O_3 AND STEARIC ACID TO RECOVER WASTE OIL IN WATER

Mai Van Tien [1], Pham Ba Viet Anh[1,*], Nguyen Thuong Doan[1]

ABSTRACT

The spongy nanocomposite materials based on Al_2O_3 hybridized with stearic acid were synthesized by a hydrothermal method combined with a sol-gel combustion method. The characteristics of the materials were determined by standard methods such as Fourier-transform infrared spectroscopy (FTIR) and scanning electron microscopy (SEM). A 0.03 M NH_3 solution and a 0.05 M stearic acid solution were used to synthesize materials. The synthesis yield of Al_2O_3 nanoparticles and stearic acid hybridized Al_2O_3 spongy nanocomposites reached 96.5 % and 97.6 %, respectively. The effects of the variation of NH_3 concentrations, steric acid concentrations, and sintering temperature on the absorbability of the nanofoams were investigated. The hybrid nanomaterials were used to treat 2 types of waste oil from motorcycle engine and cooking. The results showed that 1 g of hybrid nanocomposite foams absorbed 5 mL of waste oil. This indicates that the steric acid-hybridized Al_2O_3 spongy nanomaterials could be applied for the treatment of oil pollution.

Keywords: *Nanocomposite foam, nanomaterial, stearic acid, Al_2O_3, waste oil.*

Received: 24 August 2022; revised: 19 September 2022; accepted: 22 November 2022.

1. INTRODUCTION

Oil spills and waste oil pollution are accidents that occurs during the exploitation, storage, transportation and use of oil. Oil pollution and waste oil not only negatively affect an economy, but also seriously affect an ecological environment. Recently, along with rapid socioeconomic development, Vietnam's petroleum industry has been also strongly developed. It is estimated that around 11 million tons of oil and oil products have been consumed every year. Moreover, Vietnam is located on the international maritime route of oil transportation from the Middle East to Japan in amount of up to 30 million tons per year. This implies that tens of millions of tons of oil are being circulated on the territory of Vietnam every year and therefore the risk of oil spills is very high. The fact shows that oil spill accidents have consecutively occurred for many years. For example, the accidents of the Neptune Aries in 1994 in Ho Chi Minh city, the Formosa One in 2001 in Ba Ria - Vung Tau, the My Dinh ship in 2004 in Cat Ba sea, and dozens of other small accidents in the whole country and in the petroleum industry [1-3]. In addition, around 1.5 million liters of cooking oil is consumed in Vietnam every

[1]Ha Noi University of Natural Resources and Environment

[*]Corresponding author: pbvanh@hunre.edu.vn

year. A rate of 10% - 20% of the amount is disposed after use, implying 150,000 to 300,000 liters of waste cooking oil is discharged to the environment every year [4].

In order to recover waste oil and treat oil pollution, mechanical methods using offshore oil booms, shoreline oil booms, floating barrier and vacuum equipments have been often used. Besides, there are many other treatment technologies such as chemical dispersion, biodegradation, in-situ combustion, and adsorption. The adsorption methods may be considered as more appropriate solutions for the recovery of waste oil since these methods minimize potential negative impacts on the environment [5-9].

Most of adsorbents using for oil spill treatment that were synthesized from clay, perlite, and glass wool had low adsorption capacity. Although polyurethane spongy materials had high adsorption capacity, they were very bulky. Moreover, their chemically compatibility with different oils was not high and therefore the oil treatment was not thorough [10-12]. In this work, spongy nanocomposite materials based on stearic acid-hybridized Al_2O_3 were synthesized to apply for the recovery of waste oil in water by a hydrothermal method combined with a sol-gel combustion method. The effects of NH_3 concentrations, steric acid contents, and sintering temperature on the characteristics and waste oil absorbability of the hybrid nanocomposites were investigated.

2. MATERIALS AND METHODS

2.1. Materials

Aluminum nitrate nonahydrate $Al(NO_3)_3.9H_2O$ (white solid, ≥ 99.5% purity, China), ammoniac solution (20 – 25% concentration, Vietnam), stearic acid (white solid, ≥ 98% purity, Indonesia), tergitol (≥ 99% purity, Malaysia), n-hexane (colorless liquid, ≥ 99.5% purity, China), double distilled water

Waste oil was collected from a motorcycle engine with a black color and high viscosity. Waste cooking oil was collected from the kitchen of a restaurant which has a brownish color.

2.2. Synthesis of stearic acid-hybridized Al_2O_3 nanocomposite foams

Spongy nanocomposite materials based on Al_2O_3 hybridizing with stearic acid were synthesized by a hydrothermal method combined with a sol-gel combustion method via two processes as presented in figure 1.

The synthesis procedure includes two steps, namely the synthesis of Al_2O_3 nanofiblers and stearic acid/Al_2O_3 spongy nanocomposites. Al_2O_3 nanoparticles were synthesized via the slow addition of NH_3 solutions with various concentrations of 0.1 M, 0.3 M and 0.5 M into a 25 mL of a solution containing 15 g of $Al(NO_3)_3$ until pH = 6. A suspended mixture was generated and continuous stirred for 1 h. After that, the mixture was centrifuged at a speed of 4.500 rpm for 5 min to obtain a precipitate part which was transferred to an autoclave for a hydrothermal process at 170^0C for 24 h. Subsequently, the product of the hydrothermal process was mixed with 5 g of tergitol. Finally, the mixture was sintered at 450 – 600^0C for 5 h to form Al_2O_3 nanoparticles.

Stearic acid/Al_2O_3 spongy nanocomposites were synthesized by the addition of steric acid solution in a suspension of Al_2O_3 nanoparticles. Briefly, 1 g of Al_2O_3 nanoparticles was ultrasonicated in 50 mL of distilled water for 5 min to generate a suspended solution. Then, various volumes in the range of 50 mL – 150 mL of a 0.05 M

stearic acid solution were injected in the Al_2O_3 suspension during a vigorous shaking to form milky spongy nanocomposite materials which were purified by using a filter paper.

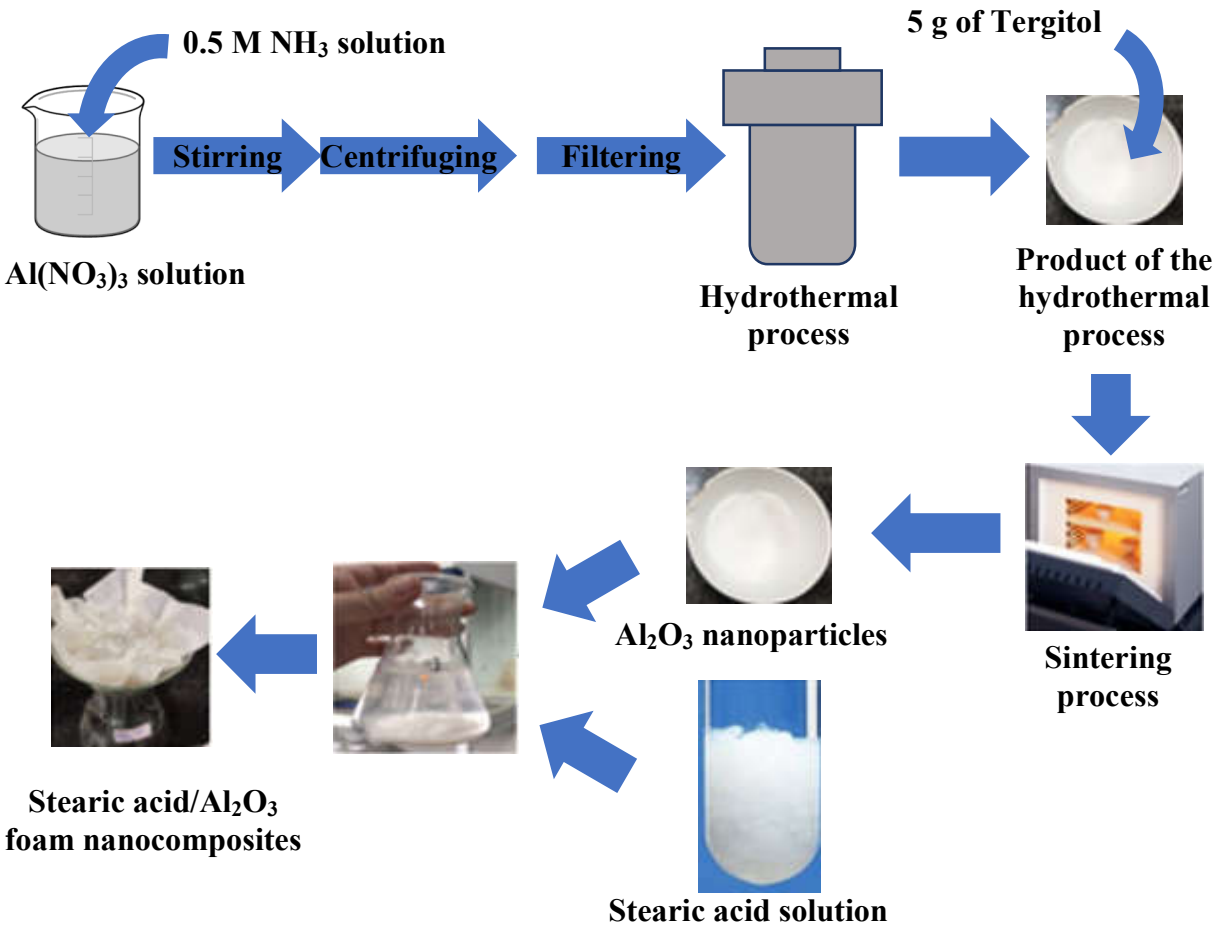

Figure 1. Schematic diagram illustrating the synthesis procedure of spongy nanocomposites based on Al_2O_3 hybridized with stearic acid.

2.3. Structure characterization of the hybrid foams

The structure characterization of the function groups of Al_2O_3 nanoparticles and stearic acid-hybridized Al_2O_3 nanocomposites was analyzed by a Fourier-transform infrared spectroscopy (FTIR) using Bruker Tensor spectrometer (Institute of Geography, VAST). The surface structure morphology of materials was determined by using a Jeol JMS 6490 Scanning Electron Microscopy (SEM).

The experimental procedure for the density determination of the nanocomposite was carried out according to TCVN 6039-1: 2015 (ISO 1183-1:2012).

2.4. Evaluation of the absorbability of the hybrid foams to waste oil

The waste oil absorbability of hybrid foams was evaluated using a static model, which was performed at the laboratory of Faculty of Environment, Ha Noi University of Nature Resources and Environment. The detail practical procedure was carried out as follows. Firstly, various volumes in the range of 1 mL to 6 mL of waste oil were added into beakers containing 50 mL distilled water, then

1 g of stearic acid/Al_2O_3 spongy nanocomposites was added to each beaker. Waste oil in water was immediately adsorbed on the spongy nanocomposites. The waste oil adsorbed nanocomposites were separated by using filter cloth or glass wood, which were dried and weighed for the determination of adsorption yield of the materials.

For the preparation of a blank sample, 1 mL of waste oil was added into a beaker containing 50 mL distilled water, then the solution was flowed through the layer of filter cloth or glass wood. Water oil adsorbed on the spongy nanocomposites was recovered via a simple mechanical compression method. All experiments were repeated three times.

3. RESULTS AND DISCUSSION

3.1. Effects of synthesis conditions on the properties of hybrid nanocomposite foams

3.1.1. Effects of the concentration variation of NH_3 solutions on the formation of Al_2O_3 nanoparticles

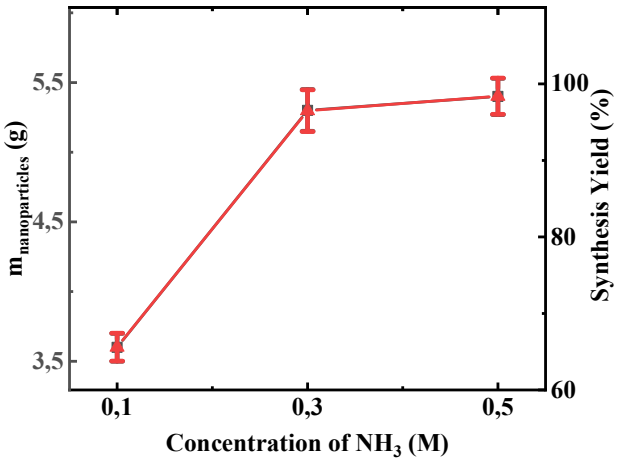

Figure 2. The effects of NH_3 concentrations on Al_2O_3 nanoparticle formation.

The effects of NH_3 concentrations on the formation of Al_2O_3 nanoparticles were detailed in Figure 2. NH_3 solutions with concentrations of 0.1 M, 0.3 M and 0.5 M were used for synthesis processes while other conditions were similar as described in section 2.2.

The obtained results showed that NH_3 concentration impacted the mass and size of Al_2O_3 nanoparticles. The formation yields of Al_2O_3 nanoparticles increased during the increase in the concentrations of NH_3 solutions. When the synthesis process achieved a theorical yield of 100%, it would generate 5.49 g of Al_2O_3 nanoparticles. It means a 0.5 M NH_3 solution could be used to synthesize the nanoparticles with a yield of 98.4%, which was higher than the yield of synthesis processes using lower NH_3 concentrations. However, low NH_3 concentrations could form the nanoparticle with smaller and more uniform sizes. It may be explained by the fact that the size of $Al(OH)_3$ precipitates formed from low concentration NH_3 solutions were smaller and more uniform, whereas $Al(OH)_3$ formed from a high NH_3 concentration tended to accumulate a large size. Therefore, the shape of Al_2O_3 nanoparticles synthesized from a high NH_3 concentration was heterogeneous. From the result, 0.3 M NH_3 solutions were used for further experiments.

3.1.2. Effects of the variation of sintering temperature

strongly impacted on the properties and waste oil adsorption capability of nanomaterials. Various temperatures in the range of 450^{0}C to 600^{0}C were used to synthesis spongy nanocomposites while other experimental conditions were fixed as described in section 2.2. The spongy nanocomposites were utilized to adsorb a waste oil sample containing 2 mL of

motorcycle waste oil in 50 mL of distilled water.

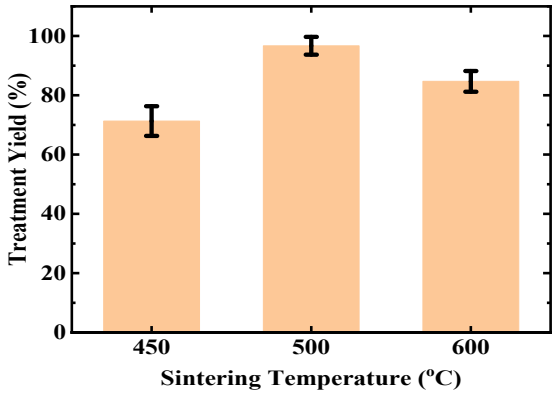

Figure 3. Effects of sintering temperature variation on the waste oil adsorption capability of spongy composites

The temperature of sintering processes Figure 3 shows the yield of waste oil treatment using stearic acid-hybridized Al_2O_3 spongy nanocomposites. The results indicated that the nanocomposites synthesized under the sintering temperature of 500^0C could adsorb waste oil with the highest yield of 96.7%. This may result from the effects of temperature on the spongy structure of stearic acid/Al_2O_3 nanocomposites.

3.1.3. Effects of the volume variation of stearic acid solutions

The effects of stearic acid content on the waste oil treatment yield of spongy nanocomposites were evaluated by using various volumes of stearic acid to synthesize the spongy nanocomposites. The synthesis yield and treatment yield of different nanomaterials are presented in figure 4.

The results show an increasing treatment yield with an increasing stearic acid volume from 50 mL to 150 mL. However, the highest synthesis yield was achieved 97.6% for a stearic acid volume of 100 mL. This probably comes from the difference between the ratios of stearic acid to Al_2O_3 nanoparticles, which altered the structure, size and spongy properties of the nanocomposites. Importantly, the experiments helped us to determine the optimal conditions of spongy nanocomposites, namely a NH_3 concentration of 0.3 M, a sintering temperature of 500^0C, and a 0.05 M stearic acid volume of 100 mL.

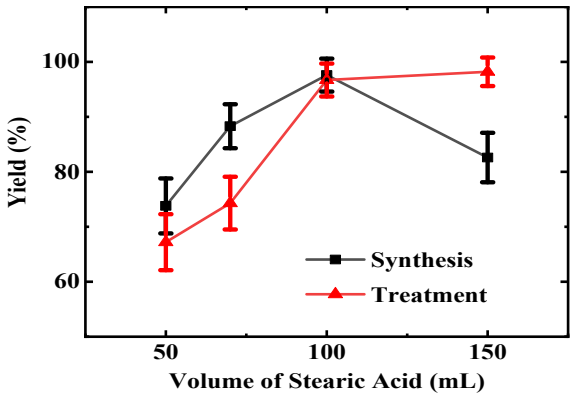

Figure 4. Synthesis yield and waste oil treatment yield of spongy nanocomposites synthesized from various volumes of stearic acid solutions

3.2. Characteristics of hybrid nanocomposite foams

3.2.1. Bond features of hybrid nanocomposite foams

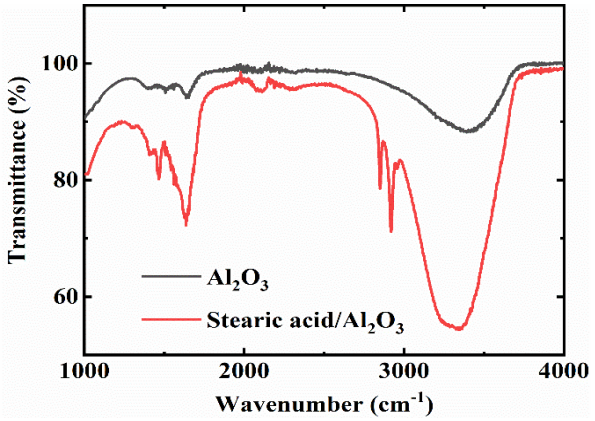

Figure 5. Fourier-transform infrared spectra of Al_2O_3 nanoparticles and stearic acid-hybridized Al_2O_3 nanocomposites

The bond features of Al_2O_3 nanoparticles and stearic acid-hybridized Al_2O_3 nanocomposites were investigated using a Fourier-transform infrared spectroscopy method. Figure 5 shows that both Fourier-

transform infrared spectra of Al_2O_3 nanoparticles and stearic acid-hybridized Al_2O_3 spongy nanocomposites exhibited absorption bands at the same wavenumbers around 1560 and 3450 cm^{-1}, which were attributed to Al-O-Al bonds and O-H bonds in H_2O molecules absorbed on the nanoparticles, respectively. Moreover, the spectrum of the spongy nanocomposites displayed various absorption bands at 2911 and 2844 cm^{-1} relating to the asymmetric and symmetric covalent vibrations of C-H bonds of stearic acid. Significantly, the characteristic band of C=O bonds of stearic acid at 1694 cm^{-1} was not observed on the spectrum, implying that stearic acid molecules created strong bonds with Al_2O_3 via a chemical process. This could probably impact the surface of materials, which formed hydrophobic and lipophilic characteristics of the stearic acid-hybridized Al_2O_3 nanocomposites.

3.2.2. Surface structures of hybrid nanocomposite foams

The surface structure of stearic acid-hybridized Al_2O_3 spongy nanocomposites was imaged by using a scanning electron microscope, which was presented in Figure 6. The SEM images indicate that the surface structure morphology of the hybrid nanocomposites was relatively spongy. The addition of stearic acid made Al_2O_3 particles tend to bind together via stearic acid molecules, resulting in the formation of a multidimensional spongy structure with high porosity.

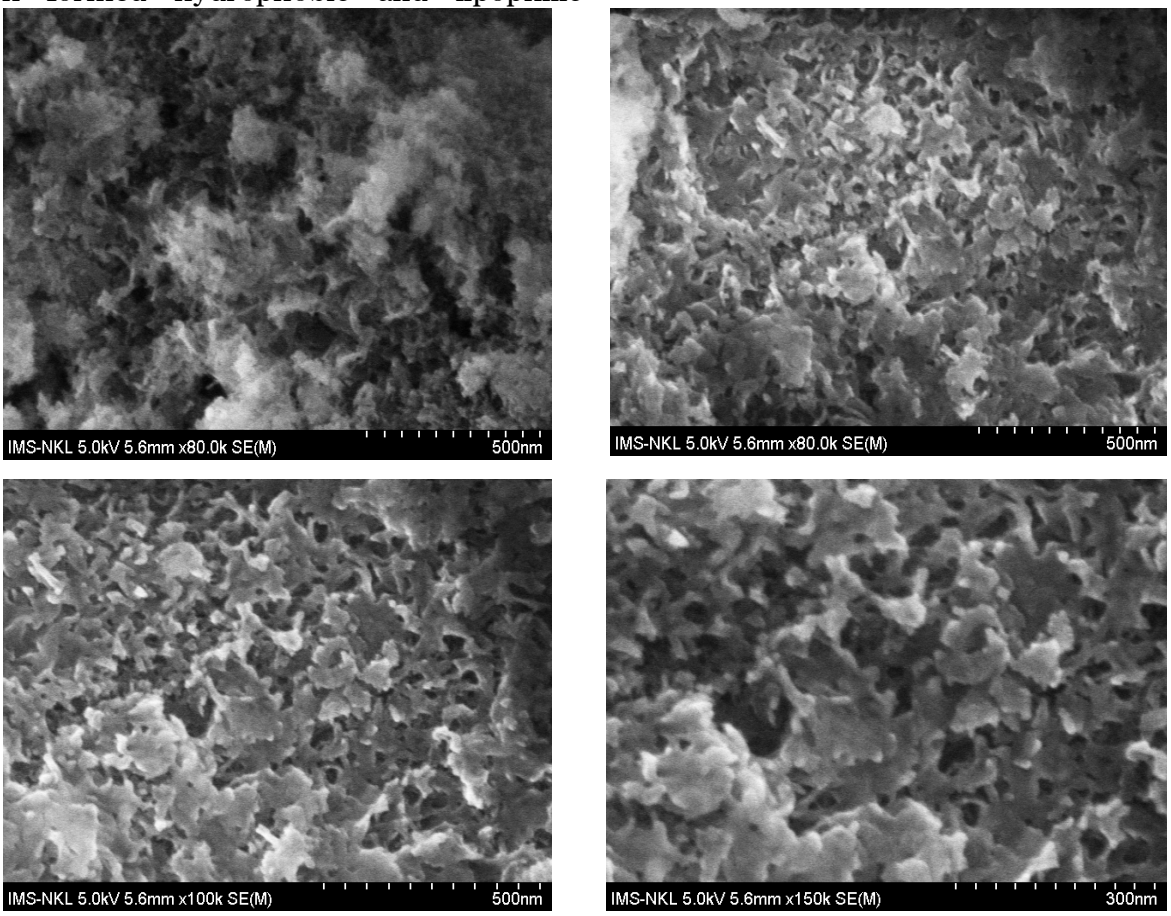

Figure 6. SEM images of spongy nanocomposites based on stearic acid-hybridized Al_2O_3

3.2.3. Density of hybrid nanocomposite foams

The density of acid-hybridized Al_2O_3 nanocomposites was determined to be 0.74 g/cm^3. The low density of the hybrid nanocomposites indicated the spongy structure of the materials, which was consistent with the surface structure analysis by SEM imaging. This result also implies that the hybrid composites could be float on water, which facilitates the treatment of waste oil floating on water since the density of waste oil is also lower than water.

3.3. Evaluation of the absorbability to waste oil of hybrid nanocomposite foams

The waste oil absorbability of stearic acid-hybridized Al_2O_3 spongy nanocomposites was evaluated by the addition of 1 g of the nanocomposites to beakers containing various volumes of waste oil in 50 mL distilled water. The results of experiments showed that the waste oil in water was immediately absorbed by the spongy nanocomposite (Figure 7).

Figure 7. Experimenting on the waste oil absorption capability of spongy nanocomposites based on Al_2O_3 hybridizing with stearic acid

When the spongy nanocomposites absorbed waste oil were separated by a filter cloth, there were no trace of waste oil in transparent filtrates for the initial volumes of waste oil in the range of 1 – 5 mL. However, there was a small amount of waste oil in the filtrate when the initial volume of waste oil was 6 mL. It implies that the spongy nanocomposites were saturated with waste oil. This result could allow us to state that the absorption capability of the spongy nanocomposites is around 5 mL of waste oil per 1 g of the material. Moreover, the stearic acid-hybridized Al_2O_3 spongy nanocomposites were also used to treat waste cooking oil in water. The result of experiments indicates that the nanocomposites could absorb the waste cooking oil with the absorption capability similar to their waste oil absorption capability. It implies the hybrid nanocomposites can be applied to treat different waste oil types.

4. CONCLUSIONS

We successfully synthesized spongy nanocomposite materials based on the hybridization of Al_2O_3 with stearic acid by using a hydrothermal method and a sol-gel method. The optimal conditions were investigated for the synthesis procedure of the hybrid spongy nanocomposites, namely a NH_3 concentration of 0.5 M, pH = 6, a 0.05 M stearic acid volume of 100 mL, and a sintering temperature of 500^{0}C. The characteristics of the hybrid nanocomposites were determined by FTIR spectroscopy, SEM imaging. The

results indicated the nanocomposites had multidimension spongy structure with a high porosity, which was consistent with the low density of the materials (0.74 g/cm^3). The nanocomposites were utilized to absorbedly treat waste oil in water with a maximum absorption capability of 5 mL/1 g. This result should open the various applicability of hybrid nanomaterials for the recovery and treatment of spilled oil and waste oil in water and can be applied for the treatment of oil pollution.

REFRENCES

1. ITOPF (2014). "*Effects of oil pollution on the marine environment*", Techical information papers 13.

2. ITOFT (2014). "*Effect of oil pollution on social and economic activities*", Technical information paper 12.

3. ITOFT (2014). "*Use of sorbent materials in oil spill response*", Technical information paper 8.

4. USDA's Foreign Agricultural Service (2012). "Global Agricultural Information Network Report".

5. Bro-Rasmussen F (1996). "Contamination by persistent chemicals in food chain and human health", *Sci. Total Environ.*, 188(1), pp. 45-60.

6. Olov Fast, Christer Colliander (1994). "A new tool for oil spill responders", *Spill science and Technology Bulletin*, 1(2), pp. 173-174.

7. Pasila A (2004). "A biological oil adsorption filter", *Marine Pollution Bull*, 49(11-12), pp. 1006-1012.

8. B .R. Simonovic, D. Arandelovic, M. Jovanovic, B. Kovacevic, L. Pezo, A. Jovanovic (2009). "Removal of mineral oil and wastewater pollutants using hard coal", *Chem. Ind. Chem. Eng. Q.*, 15, pp.57-62.

9. A. E. Bence, K. A. Kvenvolden, M. C. Kennicutt (1996). "Organic geochemistry applied to environmental assessments of Prince William Sound, Alaska, after the Exxon Valdez oil spill - A review", *Org. Geochem.*, 24, pp. 7-42.

10. R. Camilli, C. M. Reddy, D. R. Yoerger, B. A. S. Van Mooy, M. V. Jakuba, J. C. Kinsey (2010). "Tracking hydrocarbon plume transport and biodegradation at Deepwater Horizon", *Science*, 330, pp. 201-204.

11. J. Pinto, A. Athanassiou, D. Fragouli (2018). "Surface modification of polymeric foams for oil spills remediation", *J. Environ. Manage.*, 206, pp. 872-889.

12. R. MacDonald, D.M. Kammen, M. Fan (2014). "Science in the aftermath: investigations of the DWH hydrocarbon discharge", *Environ. Res. Lett.*, 9, pp. 125006 (1-2).

WRITING AND SUBMITTING

1. The Vietnam Journal of Agriculture and Rural Development publishes scientific articles announcing scientific research works with new scientific content, overview articles on the agriculture and rural development sector that have not been submitted for publication in any kind of journals

2. Articles can be written in Vietnamese (published in the Journal by Vietnamese language) or in English (published in the Journal by English language), drafted on a computer, lines separated by 1, 2 (Paragraph/Line spacing Multiple at 1,2), using the font Times New Roman, font size 12, with a length of no more than 10 pages of A4 size paper including references.

3. Keywords are presented in alphabetical order, from 3 to 5 words. Keywords in Vietnamese and English must have the same content and meaning of the word. The abstract must be no more than 350 words in length, without newline, in font size 10, including: Briefly stating the purpose, research method, and main research results. Articles written in Vietnamese must have abstracts in both English and Vietnamese and must not differ in content or meaning.

4. Articles must be presented in the following order: Title of the article in Vietnamese and English, author(s), author(s) agency name, abstract, keywords, content of the article , acknowledgments (if any), references. Author contact must be indicated with office address, email, and phone number on the front page of the manuscript. Vietnamese proper names must have enough accent marks, including articles in English.

5. References are presented in order of citation and numbered in square brackets in the order they appear in the article and in the list of references.

+ For documents that are articles in the Journal, write in full in the following order: Author's name, year of publication, title of article, title of journal, volume, number, page.

+ For documents being books, write in full in the following order: Name of author, year of publication, title of book, publisher, place of publication.

If the article is in English, any references that are not in English must be translated into English and captioned in the original language in parentheses.

6. The Vietnam Journal of Agriculture and Rural Development implements the submission process, the online review process on the Journal's software system and uses the database of published Journal, to suggest collaborators, reviewers and readers access the website: http://tapchikhoahocnongnghiep.vn/ and follow the instructions.

7. For details, please contact: Journal of Agriculture and Rural Development; No. 10 Nguyen Cong Hoan, Ba Dinh, Hanoi; Phone: 024.37711070; 024.38345457; 024.37716634. Email: bbtnongnghiep@gmail.com.